Investigating Systemic Aging and its Effects on Aged Tissues by Utilizing a Small Animal Blood Exchange Model

by

Melod Mehdipour-Mossafer

A dissertation submitted in partial satisfaction of the

requirements for the degree of

Joint Doctor of Philosophy
with the University of California, San Francisco

in

Bioengineering

in the

Graduate Division

of the

University of California, Berkeley

Committee in charge:

Professor Irina Conboy, Chair
Professor Niren Murthy
Professor Guo Huang

Spring 2022

Abstract

Aging is characterized as a progressively worsening loop where an accumulation of aberrant molecules and cells lead to a plethora of ailments. Tissue homeostasis gradually falters leading to inadequate resident stem cell responses, persistent inflammation, fibrosis, and metabolic derangements. Furthermore, organ secretome profiles of aging individuals shift from factors that bolster tissue health and regeneration to a milieu that progressively impairs tissue function. These harmful factors accumulate in the blood and are distributed throughout the body. Heterochronic parabiosis experiments have shown that the systemic environment can impact organ regeneration. Young blood can rejuvenate the performance of aged tissue stem cells, whereas old blood can negatively affect those of the young. This work strongly reinforces the paradigm which maintains that mammalian aging is plastic, yet the translatability of this work remains elusive. It is also unclear whether young blood factors are necessary for rejuvenation. In this dissertation, a preclinical model that mimics plasmapheresis was developed to enable immediate translation to therapies for aged humans. Plasmapheresis is an FDA-approved treatment modality where plasma is extracorporeally separated from the blood, replaced with a physiologic fluid, and transfused back into the bloodstream. We demonstrate that the dilution of aged blood plasma rejuvenated the muscle and brain. The plasma dilution studies introduced a novel paradigm which holds that young blood factors may not be essential for rejuvenation; a neutral-age physiological fluid could suffice in this regard. These works broaden our understanding of systemic aging and suggest a novel repositioning of plasmapheresis to improve the health span of aged people.

Table of Contents

List of Figures

Acknowledgements

The research described in this dissertation was supported by grants from National Institute of Health, QB3 Calico Award, and Open Philanthropy award to Professor Irina Conboy, and the National Science Foundation Graduate Research Fellowship to Melod Mehdipour. I thank Mary West, PhD and the CIRM/QB3 Shared Stem Cell, Cell and Tissue Analysis Facility at UC Berkeley for use of the Zeiss Axioimager microscope and cryotomes. I thank my thesis advisor Professor Irina Conboy and Dr. Michael Conboy for mentoring, guiding, and integrating these studies. I thank Cameron Kato for his contributions that are provided in Chapter 2, Professor Yi Zuo of the University of California, Santa Cruz and her former postdoctoral fellow and now Assistant Professor Chia-Chien Chen of Duke Kushan University for their contributions to Chapter 3. I also thank the following for their contributions to Chapter 3: Taha Mehdipour for his contributions to Figures 2 & 3, Dr. Michael Conboy for performing experimental TA muscle injures in mice for Figure 3, and Professor Ok Hee Jeon of Korea University College of Medicine for oral gavage administration of ABT263 in aged mice for Figure 3. I would also like to thank all of the members of Conboy lab. I thank *Aging* for the publication of the research presented in Chapter 2. I would also like to thank *GeroScience* for publication of the research presented in Chapter 3 of this dissertation. I thank Cameron Kato and Taha Mehdipour for providing me with Letters of Consent for use of their primary data and notebook entries included at the ends of Chapters 2 and 3, respectively.

Dedication

In the Name of God, Most Gracious, Most Merciful

First and foremost, I would like to thank God for granting me health, determination, wits, and the strength to persevere.

I would like to dedicate my thesis dissertation to:

My mother Susan Mehdipour, and my father, Mehdi Mehdipour, for raising me to be the person that I am today.

My brother and best friend, Taha Mehdipour.

My uncle, Mojtaba Shobeiri, my aunt, Maryam Shobeiri, and my cousins, Shobeir Shobeiri & Amir Shobeiri, for their unwavering and pivotal support throughout my life.

The rest of my family members throughout the world. Thank you for all the love and support.

My late aunt, Akram Ghorbani, my late uncle, Mahmood Saghirdar, my late cousin Namrood Nozari, and any other soul who has tragically succumbed to COVID-19.

Introduction

Aging is a universal process that espouses a plethora of physiological and molecular changes[1,2]. It is associated with the impairment of stem cell activation, which leads to the decline of tissue function[1–4]. Old and damaged or unrepaired tissues perturb homeostasis in surrounding tissues by secreting factors into circulation. These factors may not only serve as biomarkers for specific age-associated pathologies but may also induce a variety of degenerative pathologies[3,5]. In all, aging can be characterized as a detrimental loop where damaged macromolecules and cells along with impaired tissue function can collectively perpetuate one another. This includes but is not limited to senescent cells, chronically active immune cells, and the senescence associated secretory phenotype (SASP) that perpetuates tissue damage. This loop will ultimately be responsible for accumulated metabolic irregularities, fibrosis, and chronic inflammation[3,6]. These phenomena are depicted in Figure 1 and are strongly associated with increased susceptibility to chronic diseases that accompany aging.

Previously, prevalent theories of declining tissue function with respect to age focused on cumulative cell intrinsic alterations such as telomere attrition, DNA damage, oxidative damage, and mitochondrial dysfunction[7]. Though this may be true for differentiated cells, stem cells appear to age "extrinsically" and maintain a degree of "youth" that could result from quiescence, which is the default for virtually all postnatal stem cells[7–13]. The regenerative capacity of stem cells appears to persist throughout life but the biochemical cues that regulate these cells change with age in ways that cause the abandonment of tissue maintenance and repair in aged individuals[7,9].

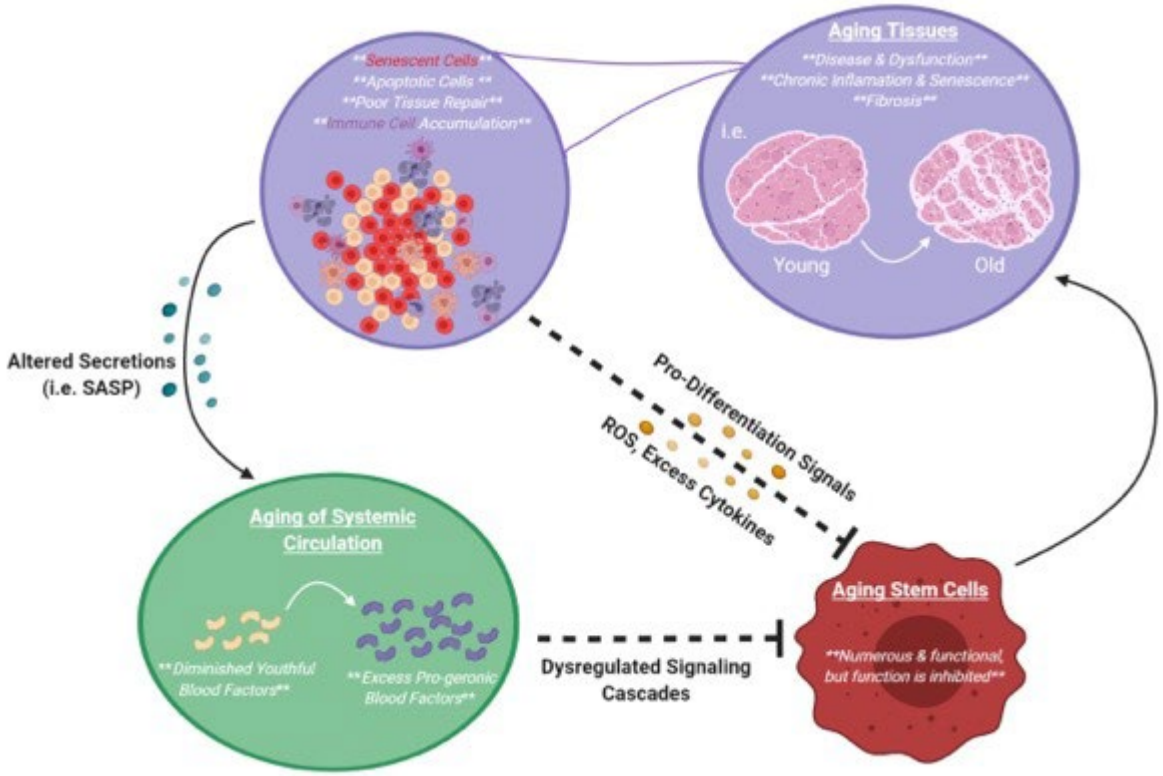

Figure 1. The detrimental loop perpetuated by mammalian aging. Factors that promote degenerative phenotypes with advanced age may be present to some extent in young individuals but ultimately accumulate as age advances. This causes dysregulated signaling cascades that attenuate tissue stem cell function and ultimately cause tissue 77dysfunction. Damaged cells such as senescent and apoptotic cells can accumulate within these tissues. Immune cells can infiltrate these damaged tissues and may contribute to the secretion of excess cytokines, pro-differentiation signals. Senescent cells can secrete senescence-associated secretory phenotype (SASP) factors which can further alter systemic proteomic profiles and stem cell responses. Figure was generated on biorender.com.

Heterochronic parabiosis studies have demonstrated that these biochemical cues can be recalibrated to health-youth, thereby rescuing the regenerative capacity of old stem cells *in vivo*[10,14–17]. Conversely, age-related changes in these biochemical signals can make stem cells from young animals behave much like older stem cells[8,18].

The robust rejuvenation of representative organs from the three developmental germ layers (muscle, liver, and brain) has sparked great interest in leveraging potentially medical properties of young blood factors. This arises from a predominantly held conclusion from the heterochronic parabiosis studies which maintains that the function of old stem cells can be enhanced upon the exposure of young systemic milieu[7]. From this originated the notion that a "systemic silver bullet" (ie one circulating molecule) can bring about rejuvenation across multiple tissues simultaneously. Aging is a multi-genic process, meaning that changes to multiple factors contribute to phenotypes observed in aged individuals.

Young and aged blood serum have inducing or inhibitory properties *ex vivo* on stem cells that were isolated from mice and humans[7,19]. During *in vivo* studies, small volumes of young plasma were infused into aged mice and improvements to neurogenesis and cognition were observed[20]. Though promising, the effects of plasma infusions to other tissue stem cells were not investigated and health span experiments have not been performed[7,20]. In addition, the positive effects of young blood are only partial for muscle, the extent of hippocampal neurogenesis in aged mice exposed to young blood is nowhere near the levels of young mice, and no extension of lifespan by infusions of young plasma into aged mice was observed[7,8,20,21]. The profound inhibition of young organ stem cells upon exposure to aged blood was also reported[9,18,22,23]. In all, infusion small volumes of young plasma into aged subjects may not be an effective method of rejuvenating aged tissues unless the potent inhibitory components of aged plasma are removed or neutralized[7].

It is also prudent to experimentally uncouple the effects of blood and serum alone from other influences brought about by parabiosis. What also remains unclear is determining which levels of systemic factors are both necessary and sufficient for enhancing the pro-regenerative capacities of aged tissue stem cells. Above all, mixing young and old blood in culture, exposing young stem cells to aged serum, and heterochronic blood exchange studies suggest that old blood dominates over that of the young and that young blood is not a medicine.

The heterochronic parabiosis model is also fraught with a few significant effects that may confound relevant conclusions. The effects of heterochronic parabiosis are often assumed to be caused by the exchange of macromolecules found in plasma, but the physiology between two conjoined partners is far more complex[24]. The old partner benefits not just from the blood of its

young partner, but from the young animal's organs. The heart, lungs, liver, kidneys, and thymus may all contribute to remove or neutralize harmful factors or metabolites that are present in aged individuals[7]. These organs improve blood oxygenation, normalize metabolic parameters such as glucose and cholesterol profiles, and improve immune/inflammatory responses in aged animals. These collective functions are thought to greatly contribute to the rejuvenation of tissue stem cells[9,25]. Conversely, the young parabiont must maintain an aged body with poorly functioning organs[7] and this is thought to hamper the function of young tissue stem cells.

Environmental enrichment may also significantly impact tissue stem cell responses. The old parabiosis partner is placed in a more stimulating environment when sutured to a young partner than when it is stitched to an older partner. Older animals tend to be sedentary, whereas younger partners are a lot more active. An old animal is therefore obligated to be active when conjoined to a younger partner. These along with pheromones released by young animals are thought to enhance neurogenesis and synaptic plasticity[7,24,26,27].

Cytokines released from blood cells may also influence organ stem cell performance[28–30]. Wound healing capabilities of leukocytes, which decline with advanced age, could also be pertinent for adequate regeneration of injured tissues. Old parabionts may also benefit from young leukocytes in this fashion.

To sum the major findings implicated by these studies, heterochronic parabiosis serves as proof for the hypothesis that mammalian aging is plastic. Aged stem cells remain numerous and function, and an exposure to young blood can awaken regenerative responses of aged tissue stem cells while young tissue stem cell function declines. Signal transduction networks can also be reset to "youth" or "old age". At the same time, several significant demerits to the parabiosis model include the following: both the blood and organs are shared, complicating the conclusions about determinant factors. It takes roughly 7-10 days for stochastic exchange of blood to take place between partners, and the procedure is highly invasive[31]. A phenomenon known as parabiotic disease may also randomly reduce sample sizes by up to 50%[31]. Lastly, animals are connected for 4-5 weeks making it difficult to decipher the onset and duration of the reported effects.

A heterochronic blood exchange model was developed to ensure that reported changes to tissue health and regeneration arose solely from blood[24]. In place of parabiosis, mice underwent a minimally invasive procedure known as jugular vein cannulation surgery where catheters are installed in their jugular veins. The animals were then connected to a blood exchange device where the amount of blood, exchange flow rates, and the onset and duration of effects can be easily interrogated. The mice can be connected and disconnected from the device at will; no animals are surgically conjoined to each other during this process. During one blood exchange session, 150 μL of blood are exchanged between mice 15 times in order to exchange roughly 50% of blood between partners, which takes 30 minutes. **Figure 2** illustrates the heterochronic blood exchange procedure (obtained from Rebo & Mehdipour et al 2016).

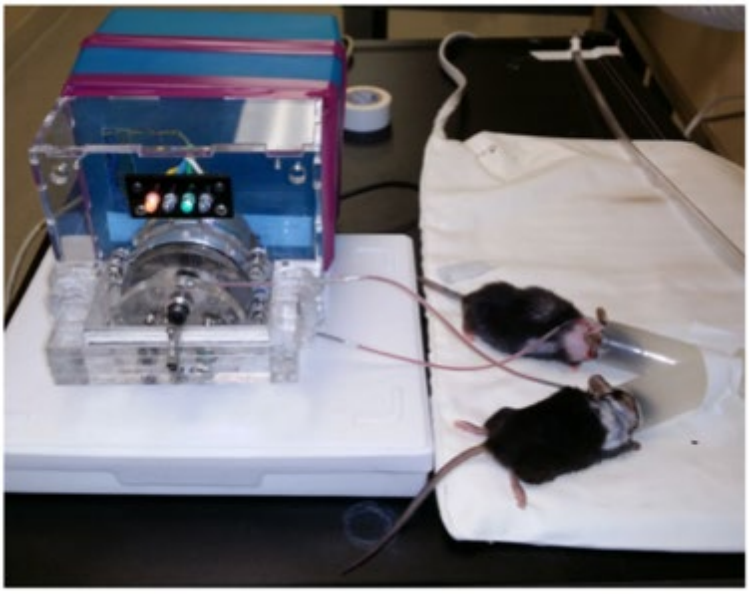

Figure 2: the heterochronic blood exchange system. A young mouse (right of the anesthesia tube) and an old mouse (left of the anesthesia tube) are connected to the programmable blood exchange apparatus while placed on a heating pad to maintain body temperature while anesthetized. Image was obtained from Rebo & Mehdipour et al 2016[24].

During heterochronic blood exchange, mice were cannulated and their blood was exchanged the day following cannulation. One day after exchange, tibialis anterior muscles from mice were experimentally injured by cardiotoxin injections. Animals were then sacrificed 5 days post injury and organs were harvested to analyze regeneration parameters[24]. In work leading to my PhD studies, it was found that muscle regeneration improves significantly in the old animal exchanged with young blood. Fibrosis becomes decreased in old mice apheresed with young blood. In a 4-limb hang test, functional performance of old exchange partners is not improved by young blood, but young mice display rapidly diminished agility/coordination/learning after they have been exchanged with old blood.

The number of proliferating neural precursor cells in the hippocampus rapidly and severely decreases in the young animal exchanged with old blood. No notable improvement in neurogenesis is observed in the old heterochronic exchange partner. Peripheral muscle injury compounds the inhibitory effect of old blood in young partners. The inhibition of hippocampal neurogenesis was rapid and uncoupled from shared organs or environmental enrichment[24].

Transfusion of young blood improves hepatogenesis while old blood inhibits it in young mice. Hepatocyte proliferation, as expected, is less prominent in animals without peripheral muscle injury. Heterochronic blood exchange also decreases the number of fibrotic clusters in aged livers. Liver adiposity is also diminished in old livers after heterochronic blood exchange[24].

Transforming Growth Factor beta-1 (TGFβ1) is was shown to increase both systemically and locally. TGFβ1/pSmad3 induction is also more pronounced within brains and muscles of aged

mice than in young animals[12,32,33]. Pharmacological inhibition of TGFβ1 signaling decreased the intensity of pSmad2/3 levels, was associated with a concomitant decline in elevated B2M levels, and improved myogenesis and neurogenesis of aged mice[12,34]. We therefore reasoned that TGFβ1 signaling may be the likely reason for the observed changes in B2M levels. While TGFβ1 expectedly increased with age, heterochronic blood exchange did not significantly alter TGFβ1 levels or pSmad3 intensity in either young or old muscle[24]. These data suggest that factors other than TGFβ1 account for the induction of B2M by aged blood in young animals[24].

Summarily, the age of tissues can be rapidly and effectively reversed between the young and old states through the heterochronicity of systemic milieu. Age-specific systemic inhibitors dominate over the rejuvenative molecules found in young blood. This is particularly evident in the effects on brain and animal performance.

Heterochronic parabiosis and blood exchange experiments established that the age of systemic milieu has a rapid effect on the health and regeneration of muscle, liver, and brain[8,20,24,33]. Unlike parabiosis however (where organs, environmental enrichment, and pheromones are also shared in addition to blood), the small animal apheresis uncoupled the effects of blood from other influences. This approach determined that the beneficial effects of young blood are dominated by the negative effects of aged blood. The overall positive effects could be explained by the dilution of aged blood factors; not necessarily by young factors[24]. Plasma exchanges are also routine treatment modalities for managing several autoimmune disorders such as thrombotic thrombocytopenic purpura, Goodpasture syndrome, and Guillan-Barré syndrome, where its mechanism of action is removing pathogenic autoantibodies[24,35,36]. The blood exchange system described here can be applied to mice or other small animals[24]. This allows for more well-controlled experiments and can be rapidly translated to combating a variety of age-related diseases with already FDA approved devices[24]. Extracorporeal blood manipulation may provide a modality of rapid translation for human use[24].

References

1. López-Otín, C., Blasco, M. A., Partridge, L., Serrano, M. & Kroemer, G. The hallmarks of aging. *Cell* **153**, 1194–1217 (2013).
2. Aunan, J. R., Cho, W. C. & Søreide, K. The biology of aging and cancer: A brief overview of shared and divergent molecular hallmarks. *Aging and Disease* (2017) doi:10.14336/AD.2017.0103.
3. Mehdipour, M. *et al.* Attenuation of age-elevated blood factors by repositioning plasmapheresis: A novel perspective and approach. *Transfusion and Apheresis Science* **60**, 103162 (2021).
4. Hung, C.-W., Chen, Y.-C., Hsieh, W.-L., Chiou, S.-H. & Kao, C.-L. Ageing and neurodegenerative diseases. *Ageing Research Reviews* **9**, S36–S46 (2010).
5. Steenman, M. & Lande, G. Cardiac aging and heart disease in humans. *Biophysical reviews* **9**, 131–137 (2017).
6. Etienne, J., Liu, C., Skinner, C. M., Conboy, M. J. & Conboy, I. M. Skeletal muscle as an experimental model of choice to study tissue aging and rejuvenation. *Skeletal Muscle* **10**, 4 (2020).
7. Conboy, I. M., Conboy, M. J. & Rebo, J. Systemic problems: A perspective on stem cell aging and rejuvenation. *Aging* vol. 7 754–765 (2015).
8. Conboy, I. M. *et al.* Rejuvenation of aged progenitor cells by exposure to a young systemic environment. *Nature* **433**, 760–764 (2005).
9. Conboy, I. M. & Rando, T. A. Heterochronic parabiosis for the study of the effects of aging on stem cells and their niches. *Cell Cycle* vol. 11 2260–2267 (2012).
10. Conboy, I. H., Conboy, M. J., Smythe, G. M. & Rando, T. A. Notch-Mediated Restoration of Regenerative Potential to Aged Muscle. *Science* **302**, 1575–1577 (2003).
11. Elabd, C. *et al.* Oxytocin is an age-specific circulating hormone that is necessary for muscle maintenance and regeneration. *Nature Communications* **5**, (2014).
12. Yousef, H. *et al.* Systemic attenuation of the TGF-β pathway by a single drug simultaneously rejuvenates hippocampal neurogenesis and myogenesis in the same old mammal. *Oncotarget* **6**, 11959–78 (2015).
13. Rando, T. A. & Wyss-Coray, T. Stem Cells as Vehicles for Youthful Regeneration of Aged Tissues. *The Journals of Gerontology: Series A* **69**, S39–S42 (2014).
14. Carlson, M. E. *et al.* Molecular aging and rejuvenation of human muscle stem cells. *EMBO Molecular Medicine* **1**, 381–391 (2009).
15. Paliwal, P., Pishesha, N., Wijaya, D. & Conboy, I. M. Age dependent increase in the levels of osteopontin inhibits skeletal muscle regeneration. *Aging* **4**, 553–566 (2012).
16. Yousef, H. *et al.* hESC-secreted proteins can be enriched for multiple regenerative therapies by heparin-binding. *Aging* **5**, 357–372 (2013).
17. Dumont, N. A., Wang, Y. X. & Rudnicki, M. A. Intrinsic and extrinsic mechanisms regulating satellite cell function. *Development (Cambridge, England)* **142**, 1572–1581 (2015).
18. Conboy, I. M. & Rando, T. A. Aging, stem cells and tissue regeneration: Lessons from muscle. *Cell Cycle* **4**, 407–410 (2005).

19. Brack, A. S., Conboy, I. M., Conboy, M. J., Shen, J. & Rando, T. A. A Temporal Switch from Notch to Wnt Signaling in Muscle Stem Cells Is Necessary for Normal Adult Myogenesis. *Cell Stem Cell* **2**, 50–59 (2008).
20. Villeda, S. A. *et al.* Young blood reverses age-related impairments in cognitive function and synaptic plasticity in mice. *Nature Medicine* **20**, 659–663 (2014).
21. Ruckh, J. M. *et al.* Rejuvenation of regeneration in the aging central nervous system. *Cell Stem Cell* **10**, 96–103 (2012).
22. Sinha, M. *et al.* Restoring systemic GDF11 levels reverses age-related dysfunction in mouse skeletal muscle. *Science* **344**, 649–652 (2014).
23. Brack, A. S. *et al.* Increased Wnt signaling during aging alters muscle stem cell fate and increases fibrosis. *Science* (2007) doi:10.1126/science.1144090.
24. Rebo, J. *et al.* A single heterochronic blood exchange reveals rapid inhibition of multiple tissues by old blood. *Nature Communications* **7**, (2016).
25. Jeong, J., Conboy, M. J. & Conboy, I. M. Pharmacological inhibition of myostatin/TGF-β receptor/pSmad3 signaling rescues muscle regenerative responses in mouse model of type 1 diabetes. *Acta Pharmacologica Sinica* **34**, 1052–1060 (2013).
26. Schaffer, D. v & Gage, F. H. Neurogenesis and neuroadaptation. *Neuromolecular Med* **5**, 1–9 (2004).
27. Jessberger, S. & Gage, F. H. Stem-cell-associated structural and functional plasticity in the aging hippocampus. *Psychology and aging* **23**, 684–691 (2008).
28. Horsley, V., Jansen, K. M., Mills, S. T. & Pavlath, G. K. IL-4 Acts as a Myoblast Recruitment Factor during Mammalian Muscle Growth. *Cell* **113**, 483–494 (2003).
29. Hai Huang Dhavalkumar D Patel, K. G. M. The immune system in aging: roles of cytokines, T cells and NK cells. *FBL* **10**, 192–215 (2005).
30. Nervi, B., Link, D. C. & DiPersio, J. F. Cytokines and hematopoietic stem cell mobilization. *Journal of Cellular Biochemistry* **99**, 690–705 (2006).
31. Conboy, M. J., Conboy, I. M. & Rando, T. A. Heterochronic parabiosis: Historical perspective and methodological considerations for studies of aging and longevity. *Aging Cell* vol. 12 525–530 (2013).
32. Carlson, M. E. *et al.* Relative roles of TGF-β1 and Wnt in the systemic regulation and aging of satellite cell responses. *Aging Cell* **8**, 676–689 (2009).
33. Carlson, M. E., Hsu, M. & Conboy, I. M. Imbalance between pSmad3 and Notch induces CDK inhibitors in old muscle stem cells. *Nature* **454**, 528–532 (2008).
34. Mehdipour, M. *et al.* Rejuvenation of brain, liver and muscle by simultaneous pharmacological modulation of two signaling determinants, that change in opposite directions with age. *Aging* **11**, 5628–5645 (2019).
35. Tsai, H.-M. Current Concepts in Thrombotic Thrombocytopenic Purpura. *Annual Review of Medicine* **57**, 419–436 (2006).
36. von Baeyer, H. Plasmapheresis in Immune Hematology: Review of Clinical OutcomeData with Respect to Evidence-Based Medicine and Clinical Experience. *Therapeutic Apheresis and Dialysis* **7**, 127–140 (2003).

Chapter 1: Rejuvenation of Multiple Tissues by Plasma Dilution

Heterochronic parabiosis was shown to rejuvenate several tissues in aged mice at some expense to the young partner[1–3]. Young blood plasma, its fractions, and its soluble factors were largely credited for the beneficial effects for parabiosis or heterochronic blood sharing. It was however, not established whether young blood is necessary for multi-tissue rejuvenation[4]. The small animal blood exchange procedure was subsequently used to replace half of the plasma with a "neutral-aged" physiological solution comprised of saline (0.9% sodium chloride) and 5% mouse serum albumin (MSA). Termed as neutral blood exchange (NBE), this system was used to dilute plasma factors while being replenished with the albumin that would otherwise be diminished if saline alone were used. A single session of NBE was shown to rejuvenate the efficiency of muscle repair, to reduce the extent of fibrosis and adiposity in the liver, and to significantly boost hippocampal neurogenesis in aged mice [4]. A pilot study was also performed using a similar FDA-approved procedure known as therapeutic plasma exchange (TPE). During TPE, intravenous catheters are connected to each of the patient's arms. Blood is drawn from the patient and is spun through a cell separation module where plasma is separated by either filtration or centrifugation[5–7]. The concentrated blood cells are simultaneously reconstituted with a solution that consists of 5% human serum albumin, normal saline, and other relevant physiological salts and metabolites[6]. This reconstituted blood mixture is then returned to the patient. Of note, the patients' own blood cells are returned to their bodies. Comparative proteomic analysis on serum from mice receiving NBE and from aged human serum obtained before and after TPE revealed a molecular resetting of signaling molecules in the systemic milieu[4]. Interestingly, numerous factors that were elevated after acute plasma dilution are chiefly responsible for coordinating healthy tissue maintenance and repair as well as modulating immune responses. TPE has also demonstrated functional blood rejuvenation, as evident by a myoblast proliferation assay[4]. Here, myoblasts in culture were treated with pre- or post-TPE serum and pulsed with bromodeoxyuridine (BrdU). Post-TPE serum treated myoblasts proliferated to a significantly greater extent than those who were treated with pre-TPE serum[4]. Ectopically added albumin does not appear to be the only determinant of rejuvenation and the levels of albumin are not altered by the NBE process. Based on these data, the hypothesize is that the dilution of systemic autoregulatory proteins that crosstalk to multiple signaling pathways has long-lasting effects on gene expression. This work improves our understanding of systemic aging and introduces a novel paradigm that not young blood factors, but plasma dilution is sufficient to broadly rejuvenated aged mammals.

The assumption of the addition of young factors being needed for rejuvenation with respect to heterochronic parabiosis and blood exchange has remained unconfirmed. To address this, we performed NBE by replacing platelet-rich-plasma (PRP) with a solution containing saline and 5% mouse serum albumin. 50% of the PRP of old and young mice was replaced with this physiological solution along with age-matched red and white blood cells being returned to each animal. We hypothesized that an acute and large dilution of age-accumulated plasma factors rapidly and robustly rejuvenates the maintenance and repair of tissues such as muscle and brain, and that young blood factors are not essential for rejuvenation. The studies of blood dilution are not feasible with parabiosis or plasma injections, as described in **Table 1**.

Repeated infusions of young mouse plasma or plasma from aged mice that underwent physical

exercise were reported to have rejuvenating properties on the brain[3,8,9]. Interestingly, 50/50 blood exchange of old mice with young blood failed to promote such a rejuvenation[10]. The differences between plasma injections and blood exchange are many, including the relatively small contribution of ectopic factors to endogenous systemic milieu in the injection approach and the fact that the factors injected through the tail vein collect in the liver and the metabolized by-products is the main differential effect[11]. In contrast, the effect of plasmapheresis through the jugular vein are truly systemic. Additionally, in plasmapheresis, there is no repeated animal handling that is typical for the cycles of plasma injections. Hence, the stress of repeated handling is reduced and the environmental differences between experimental cohorts are minimized in plasmapheresis, as compared to plasma infusions. **Table 1** illustrates key methodological differences between parabiosis, blood exchange, and plasma infusions.

Table 1

Experimental Parameter	Parabiosis	Plasma Infusions	Blood Exchange
Stress, environmental enrichment and exercise	+	+/- (repeated animal handling)	–
Shared organs	+	–	–
Blood cell sharing	+	–	+/- (as desired)
Maintaining precise control over how much blood is exchanged	–	–	+
Exchange amounts of blood exceeding 50%	–	–	+
Ability to mix designer blood solutions for exchange	–	–	+
Risk of parabiotic disease (Epigenetic mismatching)	+	+/- (might manifest with repeated infusions)	–
Concentrated in the liver	–	+	–

(+) indicates that the respective approach exhibits these characteristics and (–) indicates the opposite

To test our hypotheses under these considerations, young (2 – 4-month-old) and old (22 – 24-month-old) male mice underwent NBE. Isochronic blood exchanges comprised of young – young (YY) and old – old (OO) mice were performed[4,10]. Subsequent analysis of muscle regeneration, liver health, hippocampal neurogenesis, and blood proteomics were then performed 6 days after NBE. State the IACUC approval and ethical treatment of animals throughout this chapter, as appropriate.

Jugular vein cannulation surgeries and subsequent blood exchanges were performed as follows:

Mice were pre-anesthetized with buprenorphine and anesthetized with isofluorane oxygen to complete relaxation on a heating pad. Ophthalmic ointment was applied to each eye to precent drying[10]. The mouse was placed supine underneath a dissection microscope. The area of incision, which is just to the right of the midline, was shaven and cleaned with alternating scrubs of betadine and alcohol wipes. A vertical 1 cm incision was made in the shaven area and the right internal jugular vein was isolated by trimming the surrounding fat and fascia. 2, 4 cm pieces of 6 – 0 sutures were passed directly beneath the right internal jugular vein. Sutures were separated; one to the cranial end of the vein and the other to the caudal end. The cranial suture was

tightened to restrict blood blow while the caudal suture was loosely tightened to allow for catheter passage. A venotomy was performed with a 23G needle whose beveled end was bent 90º outward. A catheter pre-loaded with heparin flush solution was then carefully inserted into the vein. Catheter patency was ensured by flushing the saline through the line multiple times. The catheter was then anchored with a third 4 cm 6 – 0 suture at the cranial end. The mouse was then moved to a lateral decubitus position (lying on its left side). A pair of forceps was inserted through the incision site while bluntly dissecting space underneath the skin. An 18G needle was passed through the skin between the scapulae and the catheter was fed through the lumen of the 18G needle. Wound clips were then used to close the incision site and durmabond was used to secure the catheter in place. The mice were placed in their cages individually and were allowed to rest for a few hours. **Figure 1** illustrates what is mentioned above.

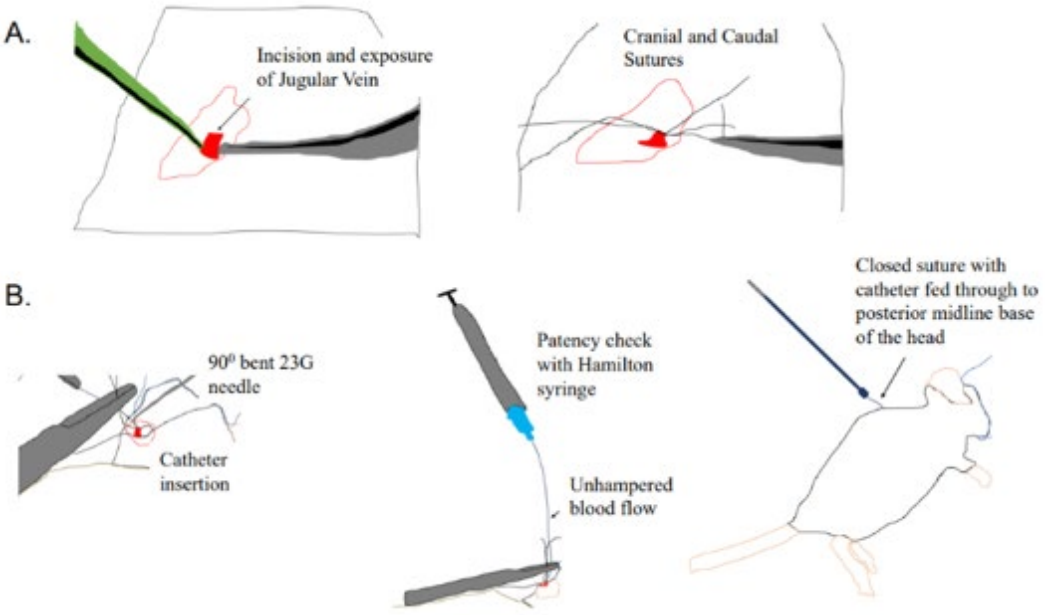

Figure 1: Major stages of jugular vein cannulation procedure (tracing of the photographs). A) Left: Initial incision site for right jugular vein cannulation and exposure of jugular vein, ensuring posterior side of the vein is well exposure and free of fatty or connective tissues; **Right:** Placement of initial two suture for top and bottom knots to be tied around the jugular vein; top knot is tied tightly to occlude blood flow and bottom knot is loosely tied until post catheter insertion. **B) Left:** Puncture of the jugular vein was created with a 23g needle with its tip bent to a 90° angle. Catheter was inserted through puncture and into vessel towards right atrium; **Middle:** Once the catheter is placed, a patency check is performed using a heparin loaded Hamilton syringe. The syringe is pushed and pulled for forward and backward flow to ensure no occlusions in the catheter. **Right:** Blunt dissection from the incision to the posterior midline of the base of the skull allows for feeding the catheter through the back.

The 5% MSA + saline solution was prepared while the cannulated mice were resting. To prepare the physiological solution comprised of 5% mouse serum albumin in saline, donor mice were anesthetized until they were completely relaxed. Once anesthetized, blood was drawn through cardiac puncture into a 3 mL hypodermic needle that was prefilled with 10 units of heparin. Occasional inversion of the syringe occurred to encourage mixing of the heparin with the blood to prevent clotting. The extracted donor blood was passed through a FACS tube to remove blood

clots and the total volume acquired was recorded. Blood samples were centrifuged at 400g for 5 minutes. The plasma fraction was decanted, and sterile saline was applied to rinse the remaining blood cells. Samples were centrifuged once again at the indicated speed and time to remove the saline. The albumin-saline solution was then added at volumes that were identical to the volumes of plasma fractions that were initially removed. Blood cells were then reconstituted in the albumin-saline solution.

Blood exchanges were performed using a syringe and Y-coupler as shown in **Figure 2**.

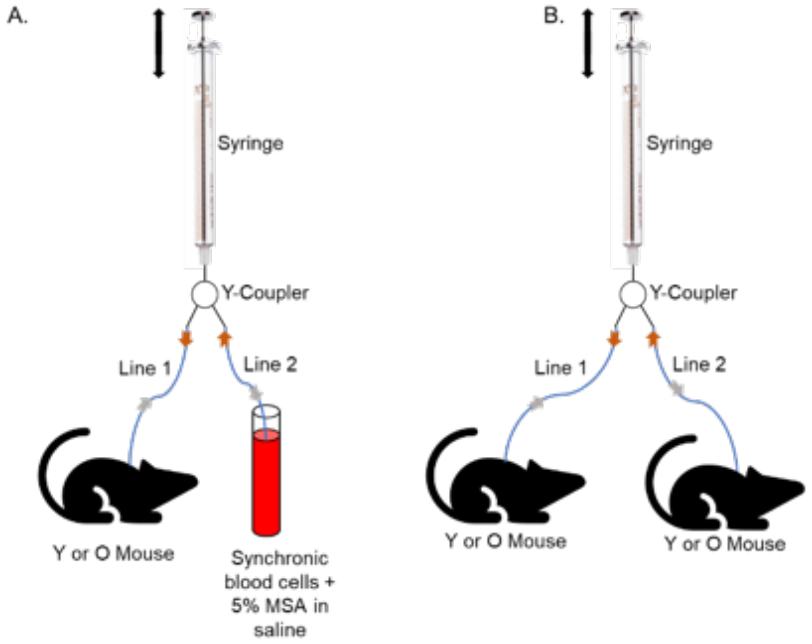

Figure 2. Blood exchanges using the Y-coupler and syringe method. Young (2-4 months of age) or old (18-24 months of age) mice or a tube containing a designer blood solution are connected to a Y-coupler. The experimenter draws blood using the syringe. Lines 1 and 2 are occluded in an alternating fashion to draw or inject blood volumes between exchange partners. **A)** depicts blood exchanges between a young (Y) or old (O) mouse and a tube consisting of age-matched donor blood cells, 5% mouse serum albumin (MSA) in 0.9% sodium chloride (saline). **B)** Blood exchanges between mice of the indicated ages.

The cannulated mice were placed under anesthesia once more for blood exchanges. Anesthetized mice are placed on a heating pad and connected to the Y-coupler/syringe apparatus as shown in **Figure 2**. Mice will be cannulated in their right jugular veins and connected to a Y-coupler and a syringe. Line 2 will be occluded by a hemostat clamp and 150 µL of blood will be drawn from the mouse through Line 1. Line 1 will then be occluded and the 150 µL of blood will be transferred to a collection tube through Line 2. While Line 1 is still occluded, Line 2 will then be submerged in a tube that contains a mixture of 5% MSA, saline, and synchronic blood cells. 150 µL of blood from this tube is drawn and then injected back into the mouse after Line 1 is opened and Line 2 is occluded. These steps result in one full exchange and will be repeated 14 times. This will ensure that ~50% of blood is either replaced with the designer blood solution or exchanged between each mouse partner. The following day after exchange, the mice received experimental cardiotoxin injections to injure their tibialis anterior muscles as performed

previously[1,10,12,13]. The mice were then sacrificed 5 days post injury and their tissues were harvested for analysis.

Muscle repair was assayed by the extent of fibrosis and formation of new myofibers that were present within injury sites by hematoxylin and eosin (H&E) staining. The minimum Feret diameter of newly formed embryonic myosin heavy chain-positive (eMyHC+) muscle fibers was quantified as published previously[1,4,10,12,14]. Just as previously published, YY muscles regenerated far better than OO[1,4,13,14]. NBE improved muscle regeneration, reduced fibrosis, and increased the minimum Feret diameter of de-novo myofibers in aged animals to the point of no significant difference with the YY cohort while NBE did not worsen these aspects of muscle repair (**Figure 3A, 3B**)[4].

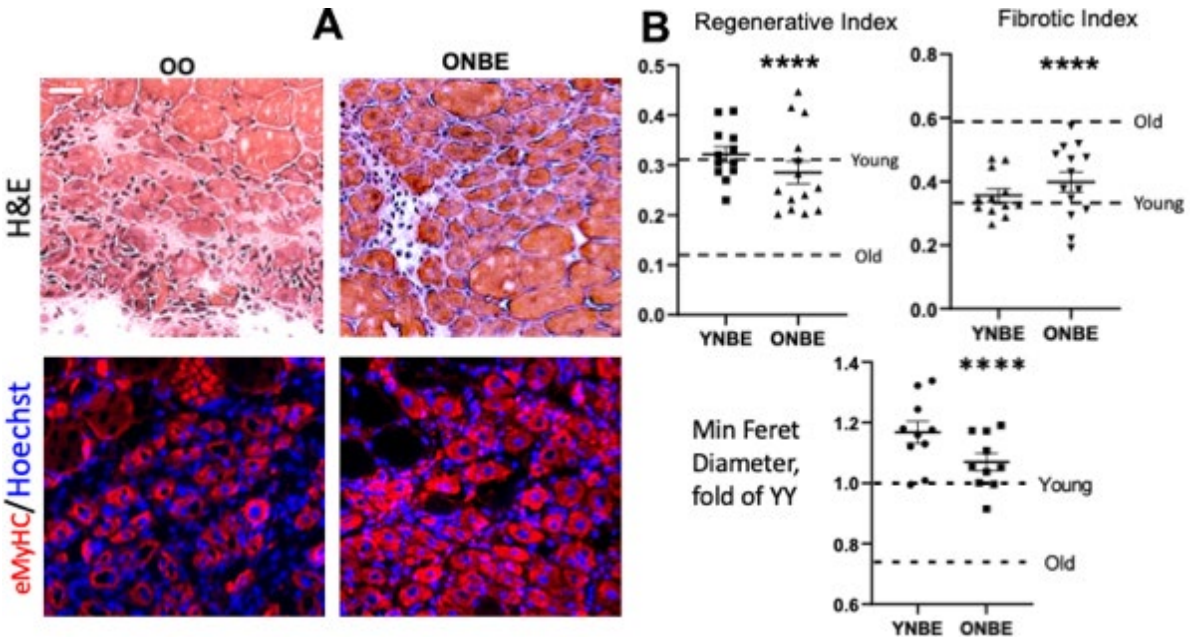

Figure 3. Rejuvenation of adult myogenesis by NBE. H&E staining and eMyHC immunofluorescence (IF) were performed on 10 µm thick cryosections. **A)** Representative images of H&E and eMyHC IF at the injury site depicting centrally nucleated nascent myofibers that are characteristically present 5 days post injury. Scale bar = 50 µm. **B)** Regeneration index: the number of centrally nucleated myofibers per total nuclei. OO vs. ONBE p = 0.000001, YY vs ONBE non-significant p = 0.4014; Fibrotic index: white devoid of myofibers areas. OO vs ONBE p = 0.000048, YY vs YNBE non-significant p = 0.1712. Minimal Feret diameter of eMyHC+ myofibers is normalized to the mean of YY[10]. OO vs. ONBE p= 3.04346E-05, YY vs. YNBE p=0.009. Data-points are TA injury sites of 4-5 YNBE and 5 ONBE animals. This figure was adapted from Mehdipour et al. 2020[4] where co-author Cameron Kato provided the eMyHC images and the minimal Feret diameter data. Camron Cato (UCB/UCSF Graduate group, Conboy lab GSR) contributed the data on H&E and Min Feret Diameter with corresponding panels of Figure 3. Please see corresponding *Excel Sheets 1 – 3* in *Chapter 1 Appendix* for reference of primary data.

Myoblast proliferation has not changed significantly at any concentration of HSA added and Western blotting confirmed that there is not net gain or loss of albumin in NBE/TPE but rather back supplementation of the procedure depleted serum albumin[4]. Antioxidant activity of sera pre-TPE versus post-TPE did not have any significant differences between these cohorts[4].

Collectively, these results establish that NBE has profoundly positive effects on myogenesis, but ectopic albumin does not appear to be the sole cause of these.

We also analyzed the extent of hippocampal neurogenesis in the subgranular zone (SGZ). Neurogenesis in the SGZ continues throughout adult life and declines with advanced age. It is also influenced by blood heterochronicity[10,14–16]. To assay the effects of NBE on neurogenesis in the SGZ, proliferation of neural stem cells within the SGZ were quantified. This was done by performing immunofluorescence against the proliferation marker Ki67 in cryosections of mouse brains (**Figure 4A**). The number of Ki67+ cells were quantified and extrapolated per hippocampus analyzed. YY mice had approximately 10-fold higher numbers of Ki67+ cells in the SGZ when compared to those of OO, as expected[10,13,16]. There was also an ~8-fold increase in hippocampal neurogenesis in aged mice after NBE with no significant reductions in hippocampal neurogenesis in young mice receiving NBE (**Figure 4B**)[4].

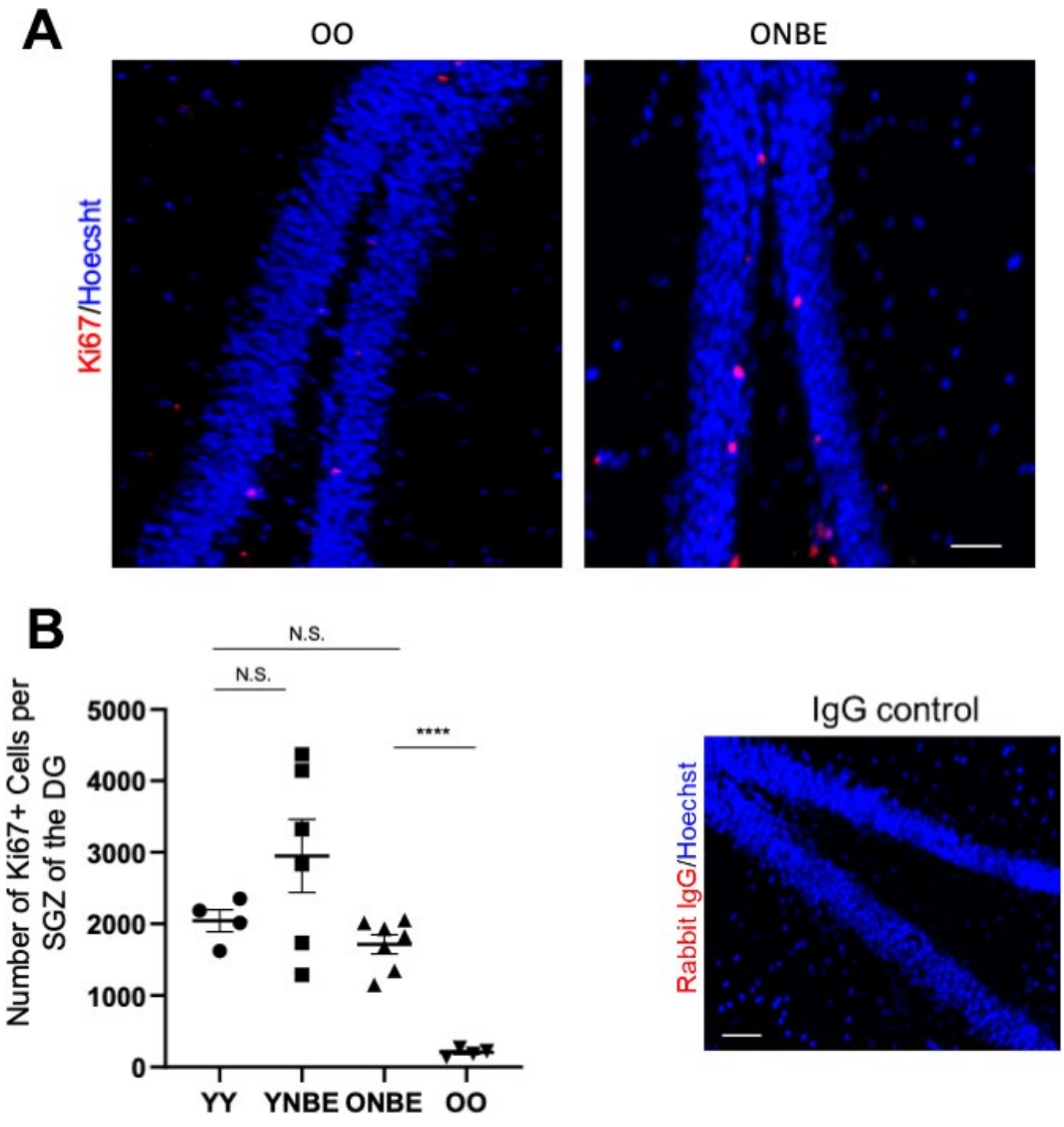

Figure 4. NBE of aged mice is significantly enhanced after NBE. A) Immunofluorescence was performed to assay for proliferative Ki67-positive cells in the subgranular zone (SGZ) of the dentate gyrus (DG). Representative images of Ki67(red)+/Hoechst (blue)+ cells in the DG are shown for OO and ONBE mice. **B)** Quantification of the number of Ki67+/Hoechst+ cells per SGZ of the DG (extrapolated from serial sections that span the entire hippocampus). ONBE mice have a ~8-fold increase in the number of these cells when compared to OO (****p-value = 0.0000145). The number of these proliferating neural precursor cells in the SGZ of YY mice is not significantly different from that of ONBE mice (N.S. p-value = 0.15235). A trend for ~44% increase in YNBE mice as compared to the YY mice, is not statistically significant (N.S. = 0.20123). Isotype-matched IgG negative control confirms low non-specific fluorescence. N=4 for YY and OO, N=6 for YNBE and N=7 for ONBE. Scale bar is 50-micron. These data demonstrate that hippocampal neurogenesis improves in old mice after just one NBE, e.g. without young blood or its fractions, and that young mice do not decline in this parameter when their blood plasma is diluted through the NBE. This figure was adapted from Mehdipour et al. 2020[4]. Please see corresponding *Excel Sheet 4* in *Chapter 1 Appendix* for reference of primary data.

This increase was larger than what was observed in heterochronic parabiosis or through the pharmacological modulation of the oxytocin and TGFβ pathways[2–4,14]. Nuclear localization of Ki67 was confirmed and non-specific immunofluorescence of isotype-matched IgG controls was found to be negligible[4]. These results were also corroborated with a BrdU proliferation assay which demonstrated that neurogenesis is enhanced upon the addition of ectopic albumin[4]. Even though this may contrast with what was found in myogenesis, these neural precursor cell proliferation results agree with previously published enhancements of retinal precursor cell proliferation by albumin[17] and with the increased efficiency of proliferation of human iPSC-derived neural precursor cells on electrospun serum albumin fibrous scaffolds[18].

A body of published work appears to consistently demonstrate that albumin can be a negative factor for brain health. These studies maintain that the blood brain barrier may become leaky with age[19,20]. Serum albumin was proposed to cross the blood brain barrier and it is found in the cerebrospinal fluid of older individuals in a positive correlation with age and certain dementias[21]. Direct infusions of albumin into the brain also caused neuro-inflammation and neuronal dysfunction through excessive TGFβ signaling[22]. In our work, the total levels of albumin are replenished rather than being diminished by NBE/TPE; thus, these negative effects on the brain were not anticipated[4].

In studies of liver health, as per the typical Conboy lab approaches[4,10], diluting old blood plasma with 5% MSA-saline diminishes adiposity and fibrosis of the aged livers and did not appear to have negative effects on the young livers[4].

The above findings are consistent with the conclusion that age-altered systemic factors inhibit the health and regeneration of multiple tissues in aged mice. Aged serum also appears to exert a dominant anti-regenerative effect on young partners in parabiosis and blood exchange[1–4,15,23–25].

To elucidate the molecular mechanisms for these broad and profound rejuvenative phenotypes, the scientists of the Conboy lab performed proteomics analysis on the samples of mouse and human blood serum and analyzed the data through heatmaps, t-SNE plots and mathematical simulations[4,26]. Even though serum was diluted by NBE/TPE, many proteins were upregulated, suggesting that their production and/or secretion was inhibited by age-elevated systemic factors, many of which regulate canonical signaling pathways and change with age in ways that are

counterproductive for tissue maintenance and repair[4,26].

Collectively, my PhD work synergistically with the findings of other scientists of the Conboy laboratory shifts the paradigm from the dominance of young factors and maintains that replacing a large volume of old blood plasma with 5% MSA in saline is sufficient for most, if not all the observed positive effects on muscle, liver, brain[4]. It also suggests the possibility of repositioning TPE for attenuating and possibly reversing the degenerative and metabolic diseases of old age.

Materials and Methods

Animals. Young (2-4 months old) and aged (18-22 months old) male C57BL/6 mice were purchased from Jackson Laboratory and the National Institute of Aging, respectively. All *in vivo* experiments and procedures were performed at the Northwest Animal Facility at the University of California, Berkeley in accordance with the policies maintained by the Office of Laboratory and Animal Care, who approved all relevant protocols.

Jugular Vein Cannulation Surgeries. Mice were administered a pre-operative dose of 0.1 mg/kg Buprenorphine subcutaneously. The mice were anesthetized with isoflurane at 0.5 – 1L/min until complete relaxation. Ophthalmic ointment was applied to each eye to prevent drying. Areas of incision were shaved with a hair trimmer and cleaned with 3 alternating scrubs of betadyne and alcohol swabs. The mouse is placed in dorsal recumbency under anesthesia on top of a heating pad set to 25ºC. Once a lack of response to toe pinch is confirmed, a 1 cm incision is made to the right of the midline. Fat and fascia are carefully trimmed with dissecting forceps (Millipore Sigma, Darmstadt, Germany) and microdissection scissors (Bio Corporation, USA) to expose the right internal jugular vein. Two silk 6 – 0 sutures are fitted underneath the vein. One suture on the cranial end is ligated tightly to impede blood flow. The caudal suture is loosely ligated. Gentle tension is applied to the vein by carefully pulling the cranial sutures taut with hemostat clamps (Global Industrial, USA). A venotomy is performed using a 23-gauge needle whose beveled end is bent 90º outward. The 1 French end of a 1 – 3 French heparinized catheter (100 U heparin/mL, Instech Labs C10PU-MJV1403) which is plugged at the 3 French end with a 22-gauge metal plug (Instech Labs, Part No. SP22/12) is inserted into the vein, and the caudal ligature is tightened. A second cranial ligature is added to secure the catheter in place. Catheter patency is confirmed by flushing the catheter with approximately 20 μL of 100 U/mL heparin by using a Hamilton syringe (Grainger, USA). Once patency has been confirmed, the catheter is plugged. The mouse is rotated to lay on its left side and blunt dissecting forceps (Millipore Sigma, Darmstadt, Germany) are used to create space underneath the skin toward the midpoint between the scapulae. An 18-gauge needle is inserted through the skin and extended toward the incision site. The plugged 3 French end is fed into the 18-guage needle and pulled through the skin at the posterior midline base of the head. Wound clips (CellPoint Scientific, Gaithersburg, USA) are used to close the incision site and Durmabond is applied to the exit point on the mouse's back. The mouse is taken off anesthesia and given Meloxicam at 5 mg/kg subcutaneously. Subcutaneous injections of Meloxicam continue daily for two additional days

post-op. The mouse is then placed in a single-housed cage and allowed to recover.

Preparation of the designer blood solution for NBEs. Red blood cells (RBCs) and peripheral blood mononuclear cells (PBMCs) were obtained from donor C57BL/6 mice to prevent blood cell depletion during NBE. Donor mice were anesthetized and their blood was collected by cardiac puncture with 3 mL hypodermic needles (Bowers Medical Supply) preloaded with 10 units of heparin (Sagent Pharmaceuticals, USA). The blood was then placed into 1.5 mL Eppendorf tubes and centrifuged for 5 min at 400 g. The plasma fraction was decanted and the blood cell pellets were reconstituted in enough normal saline (0.9% sodium chloride) to fill the Eppendorf tube). Blood samples were spun once again at 400 g for 5 minutes and the saline fraction was decanted. Blood cells pellets were now resuspended in a solution comprised of 5% mouse serum albumin (Innovative Research, USA) and normal saline. Volumes of the reconstituting albumin-saline solutions were equal to the volumes of the blood cell pellets. These blood mixtures were passed through the 50 μm mesh of FACS tubes to de-clump the cells and to filter any clots.

Blood exchanges. A 1 mL syringe with a 22-gauge leur stub (Instech Labs, Part No. LS22) connected to a 22-gauge Y-coupler (Instech Labs, Part No. SCY22) by 1 cm of 22-gauge tubing (Instech Labs, Part No. BTPE-50). 3 cm of 22-gauge tubing is attached to the other ends of the Y-coupler. A metal tubing coupler (Instech Labs, Part No. SC22/8) is fitted into the lumen of one of the 3 cm 22-gauge tubes. The Y-coupler apparatus is sterilized by drawing 10% bleach into lumen of the tubing. The bleach is discarded and replaced with 70% ethanol. Once the ethanol was discarded, the tubing is rinsed with sterile saline 3 times. Heparin saline (100 U/mL) is drawn into the lines. A lariat is formed to close the lines against each other, and the heparin is left to coat the tubing lumen for at least 1 hour at room temperature. Cannulated mice are anesthetized, placed on the heating pad in ventral recumbency, and ophthalmic ointment was applied as noted above. Connect the mouse to one end of the Y-coupler (Line 1) and connect the other end to a tube containing the designer blood solution (Line 2). A hemostat clamp was used to occlude Line 1 and 150 μL of blood was drawn from the non-occluded Line 2. Once the desired volume is reached, occlude Line 2 and then inject the blood into the mouse through Line 1. These mark 1 exchange, and each cycle was repeated 14 more times in order to attain ~50% blood exchanged. The mice were then disconnected from the Y-coupler and allowed to recover in their cages.

Experimental muscle injury. Tibialis anterior (TA) muscles of mice were injured by intramuscular injections of cardiotoxin (CTX; Sigma Aldrich), where 10 μL of CTX were injected per TA at 0.1 μL/mL. TA's were harvested five days post injury.

Tissue isolation. Mice were sacrificed in accordance with the guidelines of UC Berkeley's Office of Laboratory Animal Care (OLAC). Postmortem isolation of muscle and brain were performed where tissues were embedded in Tissue-Tek Optimal Cutting Temperature (OCT; Sakura Fintek, The Netherlands) and snap frozen in isopentane cooled to -70^{o} C with dry ice.

Tissue sectioning. OCT-embedded tissues were sectioned with a cryostat. Muscle was sectioned

to 10 μm thickness while coronal sections of the brain were obtained at 25 μm. Tissue sections were attached to gold-supplemented positively charged glass coverslip slides in preparation for immunofluorescence or histological analysis.

Hematoxylin and eosin staining. H&E staining was performed as previously published[4,10,14]: slides with mounted muscle sections were dehydrated in 70% ethanol 3 min and then placed in 95% ethanol for 30 seconds. Tissues were rehydrated in deionized water for 1 min, and then placed in hematoxylin for 5 min. Slides were then placed in 1X Scott's water for 1 min. Slides were rinsed in water for 1 min, treated with eosin for 4 min, and then rinsed in water again for 30 seconds. A final dehydration series of 70%, 95%, 99%, and 100% ethanol was performed for 1 min at each concentration. Slides were washed with xylenes twice, at 1 min per rinse. 2 drops of 50% resin/50% xylenes mounting medium were added to each slide and glass coverslips were placed. Injury sites were imaged accordingly.

Antibodies and labeling reagents. The following antibodies were diluted to 0.5 – 1 μg/mL:

- **Embryonic Myosin heavy Chain:** F1.652 clone, Developmental Studies Hybridoma Bank, University of Iowa, deposited by Blau, HM), 1:100
- **Ki67:** Abcam, Rabbit, ab16667, 1:200
- **Isotype-matched IgG's:** Sigma Aldrich, Mouse and Rabbit, 1:500 and 1:1000 respectively
- **Donkey anti-mouse Alexa 488:** Life Technologies, Invitrogen, Eugene, Oregon, A21202, lot #1975519, 1:2000
- **Donkey anti-rabbit Alexa 546:** Life Technologies, Invitrogen, Eugene, Oregon, A10040, lot #1946340, 1:2000
- **Hoechst dye for DNA staining:** Hoechst 33342, Sigma Aldrich (B2261), 1:1000

Tissue section immunofluorescence. Immunofluorescence was performed on tissue sections that were mounted on positively charged Gold Super Frost slides.

- **Muscle:** 10 μm-thick sections were blocked in 1% staining buffer (1% calf serum in 1X PBS) for 45 minutes at room temperature without fixation or permeabilization. Sections were coated in primary antibodies and incubated at 4° C overnight. The following day, the slides were rinsed in staining buffer and then coated in secondary antibodies for 2 hours at room temperature.
- **Brain:** 25 μm-thick brain sections were fixed with 4% paraformaldehyde (PFA) for 4 minutes in the dark at room temperature. The sections were washed in excess 1X phosphate buffered saline (PBS) and then permeabilized with 0.1% Triton X-100 for an additional 5 minutes over ice. Samples were washed thoroughly with 1X PBS and blocked in 1% staining buffer for 45 minutes at room temperature. The brain sections were incubated with primary antibodies overnight at 4° C. Sections were washed three times with staining buffer and coated with secondary antibodies the following day.

- 2 drops of Fluoromount (Sigma F4680) mounting media were added and coverslips were placed on each slide after a final staining buffer wash proceeding secondary antibody and Hoechst incubation. Images were obtained using a Zeiss Axioscope fluorescent microscope
- ***Data quantification and statistics.*** Data was analyzed using the Student's two-tailed t-test where p-values lower than 0.05 were considered statistically significant. Samples sizes of n=4 or larger were determined for each experiment based on power analysis.

Tissue histology and immunofluorescence. Muscle regeneration indices were calculated by counting the fractions of centrally nucleated de-novo myofibers relative to the total nuclei in 2-4 representative images per muscle section in each cohort. Muscle fibrosis was quantified by measuring areas of fibrosis within muscle injury sties. These obtained fibrotic areas were normalized to the total area of the injury site. Neurogenesis was quantified by counting the number of Ki67+/Hoechst+ cells in 200 microns of the subgranular zone. Non-paired two-tailed t-tests were performed in Microsoft Excel for all tissue analysis data.

Chapter 1 Appendix

H&E Regenerative Index Excel Sheets (Excel 1)

Young mice exchanged with young blood							**Ave**	**SE**	**P-value**			
YY-m55	237	575	0.412174			**YY**	0.353941	0.025444	0.191657	0.405241		
YY-m68	129	418	0.308612			**YNBE**	0.322365	0.024438		N.S.		0.444676
YY-m105	120	315	0.380952			**OO**	0.165723	0.008286			*	
YY-m116	103	328	0.314024			**ONBE**	0.282839	0.038657	N.S.		0.033627	N.S.
		Ave RI	**0.353941**									
						YY	**Y TPE**	**O TPE**	**OO**			
Old mice exchanged with old blood						0.412174	0.378577	0.243364	0.160584			
OO-m91	44	274	0.160584			0.308612	0.307917	0.422678	0.156584			
OO-m92	44	281	0.156584			0.380952	0.263235	0.30944	0.155367			
OO-m43	55	354	0.155367			0.314024	0.339731	0.217574	0.190355			
OO-m31	75	394	0.190355					0.22114				
		Ave RI	**0.165723**									
Old mice treated with neutral blood exchange												
	Image ID	**New Myf**	**Total Nuc**	**RI**			**Image ID**	**New Myf**	**Total Nuc**	**RI**		
O2 S1	443	61	256	0.238281		O3 S1	454	173	406	0.426108		
	444	95	290	0.327586			455	125	252	0.496032		
	445	81	270	0.3			456	110	264	0.416667		
	446	86	328	0.262195			457	127	365	0.347945		
	Sum	323	1144	0.282343			Sum	535	1287	0.415695		
O2 S2	447	80	297	0.26936		O3 S2	458	147	304	0.483553		
	448	86	252	0.34127			459	112	314	0.356688		
	449	96	293	0.327645			460	94	191	0.492147		
	Sum	262	842	0.311164			461	175	373	0.469169		
							Sum	528	1182	0.446701		
O2 S3	450	135	375	0.36								
	451	100	295	0.338983		O3 S3	462	133	333	0.399399		
	452	89	309	0.288026			463	135	300	0.45		
	453	125	362	0.345304			464	110	322	0.341615		
	Sum	449	1341	0.334825			465	140	322	0.434783		
							Sum	518	1277	0.405638		
O2 Mean	0.309444											
						O3 Mean	0.422678					
	Image ID	**New Myf**	**Total Nuc**	**RI**			**Image ID**	**New Myf**	**Total Nuc**	**RI**		
O4 S1	480	64	279	0.229391		O5 S1	57	113	470	0.240426		
	481	58	247	0.234818			58	91	505	0.180198		
	Sum	122	526	0.231939			Sum	204	975	0.209231		
O4 S2	482	74	284	0.260563		O5 S2	59	84	414	0.202899		
	483	59	238	0.247899			Sum	84	414	0.202899		
	Sum	133	522	0.254789								
							61	114	471	0.242038		
O4 mean	0.243364					O5 S3	62	97	406	0.238916		
							Sum	211	877	0.240593		
						O5 Mean	0.217574					
		Image ID	**New Myf**	**Total Nuc**	**RI**							
	O7 S1	63	74	297	0.249158							
		Sum	74	297	0.249158							
	O7 S2	65	43	203	0.211823							
		Sum	43	203	0.211823							
			66	100	465	0.215054						
	O7 S3	67	66	355	0.185915							
		Sum	166	820	0.202439							
	O7 Mean	0.22114										

Young mice treated with neutral blood exchange										
	Image ID	**New Myf**	**Total Nuc**	**RI**			**Image ID**	**New Myf**	**Total Nuc**	**RI**
Y3 S1	484	99	325	0.304615		Y1 S1	490	136	392	0.346939
	485	84	313	0.268371			491	118	400	0.295
	Sum	183	638	0.286834			Sum	254	792	0.320707
Y3 S2	486	124	388	0.319588		Y1 S2	492	123	325	0.378462
	487	73	259	0.281853			493	140	319	0.438871
	Sum	197	647	0.304482			Sum	263	644	0.408385
Y3 S3	488	110	376	0.292553		Y1 S3	494	164	381	0.430446
	489	137	367	0.373297			495	130	342	0.380117
	Sum	247	743	0.332436			Sum	294	723	0.406639
Y3 mean	0.307917					Y1 mean	0.378577			
	Image ID	**New Myf**	**Total Nuc**	**RI**			**Image ID**	**New Myf**	**Total Nuc**	**RI**
Y5 S1	38	147	543	0.270718		Y4 S1	50	115	379	0.30343
	39	131	605	0.216529			51	115	374	0.307487
	40	109	541	0.201479			Sum	230	753	0.305445
	41	100	426	0.234742						
	Sum	487	2115	0.23026			52	137	381	0.35958
						Y4 S2	Sum	137	381	0.35958
Y5 S2	42	118	459	0.257081						
	43	162	527	0.3074		Y4 S3	53	136	384	0.354167
	44	85	373	0.227882			54	139	391	0.355499
	45	153	431	0.354988			Sum	275	775	0.354167
	Sum	518	1790	0.289385						
						Y4 Mean	0.339731			
Y5 S3	46	99	383	0.258486						
	47	115	430	0.267442						
	48	134	397	0.337531						
	49	103	460	0.223913						
	Sum	451	1670	0.27006						
Y5 Mean	0.263235									

H&E Fibrotic Index Excel Sheets (Excel 2)

Young – Young Isochronic Exchange

Sample ID in Bold Red Text										
Non-injury site area (smaller value) and Total image area (larger value)										
Area of injury sire (difference between yellow highlighted values										
Computed total fibrosis area										
Fibrosis Index: ratio of computed fibrosis area and area of injury site										
YY-m55										
1	385429	130.045	0	255	1	128594	113.397	6	255	3406936
2	66094	98.917	0	255						
3	21268	136.145	0	255		3278342				
4	53704	173.912	25	247						
5	25664	183.951	34	255						
6	31106	162.784	5	255						
7	51570	123.116	6	255						
	634835									
0.193645141										
YY-m68										
1	362404	106.126	29	231	1	231486	102.628	23	223	3348810
2	56215	114.158	28	215	2	86194	110.916	31	222	
3	190951	109.211	28	223	3	19566	107.665	34	204	
4	470700	121.691	31	231		337246				
5	21250	121.69	38	208						
	1101520					3348810				
0.328928784										
YY-m105										
1	657243	138.058	0	255	1	278499	113.308	2	255	3404804
2	39455	131.158	0	255						
3	61768	128.629	4	255		3126305				
4	22595	169.853	8	255						
5	104137	171.143	9	255						
6	188511	146.199	0	255						
7	42037	137.784	1	255						
	1115746									
0.356889683										
YY-m116										
1	556176	154.739	31	231	1	707016	108.085	20	236	3406936
2	528092	111.113	17	236	2	25240	106.818	24	217	
3	67450	124.198	25	221	3	32722	111.742	17	231	
4	89082	114.079	20	234	4	15483	101.981	36	218	
	1240800				5	17622	104.628	51	218	
					6	21106	115.38	55	213	
						819189				
						2587747				
0.47949046										

Old – Old Isochronic Exchange

OO-m91a												
1	235896	118.254	3	247		1	161195	105.371	2	250		3406936
2	393636	105.423	1	254		2	57441	95.752	7	244		
	629532					3	727299	105.684	2	255		
						4	38092	107.873	18	249		
						5	877559	109.977	4	255		
							1861586					
							1545350					
0.407371793												
OO-m91b												
1	1928183	132.122	0	255		1	683751	104.994	0	248		3408534
							2724783					
0.707646444												
OO-m43												
1	501345	189.115	0	255		1	271927	162.677	0	255		3408534
2	171938	198.378	0	255								
3	323179	188.52	0	255			3136607					
4	1001411	204.202	0	255								
	1997873											
		1		197.57	0	255						
0.636953562												
OO-m34												
1	1665748	149.075	0	255		1	360699	111.63	0	255		3406936
2	138970	140.183	0	255		2	143912	113.273	0	255		
	1804718						504611					
							2902325					
0.621818025												

Old Treated with Neutral Blood Exchange

O2-443													
1	17525.16	1502.527	525	2664		1	2109.039	1548.149	261	2403			147537.5
2	8738.709	1488.287	512	3149		2	2386.631	1543.258	699	2018			
3	1415.837	1499.136	469	2377			4495.67						
4	6000.017	1487.048	527	2465									
5	1613.553	1482.583	510	2445			143041.9						
6	12068.05	1518.049	556	2458									
7	3998.104	1512.479	352	2401									
	51359.43												
0.359051709													
O2-444													
1	25486.84	1531.611	607	2611		6	6689.37	1529.495	239	2263		147539.1	
2	16996.39	1518.117	714	2366									
3	2215.541	1573.883	484	2648			140849.7						
4	2545.345	1545.64	666	2368									
	47244.11												
0.335422077													
O2-445													
6	1745.641	1608.132	674	2540		1	5171.607	1757.957	546	2769		147538.1	
7	23241.97	1524.926	234	3357		2	1552.605	1688.519	521	2715			
8	6110.055	1521.129	452	2747		3	1172.982	1710.523	732	2532			
9	14803.31	1507.432	425	2579		4	20282.99	1709.983	579	3186			
10	3085.865	1548.833	756	2595			28180.18						
11	4620.062	1582.771	613	2821									
12	6956.874	1572.275	653	2486			119357.9						
	60563.78												
0.507413281													
O2-446													
1	6609.389	33829.192	0	65535		1	4513.143	40977.55	0	65535		147538.9	
2	2121.207	31198.151	0	65535		2	3072.657	44573.08	0	65535			
3	754.981	36792.115	0	65535		3	8124.552	42643.756	0	65535			
4	11145.83	34563.709	0	65535		4	2043.827	42730.351	0	65535			
5	17783.09	29767.578	0	65535		5	1397.116	38092.601	0	65535			
	38414.5					6	1089.361	44003.489	0	65535			
							20240.66						
							127298.2						
0.301767718		O2S1 Mean											
		0.375913696											
O2-447													
1	7611.073	1350.602	711	2033		1	9165.031	1316.688	678	1718		146944.9	
2	17108.3	1310.372	485	2142		2	14696.4	1262.818	182	2157			
3	9952.462	1288.22	546	1936			23861.43						
4	19972.84	1341.551	450	2404									
5	1266.588	1270.63	403	3191			123083.5						
	55911.26												
0.454254767													
O2-448													
1	25456.26	1333.475	289	2184		1	3202.976	1540.894	864	2120		147539	
2	1148.749	1355.455	684	1884		2	3010.149	1576.029	598	2030			
3	12558.34	1297.003	540	2378		3	11207.71	1542.726	686	2130			
4	14907.22	1326.276	561	1995			17420.84						
	54070.56												
							130118.2						
0.415549685													
O2-449													
1	28591.11	1333.704	568	2217		1	4120.728	1355.296	341	2014		147539.1	
2	23005.56	1327.946	454	2433		2	3516.035	1485.734	761	2063			
3	6694.362	1372.286	681	2100		3	755.085	1442.389	989	1892			
	58291.03						8391.848						
		O2 S2 Mean					139147.3						
0.418916124		0.429573525											

O2-450												
1	2978.843	1406.401	516	2069		1	7494.274	1474.562	336	1831		147539.1
2	51774	1267.582	295	2303		2	1702.27	1474.718	739	1805		
	54752.84					3	892.582	1490.75	746	1873		
						4	1946.997	1417.027	665	2303		
							12036.12					
							135503					
0.404071119												
O2-451												
1	38171.75	1324.798	410	2007		3	1591.296	1446.705	1012	1913		147539.1
2	4889.126	1374.05	622	1743		4	3704.703	1477.909	797	1836		
	43060.88					5	2995.276	1519.648	550	1857		
						6	743.333	1534.592	633	1780		
						7	2373.631	1424.268	665	1741		
						8	1486.457	1444.466	782	1751		
						9	4105.751	1466.724	676	1754		
							17000.45					
							130538.7					
0.329870678												
O2-452												
1	3162.102	1468.841	895	1847		1	5010.917	1539.994	495	2146		147539.1
2	2877.541	1443.846	865	2042		2	2052.251	1473.549	565	2469		
3	78548.74	1291.709	388	2287			7063.168					
	84588.39											
							140475.9					
0.602155702												
O2-453												
1	50703.98	1266.551	294	2263		1	28428.76	1512.077	520	2116		147538.2
1	3416.293	1402.159	520	1910								
2	2207.741	1364.362	675	1931			119109.4					
3	4150.889	1341.313	675	1931								
4	4903.479	1242.677	324	2170								
	65382.39											
0.548927098												
			O2 S3 Mean									
O2 Avg	0.425218		0.471256149									

O3-454											
1	39221.07	1251.275	200	1965		1	16424.15	1476.634	422	1981	147539
						2	1332.632	1473.453	531	1752	
						3	1508.819	1498.013	772	1789	
						4	1728.168	1357.74	397	1880	
							20993.77				
							126545.2				
0.309937144											
O3-455											
1	2258.184	1313.21	360	1892		1	48692.5	1522.167	180	1958	147455.4
2	1010.421	1390.975	801	1779		2	2355.326	1520.18	529	1776	
3	1448.911	1304.85	352	1751		3	2861.316	1399.417	321	1973	
4	2318.091	1229.531	377	2084		4	6550.626	1419.835	275	1945	
5	4071.741	1255.516	260	2061			60459.77				
6	1808.565	1316.994	554	1836							
	12915.91						86995.61				
0.14846626											
O3-456											
1	27472.42	1305.012	252	1997		1	13525.81	1508.254	435	1917	147534.5
2	4115.111	1311.727	444	2348		2	3993.944	1466.733	737	2348	
3	4281.001	1207.048	353	1795		3	2867.972	1401.433	421	2034	
	35868.53					4	1509.131	1392.858	442	2052	
						5	5063.232	1508.331	559	1750	
							26960.08				
							120574.4				
0.297480372											
O3-457											
1	43440.29	1253.422	195	2252		1	13368.55	1447.954	426	1879	147538.8
2	19190.61	1286.774	466	1907		2	3294.814	1417.069	655	1815	
3	2231.558	1146.704	195	2010			16663.36				
	64862.46										
							130875.4				
0.495604526			O3 S1 Mean								
			0.312872075								
O3-458											
1	6190.972	1178.534	309	2368		1	11519.94	1400.993	23	2639	147536.3
2	750.717	1279.588	688	1998		2	3666.636	1420.676	462	2334	
3	5856.488	1263.227	264	2328		3	7329.736	1466.876	596	2706	
4	3038.335	1360.204	562	2230		4	6601.901	1487.061	631	2347	
5	771.83	1421.428	821	2315		5	1656.716	1292.721	293	2414	
6	1000.228	1338.345	500	2200			30774.93				
	17608.57										
							116761.4				
0.150808184											
O3-459											
1	18805.37	1262.651	233	2314		1	20754.14	1439.666	318	2579	147539.1
2	4321.564	1193.562	341	2430							
3	7746.698	1257.254	291	2346			126785				
4	6324.1	1254.957	421	2504							
	37197.73										
0.293392282											
O3-460											
1	1976.327	1347.847	663	2027		1	61853.04	1446.444	132	2721	147144.3
2	2379.351	1361.573	734	2106							
3	2857.468	1299.582	216	2411			85291.26				
4	2710.403	1309.176	593	2236							
5	1380.579	1336.687	479	2232							
6	840.058	1414.529	700	2136							
	12144.19										
0.14238488											

O3-461											
2	4319.588	1307.777	387	2526		1	722.219	1231.186	474	2410	147538.5
3	5504.115	1269.365	273	2320		2	23662.36	1511.324	270	2658	
4	3477.137	1112.157	269	2125			24384.58				
5	3993.528	1181.583	267	2495							
6	2108.103	1183.773	333	2402			123153.9				
7	784.727	1274.776	366	2270							
8	1997.648	1302.528	300	2463							
	22184.85										
0.180139201			O3 S1 mean								
			0.191681137								
O3-462											
1	7559.382	1433.562	490	2313		1	9411.63	1488.417	413	2872	147536.3
2	28482.32	1323.385	322	2569		2	1180.991	1458.413	601	2277	
3	4066.02	1302.65	481	2175		3	5537.189	1548.385	665	2294	
4	2674.521	1262.374	388	2246		4	13521.96	1445.01	327	2688	
	42782.24						7412.942				
							140123.4				
0.305318429											
O3-463											
1	11183.06	1367.437	419	2598		1	4088.59	1540.266	479	2186	147538.8
2	12790.9	1375.802	475	2592		2	36091.42	1502.575	319	2552	
	23973.96					3	2786.951	1496.819	550	2226	
							42966.96				
							104571.8				
0.229258297											
O3-464											
1	32528.27	1320.084	449	2052		1	7921.844	1488.504	588	2277	147539.1
2	15777.23	1305.853	362	2204		2	3051.959	1457.345	453	2319	
	48305.5					3	7331.505	1423.632	527	2245	
							18305.31				
							129233.8				
0.37378376											
O3-465											
1	10514.82	1259.12	414	2445		1	3166.574	1538.38	415	2593	147532.5
2	24822.76	1279.669	229	2703		2	1458.896	1370.641	377	2237	
3	3477.865	1286.128	574	1818			4625.47				
	38815.45										
							142907				
0.27161336			O3 S3 Mean								
			0.294993462								
O3 Avg	0.266516										

O4-480											
1	819.569	2960.761	1526	4095		1	2649.351	3048.477	1077	4095	147538.6
2	3467.36	2884.391	972	4095		2	2874.317	2975.922	870	4095	
3	2621.27	2740.337	860	3988		3	8336.725	3143.488	1502	4095	
4	4221.406	2683.157	880	4095		4	3277.237	2863.96	1456	4095	
5	8912.712	2664.961	891	3897		5	9629.003	2985.311	773	4095	
6	987.331	2935.229	905	3688			26766.63				
	21029.65										
							120772				
0.174126918											
O4-481											
1	10362.25	2875.191	1096	4095		1	1479.177	2905.29	668	4095	147538.3
2	2655.28	3009.742	1472	3681		2	2430.418	3054.833	1585	4095	
3	1006.989	2789.214	1328	3650		3	2987.06	3058.67	853	4095	
4	4460.724	2718.511	1039	4004		4	9967.023	3136.692	703	4095	
5	268.44	2924.838	1490	3867		5	8916.664	3008.709	981	4095	
6	559.034	2716.838	1181	4095		6	5955.918	2884.275	626	4095	
7	608.957	2961.861	1541	4095		7	2729.02	2958.225	610	4095	
8	2418.249	2900.059	1128	4095			34465.28				
9	2550.857	2797.914	976	4095							
10	1321.295	2845.742	1216	4095			113073				
11	1314.015	2925.648	1490	4095							
12	302.97	3123.381	2108	4095							
13	1848.919	2855.795	1015	4095							
14	401.36	2983.608	1852	3922							
	30079.34										
			O4 S1 Mean								
0.266016977			0.220071947								
O4-482											
1	3735.072	1691.856	843	2031		1	9528.117	1840.68	582	2107	146582.5
2	1026.854	1709.391	871	2014		2	6199.397	1754.092	446	2243	
3	2254.96	1693.483	684	2375		3	4907.535	1730.713	401	2813	
4	3983.751	1612.712	435	2813		4	1126.284	1748.333	606	2429	
5	374.943	1777.539	1459	1958		5	1252.963	1777.751	707	2153	
6	15357.15	1681.705	504	2329		6	2411.489	1769.465	663	2345	
7	2861.732	1582.278	507	2425		1	1524.628	1692.537	739	1951	
8	3941.837	1656.951	472	2463		2	998.98	1827.547	1253	2070	
	33536.3						27949.39				
0.282689285							118633.1				
O4-483											
1	19890.16	1556.786	491	2650		1	3592.896	1617.196	519	2265	147539.1
2	22491.98	1515.009	455	2387		2	2423.138	1638.581	883	2285	
3	12780.81	1504.25	502	2643		3	2541.393	1654.21	788	2310	
4	324.395	1548.464	988	1959		4	1121.291	1593.849	563	2328	
	55487.33					5	1627.802	1483.194	445	2126	
						6	2158.754	1571.731	493	2145	
							13465.27				
							134073.8				
0.413856553			O4 S2 Mean								
			0.348272919								
O4 Avg	0.284172										

O5-57												
1	130.877	159.73	7	255		1	543.994	137.81	3	255		
2	54.98	173.348	8	255								
3	26.551	135.435	8	238								
	212.408											
0.390460189												
O5-58												
1	297.483	192.778	8	255		1	15.401	143.178	9	255		544
							528.599					
0.56277632			O5 S1 Mean									
			0.476618254									
O5-59												
1	131.756	195.238	8	255		1	16.074	166.568	22	255		544
2	114.601	196.211	14	255		2	14.02	148.37	21	254		
						3	41.076	149.967	17	255		
	246.357					4	12.029	159.241	28	255		
						5	16.063	144.369	42	255		
						6	9.201	140.931	16	246		
						7	6.374	129.703	35	237		
						8	0.983	133.016	89	223		
						9	3.465	130.914	24	215		
							119.285					
0.580052506												
							424.715					
O5-61												
1	142.698	160.58	28	255		543.99						
2	169.78	138.584	23	255								
	312.478											
0.574418647												
O5-62												
1	156.834	168.678	12	255		1	16.388	101.841	19	213		544
2	39.556	154.652	15	251		2	14.469	116.467	14	242		
3	21.372	150.637	27	245		3	28.555	120.451	23	251		
	217.762					4	15.677	108.24	15	237		
							75.089					
0.464399428							468.911					
			O5 S3 Mean									
			0.519409038									
O5 avg	0.514421											

O7-63												
1	93.78	182.705	6	252		1	146.699	129.262	9	255		544
2	17.645	131.005	7	245		2	9.23	117.429	13	242		
3	18.289	113.248	8	251		3	9.256	103.685	13	233		
4	11.402	134.4	9	251		4	5.992	104.789	16	251		
	141.116						171.177					
0.378506691							372.823					
O7-64												
1	253.544	178.328	5	255		1	12.465	103.235	9	225		544
2	7.532	203.436	12	255		2	16.024	116.432	30	242		
						3	3.888	108.627	24	216		
	261.076						32.377					
							511.623					
0.510289803												
O7-65												
1	121.963	159.514	7	255		1	20.762	138.74	14	255		544
2	19.224	172.36	10	252		2	49.954	132.515	16	255		
	141.187					3	132.667	130.099	9	255		
						4	22.854	121.891	11	252		
						5	72.03	240.476	13	255		
							298.267					
0.574554496							245.733					
O7-66												
1	107.912	181.493	10	255		1	6.381	92.394	15	189		544
2	18.466	195.736	13	253		2	9.975	113.729	16	225		
3	15.142	169.401	16	255		3	9.176	98.065	11	250		
4	65.489	166.005	11	252		4	4.435	108.432	12	248		
5	11.028	212.132	13	253		5	3.703	110.926	57	240		
	218.037					6	18.874	100.762	9	228		
						7	11.814	101.84	19	226		
0.493030902						8	15.281	112.824	8	253		
						9	22.123	125.24	13	255		
							101.762					
							442.238					
O7-67												
1	178.793	201.091	6	255		1	22.381	104.267	14	248		544
2	17.548	135.303	11	240		2	79.924	104.334	6	250		
3	15.463	201.69	19	253			102.305					
	211.804											
0.479525464							441.695					
			O7 S3 Mean									
			0.486278183									
O7 Avg	0.487181											

Young Treated with Neutral Blood Exchange

Y3-484											
1	27798.999	2042.196	547	4095		5	6309.851	2100.591	718	4095	147537.962
2	8910.839	2025.245	681	4095		6	5298.39	2078.23	701	4074	
3	8085.446	1942.933	547	3168		7	9958.39	2134.041	688	4095	
4	1097.682	1932.365	518	2951		8	599.596	2144.309	921	3079	
	45892.966						22166.23				
0.366055124							125371.7				
Y3-485											
9	31269.999	2025.26	373	4095		1	31384.51	1940.123	189	3505	147261.721
10	2064.836	1956.83	457	4027		2	12542.11	2259.779	574	4095	
	33334.835						43926.62				
0.322589672		Y3 S1 Mean					103335.1				
		0.344322									
Y3-486											
1	42316.399	1879.334	176	4095		1	15400.83	1497.677	373	3941	147539.106
2	8144.833	1907.356	537	4095							
3	2519.655	1895.871	713	3233			132138.3				
	52980.887										
0.400950339											
Y3-487											
1	9552.87	2053.581	498	4095		1	53262.95	1917.104	286	4095	147539.106
2	826.85	2035.219	931	3146		2	26881.14	1651.733	225	4095	
3	9676.637	2083.77	640	3914			80144.1				
	20056.357										
		Y4 S2 Mean					67395.01				
0.297594095		0.349272									
Y3-488											
1	7540.869	2107.075	649	3847		1	23487.11	1758.398	513	3716	147534.426
2	18365.736	2034.515	357	4095		2	6234.863	1730.329	248	3530	
3	5061.464	2049.909	479	4095			29721.97				
4	4653.032	2023.383	688	3275							
	35621.101						117812.5				
0.302354286											
Y3-489											
1	10048.46	2201.771	685	4095		1	44627.21	2183.728	260	4095	147539.106
2	402.92	2135.626	845	3949							
3	9785.74	2030.776	528	4095			102911.9				
4	2172.795	2008.618	556	4010							
5	1165.598	1977.775	755	3602							
	23575.513										
0.22908443			Y3 S3 Mean								
			0.265719								
Y3 Avg	0.319771324										

Y1-490											
1	19975.336	2261.952	361	4095		1	147539.1	2091.849	299	4095	
2	14851.884	2209.672	335	4095							
3	10793.977	2205.074	613	2877							
	45621.197										
0.30921427											
Y1-491											
Same image as 490, won't quantify											
Y1-492											
1	22068.358	2042.237	278	4095		1	9501.491	2175.734	813	3570	147538.17
2	14271.946	2090.012	347	4095		2	2053.915	1855.803	349	4095	
3	5632.77	1991.456	351	3358		3	3720.408	1834.202	396	3076	
4	9694.839	2148.503	387	3049		4	9083.698	2040.171	40	3201	
	51667.913						24359.51				
							123178.7				
0.419455073											
Y1-493											
1	32235.697	2166.808	188	4095		1	22716.01	1766.738	0	4095	147539.002
2	2008.673	2350.683	905	2964		2	7023.23	2254.917	503	4095	
	34244.37					3	8745.99	2165.332	383	4095	
							38485.23				
		Y1 S2 Mean									
0.314013608		0.366734					109053.8				
Y1-494											
1	50176.463	2189.237	626	4016		1	1377.667	2112.632	573	3500	147539.106
2	836.522	2223.843	981	2739							
3	1651.723	2344.547	1029	2913			146161.4				
4	1466.592	2303.857	1203	2809							
5	2224.382	2133.856	704	3753							
	56355.682										
0.385571478											
Y1-495											
1	19841.584	2216.401	553	4095		1	17993.29	2361.461	665	3670	147534.946
2	1793.9	2245.595	632	4095		2	1920.059	2362.179	932	3292	
3	2306.131	2156.697	442	4095		3	3987.6	2191.311	452	3968	
4	719.931	2151.817	505	4071		4	2304.674	2203.958	956	3671	
5	794.192	2078.095	461	4095		5	1236.218	2313.752	424	3668	
6	1359.05	2267.419	538	4095		6	2051.731	2275.7	848	4053	
7	842.763	2158.723	365	4095		7	3851.975	2199.118	392	4095	
8	3192.16	2107.735	572	4095			33345.55				
	30849.711										
							114189.4				
0.270162651		Y1 S3 Mean									
		0.327867									
Y1-496											
1	4989.388	2137.445	552	4022		1	12196.4	2189.772	526	4095	147537.546
2	722.947	2344.421	1038	3139		2	5003.533	2177.187	591	4095	
3	1091.546	2294.083	1038	3279		3	1870.76	2010.856	489	3200	
4	1226.65	2270.457	1017	3417		4	1759.682	2171.907	903	3118	
5	352.269	2355.592	1289	3103		5	7105.915	2049.964	573	4095	
6	737.82	2165.067	786	3602			27936.29				
7	2280.961	2083.001	516	4095							
8	939.384	2116.185	629	3508			119601.3				
9	506.094	1623.681	503	2823							
	12847.059										
0.107415751											
Y1 Avg	0.300972138										

Y5-38												
1	72.846	137.987	12	225		1	57.005	102.375	12	195		544
2	67.625	114.653	10	199								
3	29.713	106.723	7	190			486.995					
	170.184											
0.349457387												
Y5-39												
1	179.859	116.224	8	206		1	51.298	111.337	20	224		544
2	15.198	140.309	13	217		2	5.731	108.37	22	190		
	195.057						57.029					
							486.971					
0.400551573												
Y5-40												
1	120.291	121.566	17	198		1	52.728	96.052	24	191		544
2	104.073	124.562	11	220								
	224.364						491.272					
0.456700158												
Y5-41												
2	95.448	99.482	10	179		1	48.888	83.841	17	175		544
3	178.896	105.664	10	193		2	6.797	80.107	27	160		
	274.344					3	13.424	78.004	20	158		
						4	1.91	76.511	27	148		
		Y5 S1 Mean					71.019					
		0.446685										
0.580031756							472.981					
Y5-42												
1	113.908	118.964	13	199		1	37.094	91.465	26	167		544
2	31.021	106.351	15	170		2	34.917	91.487	24	167		
	144.929					3	11.112	92.83	33	167		
							83.123					
0.314463512							460.877					
Y5-43												
1	86.06	114.836	8	185		1	57.92	91.447	26	178		544
2	19.922	102.962	17	171		2	9.663	88.219	28	160		
3	30.563	104.204	13	168			67.583					
4	8.656	102.056	24	161								
	145.201						476.417					
0.304777118												

Y5-44												
1	37.749	108.684	24	177		1	11.31	104.884	56	185		544
2	37.534	119.761	35	179		2	41.749	99.289	46	182		
3	40.782	101.965	29	168		3	8.121	101.509	39	170		
4	3.762	97.16	36	150		4	20.585	95.47	35	169		
5	10.046	102.862	30	153		5	13.779	96.246	34	165		
6	18.013	102.706	31	157		6	2.505	87.006	39	149		
	147.886					7	8.934	87.762	35	157		
						8	10.158	83.907	40	151		
						9	7.174	97.822	54	157		
							124.315					
0.352373804							419.685					
Y5-45												
1	76.439	111.089	11	182		1	88.49	95.632	23	169		544
2	22.25	118.818	20	186								
3	13.112	105.533	22	163			455.51					
4	15.309	128.341	24	203								
5	10.984	113.322	28	167								
	138.094											
0.303163487		Y5 S2 Mean										
		0.318694										
Y5-46												
1	230.725	112.667	5	213		1	37.797	87.628	18	167		544
2	16.686	100.545	8	170		2	6.616	93.395	17	170		
	247.411						44.413					
0.495231061							499.587					
Y5-47												
1	53.123	112.301	7	189		1	21.373	84.763	13	175		544
2	186.318	109.475	6	193		2	13.434	86.671	15	172		
3	7.415	100.476	6	174		3	3.425	93.732	17	178		
	246.856						38.232					
							505.768					
0.488081492												
Y5-48												
1	53.275	113.729	17	187		1	77.652	95.846	21	186		544
2	106.228	103.809	10	170								
3	13.577	108.32	17	172			466.348					
	173.08											
0.371139149												
Y5-49												
1	147.711	105.198	12	203		1	56.879	82.563	13	173		544
2	51.94	103.436	15	173		2	16.36	87.219	24	170		
3	46.101	100.165	11	173			73.239					
	245.752											
			Y5 S2 Mean				470.761					
0.522031349			0.469121									
Y5 Avg	0.411500154											

Y4-50												
1	44.723	112.569	31	181		1	50.776	82.873	32	176		544
2	186.293	102.528	27	179		2	19.313	82.097	34	157		
	231.016					3	4.533	75.078	38	129		
							74.622					
0.49217475							469.378					
Y4-51												
1	96.254	100.723	27	174		1	102.184	80.604	31	170		544
2	104.023	114.396	28	192								
	200.277						441.816					
0.45330409		Y4 S1										
		0.472739										
Y4-52												
1	36.193	165.048	41	255		1	14.306	240.868	73	255		544
2	72.574	168.292	31	255		2	5.513	112.832	59	251		
3	15.808	179.11	42	255		3	11.504	116.448	31	250		
	124.575					4	8.447	114.168	50	253		
						5	73.581	117.432	35	247		
							113.351					
0.289272702												
							430.649					
Y4-53												
1	178.873	170.808	36	255		1	45.09	125.334	59	254		544
							498.91					
0.35852759												
Y4-54												
1	117.233	180.714	38	255		1	44.555	129.305	39	252		544
2	45.778	155.781	44	245								
3	8.415	161.482	58	252			499.445					
	171.426											
0.343232989												
Y4-55												
1	31.752	202.744	80	255		1	51.173	136.079	57	255		544
2	90.062	171.258	67	255		2	3.825	124.232	81	220		
	121.814					3	2.116	126.631	83	210		
							57.114					
0.250189983							486.886					
Y4-56												
1	98.175	176.773	54	255		1	17.432	238.412	88	255		544
2	36.778	166.907	58	253		2	10.008	134.893	61	254		
3	8.886	213.433	88	255		3	36.004	129.787	43	253		
	143.839					4	65.936	125.551	54	249		
							129.38					
			Y4 S3 Mean									
			0.324717				414.62					
0.34691766												
Y4 Avg	0.361945681											

						Ave	Std Error	P-value			
YY	**YNBE**	**ONBE**	**OO**		**YY**	0.348947	0.058811947	0.031396	0.995197	0.568053	
0.193645	0.319771	0.425218	0.407372		**YNBE**	0.348547	0.024552718		N.S.		
0.365763	0.300972	0.266516	0.707646		**OO**	0.593447	0.064783763	*			*
0.35689	0.4115	0.284172	0.636954		**ONBE**	0.395502	0.051216101			N.S.	0.045111
0.47949	0.361946	0.514421	0.621818								
		0.487181									

Minimum Feret Diameter Excel Sheets (Excel 3)

Sample	YA	YB	YC	OA	OB	OC	Y1	Y3	Y4	Y5	Y6	O2	O3	O5	O6	O7
Fiber Diameter	79	39.956	57.519	69.87	54.926	40.31	79.286	76.327	58.909	50.684	32.111	66.024	52.476	42.854	45.333	85.208
	52.797	48.662	36.025	38.204	64.498	33.572	71.118	71.38	50.824	56.016	41.868	53.632	44.382	57.95	36	18.667
	49.477	50.262	54.813	66.198	29.12	34.667	71.467	62.936	66.68	63.386	53.333	66.667	55.249	60.926	51.051	77.161
	48.074	66.319	59.21	53.083	70.516	29.814	50.102	43.737	42.75	76.187	62.454	107.736	25.612	66.104	44.562	30.696
	54.275	64.346	37.547	36.878	43.431	45.333	29.814	64.139	82.667	84.011	48.314	63.736	59.926	71.616	39.215	57.565
	62.893	48.166	49.477	20.396	60.059	45.333	35.901	50.772	62.667	34.59	75.094	47.347	88.01	65.821	21.705	56.063
	79.196	52.426	39.598	48.166	45.353	32.985	25.157	57.519	83.352	54.471	67.987	53.367	32.469	41.655	38.759	62.667
	51.103	89.134	34.176	43.594	31.609	30.405	34.667	82.03	59.18	75.848	59.881	46.571	60.369	36.782	42.374	48.185
	46.648	48.019	60.015	31.693	36.878	32.249	25.157	56.96	73.345	50.208	58.317	51.103	50.208	49.351	4.30E+01	4.40E+01
	65.821	48.332	44.161	37.947	53.133	32.277	28.783	87.737	59.21	70.402	68.118	67.264	52.932	55.201	4.12E+01	69.179
	67.882	33.36	43.04	42.164	44.181	52.154	37.357	83.309	85.521	59.044	55.458	60.369	59.21	64.553	49.924	46.97
	50.912	76.105	52.426	28.284	65.333	28	39.643	50.772	83.501	57.72	60.458	21.705	69.564	49.621	34.998	40.552
	55.57	41.655	59.464	25.751	58.909	30.696	31.468	69.768	69.602	68.832	76.918	71.802	40.617	61.174	57.349	65.17
	63.246	36	36.974	37.947	42.164	36.393	46.034	69.346	80.554	54.39	75.625	81.802	68.104	51.777	58.241	5.26E+01
	36.878	21.705	28.032	4.95E+01	37.642	48.662	23.589	58.454	73.756	70.364	48	43.676	46.819	54.291	61.348	70.667
	46.743	43.184	42.353	49.351	53.996	36.612	50.596	62.766	49.924	76.012	61.464	43.858	38.459	79.218	65.551	39.598
	59.21	31.383	46.686	35.777	55.249	25.298	56.6	60.722	70.717	78.225	60.237	53.35	29	57.72	41.161	41.676
	45.568	34.28	48.166	32.551	59.21	52.154	42.353	54.732	43.737	75.141	66.319	42.687	71.653	61.521	64.677	4.71E+01
	61.464	45.607	53.4	34.176	78.937	64.346	73.624	66.667	55.968	21.705	56.6	49.621	51.777	62.681	7.59E+01	37.357
	44.322	35.226	45.976	25.298	35.901	40.552	41.676	54.732	65.02	96.821	37.947	50.403	42.687	82.677	36.025	5.77E+01
	24.037	42.541	47.796	42.164	58.088	51.467	50.12	34.15	77.952	86.533	49.405	62.025	76.269	66.959	61.333	6.37E+01
	49.549	55.249	50.772	32	58.134	36.393	66.68	57.581	88.04	84.327	40.617	24.909	62.936	55.698	50.684	67.594
	62.154	56.016	59.464	29.12	65.388	66.219	62.681	84.042	79.554	67.908	48.534	23.324	33.44	41.526	50.684	78.971
	52.273	60.926	69.333	42.374	52.273	52.154	23.324	62.893	74.726	37.736	69.154	35.075	35.201	50.947	57.95	6.27E+01
	26.667	39.643	44.721	2.95E+01	27.455	56.016	38.942	56.143	73.636	62.837	59.404	35.075	66.72	68.573	78.304	102.05
	63.246	41.761	53.814	26.7	32	60.296	56.253	50.684	37.428	71.653	71.318	38.873	60.868	52.273	5.55E+01	6.47E+01
	47.291	46.284	71.081	32.985	52.068	42.541	96.148	63.358	67.475	76.78	57.704	35.901	38.482	33.757	44.161	53.748
	54.275	56.253	40.2	36.099	50.12	58.439	53.748	81.41	74.595	74.595	67.383	61.072	41.161	54.422	5.63E+01	5.07E+01
	48.314	64.498	28.783	46.895	53.283	52.154	59.464	61.391	87.066	88.091	52.881	39.643	41.526	65.659	45.646	45.117
	36.271	55.714	67.882	50.315	53.946	26.466	39.576	37.357	89.492	105.232	59.21	76.513	81.071	72.602	55.698	4.25E+01
	88.01	69.538	65.862	48.917	51.863	36.099	40.354	63.805	98.097	52.154	66.88	26.566	44.322	70.855	53.946	58.667
	47.178	43.431	67.105	66.306	36.878	41.526	57.581	41.868	72.651	73.382	78.768	56.016	70.516	67.895	4.71E+01	4.27E+01
	34.176	49.495	55.458	4.27E+01	50.824	22.94	49.621	52.392	84.748	49.978	58.727	70.88	65.061	74.774	39.215	6.54E+01
	70.402	62.723	56.143	24.037	58.134	29.242	77.952	54.667	78.971	53.599	56.694	70.364	49.978	65.17	33.941	51.312
	57.689	40.552	39.777	42.667	42.999	55.825	22.784	77.345	72.111	46.686	37.759	44.821	61.982	56.063	28	68.819
	27.358	44.979	62.482	53.233	50.596	32.687	60.809	54.926	68.144	76.93	51.034	57.256	49.782	70.767	37.357	4.17E+01
	55.968	43.737	66.826	26.833	40	67.895	66.667	48.019	93.143	87.646	33.993	41.161	46.053	93.333	33.993	39.486
	53.814	41.846	56.6	37.19	25.473	49.333	41.484	57.766	53.748	61.767	28.503	80.399	51.103	65.102	51.777	54.683
	27.487	36.612	72.111	3.67E+01	40	49.603	63.231	49.621	66.212	69.179	62.254	48.074	51.863	84.095	3.89E+01	3.40E+01
	34.409	53.367	82.03	39.777	30.463	63.246	45.353	80.277	65.102	70.88	43.594	40.639	43.858	58.727	33.993	68.144
	41.846	54.715	45.607	23.627	61.867	40.705	60.604	61.391	83.245	81.377	65.875	82.645	45.333	54.926	27.487	6.84E+01
	44.322	38.39	38.759	36.878	57.95	37.047	92.27	88.04	54.715	62.667	83.533	67.699	32.551	41.676	51.88	6.86E+01
	69.051	83.522	59.21	45.509	39.777	36.612	80	53.996	89.691	84.433	78.949	75.283	46.819	69.768	3.40E+01	6.45E+01
	27.841	4.472	32.221	38.459	0	49.026	56.772	60.369	82.473	78.847	41.484	82.073	33.413	44.181	4.30E+01	53.996
	51.225	38.667	65.605	38.39	52.595	44.979	48.185	58.21	62.197	80.288	33.652	40.792	36.612	46.743	42.687	55.458
	56.079	36.878	64.346	35.876	31.016	52.068	51.294	76.187	86.461	77.345	60.648	46.38	60.369	62.681		33.993
	26.833	67.738	55.49	48.074	33.572	53.133	44	30.667	75.472	73.37	79.207	69.87	52.881	65.659		5.34E+01
	44.721	55.714	68.56	28	58.485	45.607	64.443	49.495	67.264	83.958	32.931	41.074	53.748	77.299		5.21E+01
	69.295	37.547	52.154	51.863	67.515	129.766	52.017	41.161	47.122	76.513	78.395	31.468	40.901	65.374		60.34
	48.074	56.016	32.249	32.056	48.826	72.993	58.576	35.302	87.737	89.612	69.793	94.957	57.889	62.766		4.81E+01
	40	53.814	44.402	57.889	39.215	45.976	58.317	48.332	79.342	78.44	57.395	90.99	62.025	88		33.993
	52.881	36.878	68.56	48.332	35.226	38.459	51.467	48.826	108.534	75.058	46.207	87.351	50.315	59.404		42.353
	44.02	30.229	28.844	43.533	44	36.417	59.926	50.772	48.019	72.749	54.144	50.947	67.422	87.899		40.552
	28.284	60	72.111	32.985	37.547	40.552	66.306	51.103	88.644	51.502	82.322	46.207	54.926	67.987		53.93
	65.115	39.373	35.428	32.985	44.721	48.166	40.022	76.408	68.832	58.909	72.111	69.908	66.038	74.345		5.97E+01
	51.467	34.176	47.14	40	33.36	29.963	50.772	51.294	86.953	65.388	73.091	55.12	25.473	55.682		4.41E+01
	40.2	37.357	37.947	3.82E+01	27.455	20.396	46.648	68.986	54.291	91.214	63.736	55.825	58.909	65.347		3.07E+01
	51.294	41.398	61.565	3.56E+01	31.693	48.074	32.249	51.777	81.279	100.036	65.388	74.595	57.519	47.291		24.037
	72.749	74.488	30.405	25.473	18.714	60.133	49.405	51.88	40.639	57.395	62.893	70.402	22.94	79.577		21.99
	30.667	52.068	54.029	57.271	44.979	68.534	30.696	49.549	60.237	51.777	41.868	51.863	34.769	43.676		2.56E+01
	54.275	41.161	26.667	27.487	56.253	60.237	30.782	50.12	91.214	67.908	69.602	54.667	23.739	53.4		57.519
	46.97	48.074	34.176	56.016	19.09	58.621	46.207	62.794	61.057	81.169	72.16	73.442	74.595	29.963		62.039
	52.273	60.237	42.937	38.759	43.676	61.651	30.463	54.39	63.175	64.346	75.672	33.44	57.442	40.639		58.134
	33.941	52.154	37.9	39.395	41.526	56.772	75.625	50.772	65.006	53.333	59.18	64.139	54.975	64.801		37.071
	55.682	49.171	36.878	31.127	14	45.976	37.547	79.286	58.241	36.271	49.495	121.45	57.889	53.099		71.005
	40.486	56.395	46.207	48.166	57.349	35.428	70.073	65.02	61.464	57.766	28.503	52.154	43.98	75.637		9.02E+01
	46.648	65.115	62.254	4.53E+01	64.801	46.819	51.103	65.456	84.937	85.676	73.624	71.678	65.374	47.647		62.893
	37.736	34.176	54.732	28	32.441	66.306	43.676	41.355	50.262	57.069	33.333	83.958	40.111	51.103		48.314
	46.648	39.395	40.792	32.028	36.685	10	45.353	74.964	53.35	91.263	56.694	38.942	39.777	84.433		69.959

	62.681	61.464	52.068	44.382	68.352	43.41	41.526	87.076	83.756	65.006	56.143	92.347	37.428	80.543		53.682
	52	45.412	41.074	40.089	44.181	28.347	73.961	61.057	46.571	69.87	56.772	48.074	68.326	49.621		5.12E+01
	49.477	56.079	65.456	40.792	40.2	70.174		57.889	41.333	76.012	61.695	50.684	76.965	51.502		4.24E+01
	68.832	48.662	60.926	43.081	52.932			69.141	27.487	40.486	69.602	49.603	37.924	69.997		6.00E+01
	52.747	52.154	56.269	56.143	54.39			52.831	44.701	52.392	66.88	54.975	50.191	34.769		4.73E+01
	100.779	70.855	46.686	40.792	62.837			54.406	63.344	68.209	55.12	73.961	48.826	65.102		79.878
	41.398	48.899	51.777	40.792	58.545			70.767	91.078	39.215	60.722	33.333	40.022	74.345		
	51.294	52.273	49.062	65.862	27.358			29.364	61.348	85.271	53.083	31.383	53.099	65.006		
		71.467	29.605	35.428	21.541			47.347	70.415	35.503	51.932	60.604	60.237	43.184		
		67.145	38.181	31.241	41.183			58.485	75.484	58.576	78.667	72.786	67.987	80.708		
		54.861	48.314	47.347	67.383			45.568	63.68	57.519	20.396	94.3	21.499	82.419		
		45.568	41.074	53.55	57.519			66.667	84.042	82.796	49.333	77.62	53.748	98.387		
		78.768	44.322	54.975	46.034			70.364	66.212	92.424	54.861	57.704	60.133	72.541		
		54.406	32.249	4.60E+01	54.683			54.144	68.118	69.602	61.651	60.648	70.98	42.999		
		53.367	31.693	43.184	53.996			67.699	32.221	90.755	49.978	78.031	55.57	83.192		
		48.662	55.201	32.931	46.667			61.464	32.687	29.814	72.541	102.207	32.469	49.603		
		55.714	47.479	56.143	60.015			35.901	61.464	73.817	69.602	63.246	43.858	80.022		
		54.683	41.161	22.784	74.964			62.723		67.422	68.261	78.429	52.881	55.249		
		52.017	40.814	34.59	30.926			63.61		45.333	59.059	58.682	45.607	55.201		
		89.492	45.255	40.2	36.974			63.344		84.548	39.373	76.269	41.526	57.581		
		44.701	44.721	49.171	33.36			55.714		60.296	41.526	76.012	40.705	54.144		
		65.388	60.722	34.667	74.595			48.185		63.063	62.681	75.141	35.428	50.684		
		69.295	58.134	50.772	41.761					79.755	59.628	54.715	49.924	28.032		
		58.21	34.667	36.222	59.703					45.568	59.539		50.824	66.198		
		77.746	53.666	24.585	45.509					66.999	69.051		63.344	57.519		
		54.406		30.463	45.607					55.714	35.226		37.642	43.41		
		44.081		38.181	33.993					71.118	52		61.867	88.413		
		34.28		26.965	64					63.063	62.254		40.552	61.637		
		36.612		37.357							43.533		49.924	49.549		
		41.355		46.034							71.268		38.759	62.039		
		52.068		5.02E+01							58.682		29.242	77.746		
		61.333		4.14E+01							48.185		62.254	51.294		
		45.412		52							38.873		56.772	63.175		
		60.133		60.941							60.369		71.467	49.782		
		66.104		34.769									43.184	63.847		
		58.682		28.284									58.576	50.049		
		70.667		24.585									54.715	31.693		
		57.271		34.769									60.868	62.34		
		61.391		32.441									68.144	60.604		
		76.292											45.879			
		52.747														
		68														
		72.308														
		52.392														
		84.706														
		68														
		54.813														
		62.154														
		42.667														
		49.495														
		65.673														
		60.369														
		60.458														
		63.736														
		46.226														
		53.93														
		44.141														
		64.498														
		59.881														
		52.392														
		60.941														
		73.563														
		53.233														
		41.655														
		50.912														
		61.29														
		53.333														
		39.395														
		73.636														
		38.667														
		57.889														
		59.044														
		62.025														
		41.846														
		43.184														
		27.487														
		54.029														

	YA	YB	YC	OA	OB	OC	Y1	Y3	Y4	Y5	Y6	O2	O3	O5	O6	O7		T test	
Mean	51.05816	52.78562	49.30903	40.13547	46.645072	45.89861	50.80914	59.18844	68.3322	67.502835	57.6766	59.90629	51.09904	60.81314	46.70933	53.7716		YY v YNBE	0.071739
Median	51.103	52.5865	47.981	38.4245	45.607	45.333	50.102	57.889	68.131	69.179	59.21	57.48	51.103	61.3475	44.562	53.748		OO v ONBE	0.037821
Normalized to Young			YY avg =	51.05093														YY v OO	0.040658
Mean	1.000141	1.033979	0.965879	0.786185	0.9136967	0.899075	0.995264	1.1594	1.33851	1.3222644	1.129785	1.173461	1.000942	1.191225	0.914955	1.053293		YY v ONBE	0.383432
Median	1.010803	1.040146	0.949051	0.760026	0.9020937	0.896674	0.991004	1.145028	1.347612	1.3683412	1.171157	1.136938	1.010803	1.213436	0.881424	1.06312			
Converted to Micro		148 pixels = 50 microns																Oc v Oe	0.037821
Mean	17.24938	17.83298	16.65846	13.55928	15.75847	15.50629	17.16525	19.99609	23.0852	22.805012	19.48534	20.23861	17.26319	20.54498	15.78018	18.16608			
Median																			
Melod's Data		Melod's Normalized to YY			My results with Melod's (normalized to YY)					OO v ONBE	YY v OO	YY vYNBE	YNBE v ONBE						
YY	OO	YY	OO		YY	OO	YNBE	ONBE		0.0018027	0.00078	0.009905	0.177086						
54.50927	35.15393	0.953378	0.614849		1.0001414	7.86E-01	0.995264	1.173461											
6.00E+01	30.2322	1.05E+00	0.528767		1.0339794	0.913697	1.1594	1.000942											
6.19E+01	42.95553	1.08E+00	0.7513		0.9658791	0.899075	1.33851	1.191225											
5.22E+01	39.71067	9.14E-01	0.694547		0.9533776	0.614849	1.322264	0.914955											
					1.05E+00	0.528767	1.129785	1.053293											
					1.08E+00	0.7513													
					9.14E-01	0.694547													
					YY avg	OO avg													
					1	7.41E-01													

Neurogenesis Excel Sheets (Excel 4)

	Ki67+/H+		
O5--100 um			
Section 1			
1,2	5		
3,4	4	Total	
5,6	3	12	
Section 2			
7,8	10		
9,10	5		
11,12	4	Total	
13,14	1	20	
Section 3			
15,16	8		
17,18	4		
19,21	4	Total	
20,22	2	18	
Section 4			
23,24	8		
25,26	5		
27,28	5	Total	
29,30	1	19	
O5 grand total		**69**	
Extrapolated total		**1932**	

	Ki67+/H+		
O6--100 um			
Section 1			
1,2	6		
3,4	2		
5,6	1	Total	
7,8	0	9	
Section 2			
9,10	6		
11,12	4	Total	
13,14	1	11	
Section 3			
15,16	8		
17,18	4		
19,21	1	Total	
20,22	6	19	
Section 4			
23,24	1	Total	
25,26	1	2	
O6 grand total		**41**	
Extrapolated total		**1148**	

	Ki67+/H+		
O7--100 um			
Section 1			
7,8	5	Total	
9,10	3	8	
Section 3			
1,2	4		
3,4	5	Total	
5,6	1	10	
Section 4			
11,12	7		
13,14	7	Total	
15,16	3	17	
Section 5			
17,18	4		
19,20	7	Total	
21,22	2	13	
O7 grand total		**48**	
Extrapolated total		**1344**	

	Ki67+/H+		
OMM-Delta--75 um			
Section 1			
40,41	5		
42,43	7	Total	
44,45	3	15	
Section 2			
46,47	5		
48,49	8		
50,51	8	Total	
52,53	5	26	
Section 3			
54,55	4		
56,57	5		
58,59	3	Total	
60,61	1	13	
OMM-Delta Grand total		**54**	
Extrapolated total		**2016**	

	Ki67+/H+		
OMM-Gamma--75 um			
Section 1			
62,63	5		
64,65	11		
66,67	4	Total	
68,69	3	23	
Section 2			
70,71	2		
72,73	11		
74,75	5	Total	
76,77	0	18	
Section 3			
78,79	4		
80,81	6		
82,83	3	Total	
84,85	1	14	
OMM-Delta Grand total		**55**	
Extrapolated total		**2053.333**	

	Ki67+/H+		
OMM-Beta--75 um			
Section 1			
86,87	6		
88,89	7		
90,91	3	Total	
92,93	0	16	
Section 2			
94,95	4		
96,97	4		
98,99	3	Total	
100,101	5	16	
Section 3			
102,103	4		
104,105	7		
106,107	2	Total	
108,109	0	13	
OMM-Beta Grand total		**45**	
Extrapolated total		**1680**	

	Ki67+/H+		
OMM-Alpha--75 um			
Section 1			
110,111	8		
112,113	7	Total	
114,115	2	17	
Section 2			
116,117	6		
118,119	2		
120,121	8	Total	
122,123	1	17	
Section 3			
124,125	9		
126,127	2		
128,129	2	Total	
130,131	2	15	
OMM-Beta Grand total		**49**	
Extrapolated total		**1829.333**	

Old NBE Mean	**1714.667**
Standard Error	**124.6316**

	Ki67+/H+	
Y4--100 um		
Section 1		
1,2	4	
3,5	6	Total
4,6	1	11
Section 2		
7,8	10	Total
9,10	8	18
Section 3		
11,12	5	
13,14	6	Total
15,16	5	16
Section 4		
17,18	9	
19,20	4	Total
21,22	4	17
Y4 grand total		**62**
Extrapolated total		**1736**

	Ki67+/H+	
Y5--100 um		
Section 1		
1,2	3	
3,5	5	Total
4,6	5	13
Section 2		
7,8	3	
9,10	5	Total
11,12	2	10
Section 3		
13,14	0	
15,16	5	Total
17,18	7	12
Section 4		
13,14	3	
15,16	5	Total
17,18	3	11
Y5 grand total		**46**
Extrapolated total		**1288**

Y6--75 um		
Section 1		
1,2	8	
3,5	15	
4,6	6	Total
7,8	1	30
Section 2		
9,10	6	
11,12	9	Total
13,14	2	17
Section 3		
15,16	15	
17,18	5	
19-2,20	9	Total
19,21	0	29
Y6 grand total		**76**
Extrapolated total		**2837.333**

YMM-Alpha--75 um		
Section 1		
0,1	17	
2,3	14	
4,5	4	
6,7	1	
8,9	3	Total
10,11	0	39
Section 2		
12,13	14	
14,15	14	
16,17	8	
18,19	2	
20,21	7	Total
22,23	4	49
Section 3		
24,25	14	
26,27	3	
28,29	2	
30,31	4	Total
32,33	0	23
YMMAlpha grand to		**111**
Extrapolated total		**4144**

YMM-Beta--75 um		
Section 1		
34,35	13	
36,37	12	
38,39	8	Total
40,41	3	36
Section 2		
42,43	13	
44,45	10	Total
46,47	3	26
Section 3		
48,49	16	
50,51	8	
53,54	1	Total
54,55	2	27
YMMBeta grand tota		**89**
Extrapolated total		**3322.667**

YMM-Delta--75 um		
Section 1		
56,57	20	
58,59	13	Total
60,61	6	39
Section 2		
62,63	24	
64,65	27	Total
66,67	7	58
Section 3		
68,69	10	Total
70,71	10	20
YMMDelta grand tot		**117**
Extrapolated total		**4368**

YNBE Mean	**1953.778**
Standard Error	**460.3183**

YA--50 um				YB--100 um				YC--75 um				YMM1--50 um			
Section 1				Section 1				Section 1				Section 1			
1,2	2			1,2	11			1,3	16	Total		0,1	5		
3,4	7			3,4	9	Total		4,6	9	25		2,3	7		
5,6	3	Total		5,6	2	22						4,5	8	Total	
7,8	1	13						Section 2				6,7	3	23	
				Section 2				7,9	6						
Section 3				7,8	2	Total		10,12	3	Total		Section 2			
9,10	8			9,10	3	5		13,15	5	14		8,9	4		
11,12	4											10,11	2		
13,14	4	Total		Section 3				Section 3				12,13	1	Total	
15,16	7	23		11,12	3			16,18	9			14,15	9	16	
				13,14	5	Total		19,21	8	Total					
YA grand total		**36**		15,16	3	11		22,24	7	24		**YMM1 Grand Total**			**39**
Extrapolated total		**2016**										**Extrapolated total**			**2184**
				Section 4				**YC grand total**		**63**					
				17,18	7			**Extrapolated total**		**2352**					
				19,20	8	Total									
				21,22	5	20									
				YB grand total		**58**									
				Extrapolated total		**1624**									
		Young Isochronic Control Mean				**2044**									
		Standard Error				**284.6284**									

OA--75 um				OB--125 um				OC--100 um				OMM3--50 um			
Section 1				Section 1				Section 1				Section 1			
76,78	2			1,2	1			1,2	0			24,25	1		
79,81	0	Total		3,4	1	Total		3,4	0	Total		26,27	0		
82,84	0	2		5,6	1	3		5,6	0	0		28,29	1	Total	
												30,31	0	2	
Section 2				Section 2				Section 2							
85,87	2			7,8	0			7,8	1			Section 2			
88,90	1	Total		9,10	1	Total		9,10	1	Total		32,33	1		
91,93	0	3		11,12	0	1		11,12	1	3		34,35	1		
												36,37	0	Total	
Section 3				Section 3				Section 3				38,39	0	2	
94,96	0			13,14	1			13,14	0						
97,99	0	Total		15,16	1	Total		15,16	1	Total		**OMM3 Grand total**			**4**
100,102	0	0		17,18	0	2		17,18	0	1		**Extrapolated total**			**224**
OA grand total			**5**	Section 4				Section 4							
Extrapolated total			**186.6667**	19,20	2			19,20	0						
				21,22	1			21,22	1	Total					
				23,24	0	Total		23,24	0	1					
				25,26	0	3									
								OC grand total			**5**				
				Section 5				**Extrapolated total**			**140**				
				27,28	1										
				29,30	1										
				31,32	1	Total									
				33,34	0	3									
				OB grand total			**12**								
				Extrapolated total			**268.8**								
			Old Isochronic Control Mean				**204.8667**								
			Standard Error				**47.79804**								

	Ave	Std Error	P-Value		
YY	2044	155.8974	0.201232		0.152355
YNBE	2949.389	510.693	*		
OO	204.875	27.37284		*	
ONBE	1714.571	131.4103		1.45E-05	*
	8.368866				
OO	**ONBE**	**YNBE**	**YY**		
186.7	1932	1736	2016		
268.8	1148	1288	1624		
140	1344	2837.333	2352		
224	2016	4144	2184		
	2053	3323			
	1680	4368			
	1829				

References

1. Conboy, I. M. *et al.* Rejuvenation of aged progenitor cells by exposure to a young systemic environment. *Nature* **433**, 760–764 (2005).
2. Villeda, S. A. *et al.* The ageing systemic milieu negatively regulates neurogenesis and cognitive function. *Nature* **477**, 90–96 (2011).
3. Villeda, S. A. *et al.* Young blood reverses age-related impairments in cognitive function and synaptic plasticity in mice. *Nature Medicine* **20**, 659–663 (2014).
4. Mehdipour, M. *et al.* Rejuvenation of three germ layers tissues by exchanging old blood plasma with saline-albumin. *Aging* **12**, 8790–8819 (2020).
5. Kiprov, D. D. Guest editorial. *Transfusion and Apheresis Science* **28**, 163–164 (2003).
6. Kiprov, D. D. & Hofmann, J. C. Plasmapheresis in Immunologically Mediated Polyneuropathies. *Therapeutic Apheresis and Dialysis* **7**, 189–196 (2003).
7. Kiprov, D. D., Dau, P. C. & Morand, P. The effect of plasmapheresis and drug immunosuppression on T-cell subsets as defined by monoclonal antibodies. *Journal of Clinical Apheresis* **1**, 57–63 (1983).
8. Horowitz, A. M. *et al.* Blood factors transfer beneficial effects of exercise on neurogenesis and cognition to the aged brain. *Science* **369**, 167–173 (2020).
9. de Miguel, Z. *et al.* Exercise plasma boosts memory and dampens brain inflammation via clusterin. *Nature* **600**, 494–499 (2021).
10. Rebo, J. *et al.* A single heterochronic blood exchange reveals rapid inhibition of multiple tissues by old blood. *Nature Communications* **7**, (2016).
11. Zhang, G., Budker, V. & Wolff, J. A. High Levels of Foreign Gene Expression in Hepatocytes after Tail Vein Injections of Naked Plasmid DNA. *Human Gene Therapy* **10**, 1735–1737 (1999).
12. Elabd, C. *et al.* Oxytocin is an age-specific circulating hormone that is necessary for muscle maintenance and regeneration. *Nature Communications* **5**, (2014).
13. Yousef, H. *et al.* Systemic attenuation of the TGF-β pathway by a single drug simultaneously rejuvenates hippocampal neurogenesis and myogenesis in the same old mammal. *Oncotarget* **6**, 11959–78 (2015).
14. Mehdipour, M. *et al.* Rejuvenation of brain, liver and muscle by simultaneous pharmacological modulation of two signaling determinants, that change in opposite directions with age. *Aging* **11**, 5628–5645 (2019).
15. Conboy, I. M. & Rando, T. A. Aging, stem cells and tissue regeneration: Lessons from muscle. *Cell Cycle* **4**, 407–410 (2005).
16. Kuhn, H. G., Dickinson-Anson, H. & Gage, F. H. Neurogenesis in the dentate gyrus of the adult rat: age-related decrease of neuronal progenitor proliferation. *J Neurosci* **16**, 2027–2033 (1996).
17. Yang, J., Klassen, H., Pries, M., Wang, W. & Nissen, M. H. Vitreous humor and albumin augment the proliferation of cultured retinal precursor cells. *Journal of Neuroscience Research* **87**, 495–502 (2009).
18. Hsu, C.-C., Serio, A., Amdursky, N., Besnard, C. & Stevens, M. M. Fabrication of Hemin-Doped Serum Albumin-Based Fibrous Scaffolds for Neural Tissue Engineering Applications. *ACS Applied Materials & Interfaces* **10**, 5305–5317 (2018).

19. Montagne, A. *et al.* Blood-brain barrier breakdown in the aging human hippocampus. *Neuron* **85**, 296–302 (2015).
20. Goodall, E. F. *et al.* Age-associated changes in the blood-brain barrier: comparative studies in human and mouse. *Neuropathol Appl Neurobiol* **44**, 328–340 (2018).
21. Musaeus, C. S. *et al.* Cerebrospinal Fluid/Plasma Albumin Ratio as a Biomarker for Blood-Brain Barrier Impairment Across Neurodegenerative Dementias. *Journal of Alzheimer's Disease* **Preprint**, 1–8 (2020).
22. Senatorov, V. v *et al.* Blood-brain barrier dysfunction in aging induces hyperactivation of TGFβ signaling and chronic yet reversible neural dysfunction. *Science Translational Medicine* **11**, eaaw8283 (2019).
23. Conboy, I. M. & Rando, T. A. Heterochronic parabiosis for the study of the effects of aging on stem cells and their niches. *Cell Cycle* vol. 11 2260–2267 (2012).
24. Conboy, I. M., Conboy, M. J. & Rebo, J. Systemic problems: A perspective on stem cell aging and rejuvenation. *Aging* vol. 7 754–765 (2015).
25. Katsimpardi, L. *et al.* Vascular and Neurogenic Rejuvenation of the Aging Mouse Brain by Young Systemic Factors. *Science (1979)* **344**, 630–634 (2014).
26. Mehdipour, M. *et al.* Plasma dilution improves cognition and attenuates neuroinflammation in old mice. *Geroscience* (2020) doi:10.1007/s11357-020-00297-8.

04/26/2022

To whom it may concern,

I grant Melod Mehdipour permission to use my data and notebook entries from Figure 2 of the manuscript *Rejuvenation of three germ layers tissues by exchanging old blood plasma with saline-albumin* (doi: 10.18632/aging.103418) for Chapter 2 of his thesis.

Sincerely,

Cameron Kato

Chapter 2: Plasma Dilution Improves the Brain Health of Aged Mice

The work presented in the previous chapter established that young systemic factors are not causal, not are necessary for the broad rejuvenative phenotypes exhibited in mammalian tissues. Neutral blood exchange (NBE) resets the signaling milieu of blood to a pro-regenerative state after the dilution of plasma. Muscle repair, liver health, and hippocampal neurogenesis were all improved after NBE[1]. Here, the rejuvenative phenotypes of NBE are expanded upon by focusing on the neuroinflammation and cognition-short term memory. These findings confirm the notion of rejuvenation through diluting age-elevated systemic factors and demonstrate that the observed rejuvenation was not simply by reducing senescence[2].

Brain aging is associated with a progressive loss of functionality that is largely attributed to an accumulation of activated microglia (the brain's resident myeloid cells)[2,3]. Age-associated changes in brain function were also once considered inevitable and permanent[1,4]. However, heterochronic parabiosis studies have challenged this assertion by demonstrating that brain functionality can indeed be plastic, even as one advances in age[5–7]. Several candidate protein factors identified in young or aged blood were suggested to influence the plasticity of brain aging. Despite there being some controversy to the actual age-specific levels of some of the factors, these include GDF11, B2M, CCL11, and TIMP2[6,8–10]. These studies also lacked evidence pertaining to health span[11]. Young blood plasma transfusions in the clinic were not remarkable for any improvements to brain health either[12]. In addition, heterochronic blood exchange experiments—where the influences of shared organs and environmental enrichment—have shown that young blood does not rejuvenate the old brain[13].

Our NBE data demonstrated that young blood is not the primary determinant of rejuvenation. Instead, diluting aged blood plasma with 5% mouse serum albumin (MSA) and saline yielded a robust resetting of systemic signaling milieu to health/youth while rejuvenating multiple tissues[1]. The study of the brain in thar report was limited to hippocampal neurogenesis[1,2]. Here, the work on other important facets of brain health were studied.

Young (2-4 months) and old (22-24 months) male C57/B6 mice underwent the NBE procedure while isochronic exchanged were performed between young and old mice (YY and OO respectively) as previously described[1]. Six days after blood exchange, cognitive performance tests were performed. The mice were then sacrificed, their brains were harvested for analysis, and blood proteomics assays were performed[13–16] (**Figure 1a, 1b**).

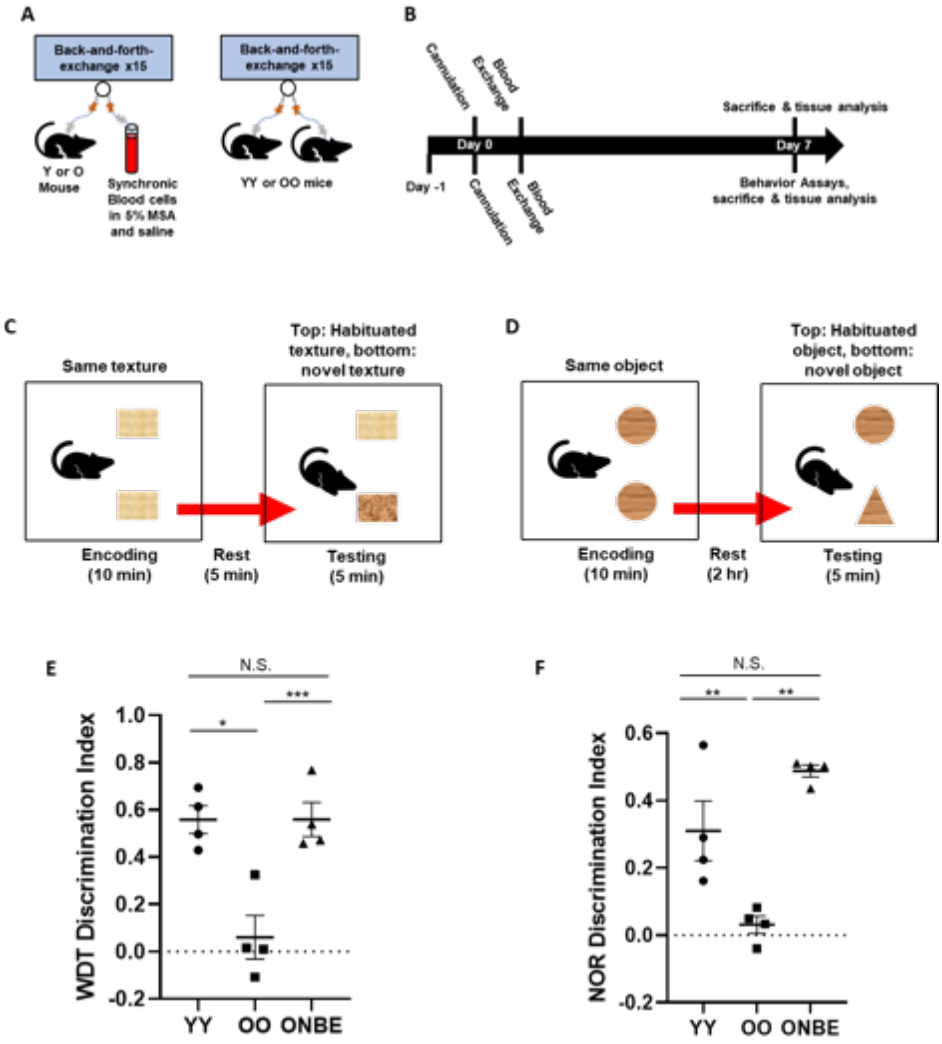

Figure 1. NBE improves the cognitive performance of old mice in a quick and robust fashion. NBE quickly and robustly improves the cognitive performance of old mice. **A)** Experimental schematic. Catheters were installed into the jugular veins of young or old mice, which had 50% of their blood plasma exchanged with normal saline (0.9% sodium chloride), 5% mouse serum albumin (MSA), and synchronic blood cells, as previously published [21]. **B)** Timeline. At day 1, mice were habituated for whisker discrimination (WD) and novel object recognition (NOR) behavioral tests. These mice underwent jugular vein cannulation on day 0 and blood exchange at day 1. WD and NOR assays were performed on day 6. Blood samples and brain were collected for tissue analysis. **C)** Schematics of mice performing the whisker discrimination task and **D)** novel object recognition assays. **E)** OO mice performed poorly when compared to YY mice, as expected (*p value = 0.024). ONBE mice were much better at discriminating between habituated and novel textures versus OO animals (***p value < 0.00001). Interestingly, ONBE mice were able to discriminate between novel and habituated textures as effectively as YY mice (N.S. p value = 0.01). f Similar trends were observed with novel object recognition studies. YY versus ONBE N.S. p value = 0.99, YY versus OO **p value < 0.004, OO versus ONBE **p value < 0.006. p values were obtained by one-tailed Student's t test, e.g., as typical for evaluating the extent of the differences in the means from three independent treatment groups, rather than comparing each group to another. N of YY = 4, N of OO = 4, and N of ONBE = 4 for each behavioral assay. This figure was adapted from Mehdipour et al. 2021[2], and these experiments were performed with Dr. Chia-Chien Chen. See corresponding *Excel Sheets 1 – 4* in *Chapter 2 Appendix* for reference of primary data.

Age-related changes in cognition occur naturally in mammals and they are typically associated with a decline in learning and memory[17]. Aged individuals display poor cognition in terms of deciphering between novel textures or objects when compared to young animals[6,7,9,16,18,19]. This aspect of cognition can be measured by the whisker discrimination task (WDT). Here, the quality of short-term memory is assessed by sensory processing through the barrel cortex and memory through hippocampus[19]. The novel object recognition test operates in a similar fashion where sensory and memory information is processed through the hippocampus and perirhinal regions[15,20]. Aged mice typically exhibit poorer capabilities to distinguish between novel objects or textures when compared to young animals[16].

The WDT and NOR test were performed after NBE in aged mice as well as in YY and OO isochronic controls (**Figure 1c, 1d**). OO mice had a profound age-specific decline in both the NOR and WDT assays when compared to YY animals (**Figure 1e, 1f**). Plasma dilution by NBE, however, improved cognitive performance in aged mice such that it became similar to that of the YY cohort (**Figure 1e, 1f**). These results establish that the functionality of the old brain is robustly and rapidly improved by diluting old blood plasma[2].

Neuroinflammation increases with age in both mice and humans. This may contribute to the decline in cognitive capacity in aged mammals[2,6,9,16]. We therefore asked whether improvements to cognition in aged mice after NBE correlated with diminished neuroinflammation.

Quantification of CD68+ cells (activated microglia) in cryosections of the brain in young and old mice 6 days post NBE or YY and OO exchanges was performed. An anatomical map that depicts various structures in coronal mouse brain sections is illustrated in **Figure 2a** (adapted from the Allen Brain Atlas). CD68+ cells were examined in the indicated regions. These cells were found just ventral to the dentate gyrus of the brain. Specifically, CD68+ cells were found in the thalamus, midbrain, and zona incerta of the thalamus in OO brains[2]. These areas were imaged and other parts of the OO brains were profiled, but no other region appeared to have detectable CD68+ cells. YY, YNBE, and ONBE brain sections were profiled in a similar fashion[2].

Figures 2b and **2c** demonstrate that CD68+ cells were the most prevalent in the old isochronic control brains. The relative number of these cells are minimal or virtually non-existent in young (YY) brains. These results are consistent with the previously published age-related increase in CD68+ resident brain myeloid cells[7,16,21]. The relative number of CD68+ cells dramatically decreased in aged mice after NBE (ONBE) to an extent that is similar to that of YY mice (**Figure 2b, 2c**). These results demonstrate that neuroinflammation rapidly and robustly diminished in the brains of aged mice after NBE[2].

To determine whether and to what degree the positive effects of NBE may be emulated by the ablation of senescent cells, we performed studies with the senolytic ABT263[2].

ABT263 (Navitoclax) is a chemotherapy agent that induces apoptosis in cervical, esophageal, leukemia, and lung cancer cells upon the inhibition of antiapoptotic proteins Bcl-2 and Bcl-xL[22–25]. ABT263 can also clear senescent cells through this mechanism, thereby diminishing the

relative levels of SASP[26–29]. ABT263 molecules are generally considered to be too large to cross

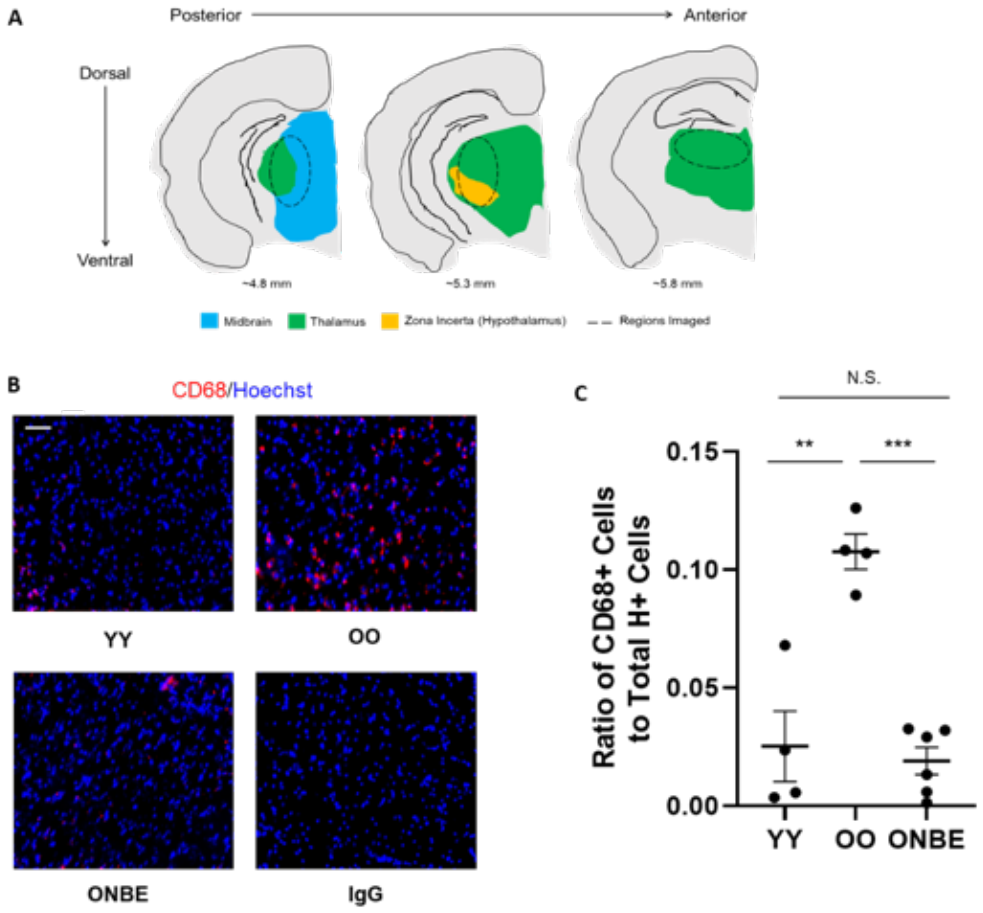

Figure 2. Neuroinflammation is reduced by plasma dilution in old mice. Neuroinflammation is reduced by a single NBE in old mice. **A)** Schematic of serial sections of 25 µm (denoted by the dashed ovals) that were taken from regions ventral to the dentate gyrus, e.g., where an apparent age-associated increase in relative number of $CD68^+$ cells was detected (green: thalamus, blue: midbrain, and orange: zona incerta of the thalamus). **B)** Immunofluorescence was performed to assay for CD68-positive (red) activated microglia in the thalamus/hypothalamus/midbrain regions of brains from mice of each cohort. Representative CD68/Hoechst double-positive cells in the specified areas are shown for YY, OO (isochronic controls), and ONBE mice. Isotype-matched IgG negative controls show the absence of non-specific fluorescence. Scale bar 50 µm. **C)** Quantification of the relative frequency of $CD68^+$/$Hoechst^+$ activated microglia in the thalamus. Neuroinflammation is substantially reduced in ONBE mice when compared to that in OO mice (***p value < 0.00002). The relative numbers of activated microglia are not significantly different between YY mice and ONBE mice (N.S. p value = 0.27). **p value YY versus OO < 0.003. p values were obtained by two-tailed Student's t test. N of YY = 4, N of OO = 4, N of ONBE = 7. This figure was adapted from Mehdipour et al. 2021[2]. See corresponding *Excel Sheet 5* in *Chapter 2 Appendix* for reference of primary data.

the blood brain barrier[30]. However interestingly, the blood brain barrier becomes porous to large proteins including peripheral SASP proteins which traverse the aged blood brain barrier and cause neuroinflammation[31–34]. In addition, the leaky blood brain barrier allows larger proteins

such as albumin to infiltrate the aging brain, further perpetuating neuroinflammation[35–37]. Peripheral senescent cell clearance by ABT 263 administration may diminish systemic SASP levels, preventing their mobilization to the brain, thereby attenuating neuroinflammation and improving hippocampal neurogenesis; however, this was not the case, because ABT263 had no/marginal rejuvenating effects, as compared to NBE [2].

Previous studies have shown that muscle injury by cardiotoxin (CTX) injections worsens hippocampal neurogenesis in mice[2,13,16]. To examine these effects in the context of ABT263, some mice received CTX injury on day 30 of the treatment while other mice have not (**Figure 3a**). Hippocampal neurogenesis in the subgranular zone (SGZ) of the dentate gyrus (DG) was quantified by counting and extrapolating the number of Ki67+ cells per hippocampus as published previously[1,2,6,7,13,16] (**Figure 3b, 3c**). The number of Ki67+ cells in the SGZ of the DG of aged mice treated with ABT263 is not significantly different from that of vehicle controls. There were also no observed differences between injured and non-injured cohorts.

The frequency of CD68+ activated microglia (which were profiled as in **Figure 2**) was also relatively elevated in old vehicle control cohorts (**Figure 3d, 3e**). Interestingly, the relative number of CD68+ cells did not change significantly in either cohort (**Figure 3e**). However, the average size of CD68 particles was found to have decreased significantly in aged mice who received ABT263 treatment (**Figure 3f**).

These results demonstrate that ABT263 does not enhance hippocampal neurogenesis but has a weaker yet measurable effect on attenuating neuroinflammation when compared to NBE[2]. These differences are apparent even though NBE and ABT263 act peripherally to reduce SASP.

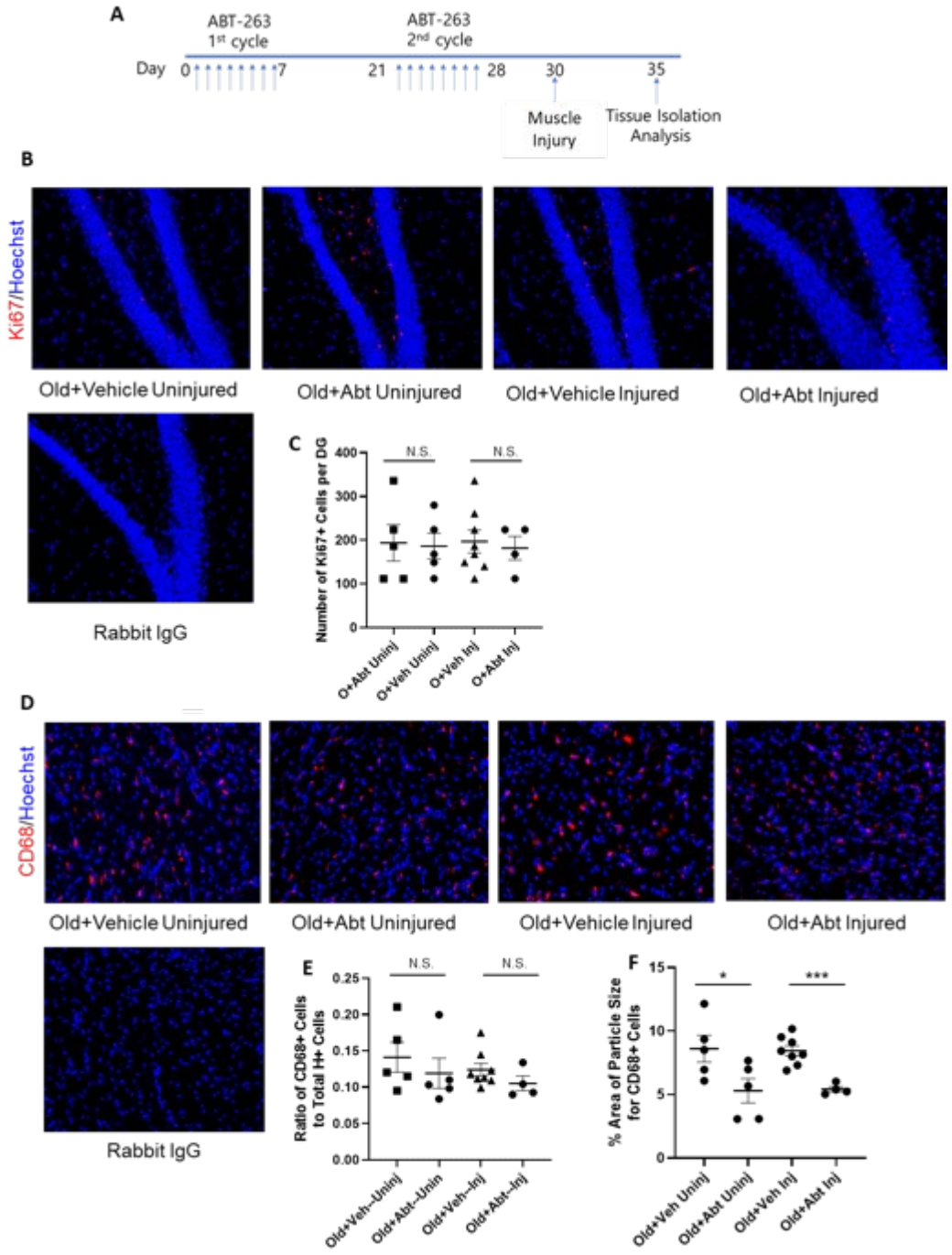

Figure 3. Effects of ABT 263 senolytic on hippocampal neurogenesis and neuroinflammation of old mice. A) Schematic of the study. There were two 7-day periods where mice were given ABT 263 or vehicle by gavage once per day. A 2-week interval followed between each 7-day gavage period. TA muscles of some mice were injected with cardiotoxin for experimental injury, while other animals were not injured. **B)** Brains were snap frozen and serially cryosectioned at 25 µm. These sections were immunoassayed with anti-Ki67 antibodies (proliferation marker), while using Hoechst to counterstain all the nuclei. Representative images of the hippocampal dentate gyrus show Ki67 (red)/Hoechst (blue) double-positive cells in subgranular zone (proliferating SGZ NPCs). **C)** Quantification of Ki-67+/Hoechst+ SGZ cells in the dentate gyrus was performed for both injured and uninjured

cohorts. ABT 263 did not improve hippocampal neurogenesis in either cohort. Old + Veh Uninj versus O + Abt Uninj p value = 0.89; Old + Veh Inj versus O + Abt Inj p value = 0.72. p values were obtained by two-tailed Student's t test. N of Old + Veh Uninj = 5, N of Old + Abt Uninj = 5, N of Old + Veh Inj = 8, N of Old + Abt Inj = 4. **D)** Immunofluorescence was performed for CD68 (activated microglia marker). Representative images of CD68 (red)/Hoechst (blue) double-positive cells. **E)** Quantification of CD68+/Hoechst+ cell frequency in the brain was performed for the injured and uninjured cohorts. ABT 263 did not attenuate CD68+ cell frequency. Old + Veh Uninj versus O + Abt Uninj p value = 0.47; Old + Veh Inj versus O + Abt Inj p value = 0.21. N.S. non-significant. **F)** CD68 cluster size per cell analysis was performed on Fiji. The size of CD68 clusters was significantly reduced by ABT 263. Old + Veh Uninj versus O + Abt Uninj p value = 0.05; Old + Veh Inj versus O + Abt Inj p value < 0.0005. p values were obtained by two-tailed Student's t test. For all experiments: N of Old + Veh Uninj = 5, N of Old + Abt Uninj = 5, N of Old + Veh Inj = 8, N of Old + Abt Inj = 4. Scale bar = 50 μm. There was no non-specific fluorescence in isotype-matched IgG negative controls. This figure was adapted from Mehdipour et al. 2021[2]. Taha Mehdipour (UCB Undergraduate student, Conboy lab) contributed the data on neurogenesis and neuroinflammation with corresponding panels of Figure 3. Professor Ok Hee Jeon of Korea University College of Medicine provided Figure 3A and administered the oral gavage of ABT263 in aged mice. Dr. Michael Conboy performed the experimental TA muscle injuries. See corresponding *Excel Sheets 6 – 8* in *Chapter 2 Appendix* for reference of primary data.

These results demonstrate that aged mice performed better in novel object recognition (NOR) and whisker discrimination tasks (WDT) after NBE. These results are accompanied by a reduction in neuroinflammation after NBE as well.

Interestingly, the senolytic ABT263 had limited effects on neuroinflammation and did not alter the extent of hippocampal neurogenesis in aged mice. Other projects that complemented my studies and were included in the same research paper showed that ABT263 and NBE diminished senescence-associated βGal (SA- βGal) activity in brain parenchyma. This implies that peripheral senescence propagates to the brain and that senolytics or NBE that are both acting peripherally attenuate it in the brain, but the rejuvenative effects of NBE on reduction of neurodegeneration and neuroinflammation were seen only in the NBE approach or were more robust than that of ABT263[2].

There is substantial interest in developing senolytic therapies that treat age-associated diseases. ABT263 is of great clinical interest since a number of studies have shown that it can treat a variety of cancers[38–40]. Its senolytic effects seem to be exerted on peripheral tissues, but it must be primed with additional chemotherapeutic drugs to have an effect on brain tumors [41,42]. The fact that NBE exerted a stronger effect on brain rejuvenation than ABT263 suggests that resetting systemic milieu by plasma dilution is more robust than peripheral clearance of senescent cells[2]. The data presented in my thesis therefore support the notion that age-elevated systemic senescence and SASP may induce central senescence[31–34].

CD68 cluster size reduction observed in this work may be associated with modest attenuation of neuroinflammation[43] by ABT263. One of the proposed mechanisms of Alzheimer's disease also involves a reduction in neuroinflammation[44]. It would be interesting to determine whether ABT263 may be effective in such applications.

In another agreement with my studies, the results of comparative proteomics, e.g., another part of this large collaborative work, demonstrated that the dilution of aged blood plasma yielded an

increase in the levels of protein factors that promote and maintain the functional health of the brain, both mice and humans[2]. These protein factors were found to share the following general functions: improving neuroprotection, attenuating neuroinflammation, diminishing neurotoxicity, enhancing neural stem cell proliferation, and enhancing the differentiation of neural stem cells[2].

Plasma exchange yields great therapeutic potential to treat many age-related diseases simultaneously, particularly those pathologies that pertain to brain health and function. The use of TPE was investigated for its effectiveness in treating mild-to-moderate Alzheimer's disease. A phase I study that began in 2005 and concluded in 2009 demonstrated that cognition and cerebrospinal fluid levels of Amyloid-beta changed little, while hippocampal volume and frontal and temporal cortex perfusion increased during a 6-month follow up[2,44,45]. A larger phase II study that began in 2007 and ended in 2017 was performed with a more intense plasma exchange regimen. This phase II study found that cognitive decline in patient's was wither statistically significant or clinically significant[44,46,47]. However, behavioral, functional, and cognitive improvements were not statistically significant[48]. Multicenter clinical trials are currently underway to investigate the potential benefits of TPE in Alzheimer's patients[44,48].

Our work agrees with these clinical trial results and expands to rejuvenative phenotypes. These data also suggest that brain diseases, as well as physiological brain aging, can be prevented and/or attenuated at some point. The dilution of age-accumulated plasma factors can restore brain health back to health/youth. Furthermore, systemic factors that bolster brain health are elevated after NBE and TPE. This implies that additional pharmacological approaches can be taken to rejuvenate the brain[2].

We have previously shown that treating aged mice with a combination of an Alk5 inhibitor (that attenuates excess TGFβ signaling) and ectopic oxytocin also reduces neuroinflammation, enhances hippocampal neurogenesis, and improved cognition in aged animals[16]. The overall effects of NBE are stronger than those of the Alk5 inhibitor-oxytocin drug combination. This suggests that the profound rejuvenation observed after NBE operates by multiple mechanisms[2]. [12]Summarily, this work agrees with and further strengthens the paradigm that diluting age-accumulated plasma factors is necessary and sufficient for broad and profound rejuvenation across multiple tissues.

Materials and Methods

Animals. All in vivo experiments and procedures were performed in accordance with the policies and approved procedures set by the Office of laboratory Animal Care at the University of California, Berkeley and the Buck Institute for Research on Aging. Young male C57BL/6 mice (2 months old) were purchased from Jackson Laboratory while old mice of 18 months of age were purchased from the National Institute of Aging (NIA). Both young and aged mice were allowed to acclimate at the same animal facility for several weeks prior to the above studies. All mice were fed identical diets.

Number of animals. A power analysis was performed to determine the sample sizes in a similar fashion to what was published[1].

Jugular vein cannulation surgery and blood exchange procedures. These procedures were performed as previously published[2,13] and as discussed in Chapter 2 of this thesis.

Note: all equipment used for these procedures were sterilized by an autoclave or bead sterilizer. The bead sterilizer was used upon repeated contact of equipment with multiple mice. Briefly, mice were dosed with buprenorphine (0.1 mg/kg) and anesthetized with 1 – 3% isoflurane in oxygen to full relaxation. Ophthalmic ointment was applied to prevent drying of each eye. Mice were shaven around their necks and rested in dorsal recumbency. Betadine scrub was applied to their bare skin and wiped with isopropanol alcohol wipes. This scrub technique was repeated two additional times. The mice were then placed on a sterile field. Once there was no reaction to tie pinch, a 1 – 1.5 cm incision was made to the right of the midline and the right internal jugular vein was exposed. Once isolated, a 6 – 0 silk suture ligated the cranial end of the vein. Gentle tension was applied to the ligated end of the vein. Another 6 – 0 silk suture was used to loosely ligate the caudal end of the vein. A 23-guage needle with its beveled end bent outward to 90^{o} was used to perform the venotomy. A pre-heparinized 1-Fr-to3-Fr catheter was promptly inserted at its 1 French end. Once patency was confirmed, the catheter was plugged, and an additional cranial ligature was made to secure the catheter in its place. Mice were then rested in left lateral decubitus to thread the catheter between their scapulae. Blunt forceps were used to create space underneath the skin, passing the incision site to the scapulae. A 16-guage needle was positioned between the scapulae and inserted underneath the skin at the level of the incision site. The plugged end of the catheter was fed through the lumen of the 16-guage needle. Wound clips were used to close the incision site and the catheter protruding the skin was secured with a drop of Durmabond. Mice were taken off anesthesia and dosed with subcutaneous Meloxicam (5 mg/kg) for 7 days post-procedure.

To prepare the designer blood solution, blood from young or aged donor mice was obtained by terminal cardiac puncture and anticoagulated with 3 units of heparin. Blood samples were centrifuged at 500 g for 5 min. The plasma fraction was carefully removed and blood cell pellets were resuspended in normal saline and then spun down once more at 500 g for 5 min. The saline fraction was removed and replaced with an equal volume of 5% MSA in normal saline. These blood mixtures were passed through a FACS mesh cap to de-clump the cells and filter out any remaining clots.

Blood exchanges were performed a few hours after cannulation surgeries and immediately after the designer blood solutions were prepared. Mice were anesthetized with 1 – 3% isoflurane in oxygen while resting in ventral recumbency. Catheters were flushed with 3 units of heparin saline. 150 μL of blood was exchanged between mice or between mice and a tube containing the designer blood solution. The exchanges were repeated for a total of 15 times in order to attain 50% replacement of blood plasma with saline and albumin fluid or 50% synchronic exchanges. Once completed, the catheters were plugged, and the mice were taken off anesthesia. Mice were allowed to recover in their cages.

ABT 263 treatment. 22 – 24-month-old male mice from the National Institute on Aging were treated with ABT 263 (APExBIO, USA) diluted in 10% ethanol, 30% polyethylene glycol 400, and 60% Phosal 50 PG (Lipoid, Germany). ABT 263 was administered by oral gavage at 50 mg/kg per day for 7 days per cycle for two cycles within a 2-week interval between cycles.

Cardiotoxin muscle injury. Tibialis anterior (TA) muscles of mice were injured by intramuscular injections of cardiotoxin (CTX; Sigma Aldrich), where 10 μL of CTX were injected per TA at 0.1 μL/mL. TA's were harvested five days post injury.

Tissue isolation. Mice were sacrificed per the guidelines of OLAC at UC Berkeley and Buck Institute. Blood was collected by terminal cardiac puncture and was allowed to clot completely at room temperature for at least 30 min. Clotted blood samples were centrifuged at a speed of 5000 g for 5 min and the serum fraction was collected. Brains were isolated and collected post-mortem as well. Tissues were embedded in Tissue-Tek Optimal Cutting Temperature and snap frozen in isopentane that was cooled to -70ºC with dry ice.

Tissue sectioning and brain mapping. OCT-embedded coronal brain sections at 25 μm thickness were obtained with a cryostat. Sections were collected on gold-supplemented positively charged glass coverslip slides. The cryostat was used to locate the midbrain, thalamus, and hypothalamus of regions described above. These brain regions were located approximately 4.5 – 4.8 mm from the most posterior end of the cerebellum. Subsequent tissue sections were collected for another 1 mm passing this mark.

Antibodies and labeling reagents. The following antibodies were used at 0.5 – 1 μg/mL:

- CD68: Abcam, Rabbit, ab125212, 1:500
- Ki67: Abcam, Rabbit, ab16667, 1:200
- Isotype-matched IgGs; Sigma Aldrich, Rabbit, 1:1000
- Donkey anti-rabbit Alexa 546: Life Technologies, Invitrogen, Eugene, Oregon, A10040, lot #1946340, 1:2000
- Hoechst dye was used to stain DNA: Hoechst 33342, Sigma Aldrich (B2261), 1:1000

Immunofluorescence of brain samples. Sectioned mouse brains were fixed in 4% paraformaldehyde for 4 min at room temperature. Subsequently, these sections were rinsed with 1X phosphate-buffered saline (PBS) several times at 2-3 min per rinse. They were then permeabilized with 0.1% Triton X-100 on ice for 5 min. Samples were then rinsed and blocked with 1% staining buffer (1% calf serum in 1X PBS) 3 times at 2-3 min per rinse. Samples were then incubated with primary antibodies overnight at 4ºC. The following day, sections were washed 3 times with staining buffer and then incubated with secondary antibodies for 2 hours. Samples were then washed 3 times with staining buffer. 2 droplets of Fluromount (Sigma F4680) were then added to each slide and cover slips were placed on top of samples.

Behavioral Assays. The whisker-dependent texture discrimination test was performed as previously described[14,15]. The encoding, resting, and testing phases lasted 10, 5, and 5 min,

respectively. The novel object recognition (NOR) test was also conducted as previously described[14–16] with the encoding, resting, and the testing phases set to 10 min, 2 hours, and 10 min, respectively. Modifications of encoding ad testing durations are intended to accommodate for the slow movement of aged mice. Behavioral analyses were performed with the analyst blinded to the identity and conditions of the mice (i.e., age and type of treatment).

Data quantification and statistics. Neurogenesis was quantified by counting the number of Ki67+/H+ cells in 200 μm of the SGZ from each mouse as previously described[1,2,16]. Neuroinflammation was scored by counting the number of CD68+ cells relative to the number of nuclei counted per field of view. Mapping strategies were described in Figure 2. All analyses were performed on tissue sections that were imaged at 20X magnification. Non-paired, one-tailed, and two-tailed Student's t-tests were performed on Microsoft Excel for all tissue analysis data.

Chapter 2 Appendix

Novel Object Recognition Testing Excel Sheets (Excel 1)

Animal #	Condition	Habituated (1/2 speed, in seconds)	Novel (1/2 speed, in seconds)		% Novel / Total	Disc Index
YY1	YY	25.99	65.19		0.714959421	0.429918842
YY2	YY	30.98	92.43		0.748966858	0.497933717
YY3	YY	12.24	67.86		0.847191011	0.694382022
YY4	YY	3.37	14.06		0.806655192	0.613310384
OO1	OO	26.33	26.88		0.505168201	0.010336403
OO2	OO	4.72	3.8		0.44600939	-0.10798122
OO3	OO	5.33	5.5		0.507848569	0.015697138
OO4	OO	10.8	21.2		0.6625	0.325
OMM1 (alpha)	OMM - designer fluid infused	25.31	84.51		0.769531961	0.539063923
OOM2 (beta)	OMM - designer fluid infused	10.44	79.81		0.88432133	0.768642659
OOM3 (gamma)	OMM - designer fluid infused	33.98	91.62		0.729458599	0.458917197
OOM4 (delta)	OMM - designer fluid infused	39.79	110.98		0.736088081	0.472176162

YY	% Novel / Total	Disc Index
avg	0.779443121	0.558886241
stdev	0.05892714	0.117854281
sem	0.02946357	0.05892714

OO	% Novel / Total	Disc Index
avg	0.53038154	0.06076308
stdev	0.092587606	0.185175212
sem	0.046293803	0.092587606

OMM	% Novel / Total	Disc Index
avg	0.779849993	0.559699985
stdev	0.071821815	0.143643631
sem	0.021655092	0.043310184

t-tests	
YY vs. OMM	0.99329526
YY vs. OO	0.003938487
OO vs. OMM	0.005333457

	Disc Index	
	Avg	SEM
YY	0.558886241	0.05892714
OO	0.06076308	0.092587606
OMM	0.559699985	0.043310184

Novel Object Recognition Encoding Excel Sheets (Excel 2)

Y-Y	Left	Right	Total
avg	17	17	34
stdev	6.055301	6.480741	12.51666
sem	3.02765	3.24037	6.258328

O-O	Left	Right	Total
avg	6	6.75	12.75
stdev	2.708013	2.872281	5.5
sem	0.816497	0.866025	1.658312

OMM	Left	Right	Total
avg	6.5	6.25	12.75
stdev	2.516611	3.304038	5.737305
sem	0.758787	0.996205	1.729862

Average			
	Left	Right	Total
YY	17	17	34
OO	6	6.75	13
ONBE	6.5	6.25	12.75

SEM			
	Left	Right	Total
Control	3.02765	3.24037	6.258328
7d RS	0.816497	0.866025	1.658312
7d RS + Mino	0.758787	0.996205	1.729862

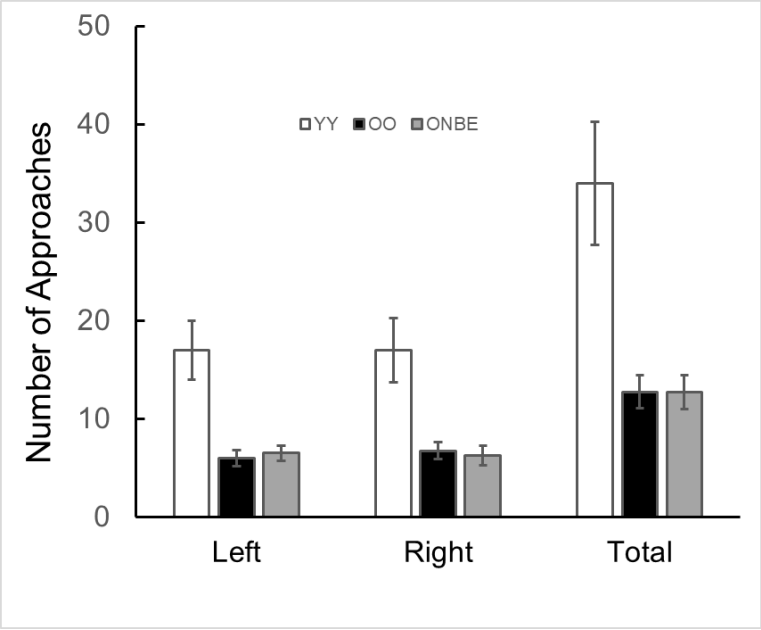

Whisker Discrimination Task Testing Excel Sheets (Excel 3)

Animal #	Condition	Habituated (1/2 speed, in seconds)	Novel (1/2 speed, in seconds)		% Novel / Total	Disc Index
YY1	YY	25.99	65.19		0.714959421	0.429918842
YY2	YY	30.98	92.43		0.748966858	0.497933717
YY3	YY	12.24	67.86		0.847191011	0.694382022
YY4	YY	3.37	14.06		0.806655192	0.613310384
OO1	OO	26.33	26.88		0.505168201	0.010336403
OO2	OO	4.72	3.8		0.44600939	-0.10798122
OO3	OO	5.33	5.5		0.507848569	0.015697138
OO4	OO	10.8	21.2		0.6625	0.325
OMM1 (alpha)	OMM - designer fluid infused	25.31	84.51		0.769531961	0.539063923
OOM2 (beta)	OMM - designer fluid infused	10.44	79.81		0.88432133	0.768642659
OOM3 (gamma)	OMM - designer fluid infused	33.98	91.62		0.729458599	0.458917197
OOM4 (delta)	OMM - designer fluid infused	39.79	110.98		0.736088081	0.472176162

YY	% Novel / Total	Disc Index
avg	0.779443121	0.558886241
stdev	0.05892714	0.117854281
sem	0.02946357	0.05892714

OO	% Novel / Total	Disc Index
avg	0.53038154	0.06076308
stdev	0.092587606	0.185175212
sem	0.046293803	0.092587606

OMM	% Novel / Total	Disc Index
avg	0.779849993	0.559699985
stdev	0.071821815	0.143643631
sem	0.021655092	0.043310184

t-tests	
YY vs. OMM	0.99329526
YY vs. OO	0.003938487
OO vs. OMM	0.005333457

	Disc Index	
	Avg	SEM
YY	0.558886241	0.05892714
OO	0.06076308	0.092587606
OMM	0.559699985	0.043310184

Whisker Discrimination Task Encoding Excel Sheets (Excel 4)

Animal #	Approach left	Approach right	Total Approaches	Condition
YY1	13	12	25	YY
YY2	23	21	44	YY
YY3	13	16	29	YY
YY4	14	16	30	YY
OO1	6	7	13	OO
OO2	9	9	18	OO
OO3	6	7	13	OO
OO4	7	7	14	OO
OMM1 (alpha)	13	12	25	OMM - designer fluid infused
OOM2 (beta)	6	7	13	OMM - designer fluid infused
OOM3 (gamma)	8	7	15	OMM - designer fluid infused
OOM4 (delta)	7	8	15	OMM - designer fluid infused

		t-tests	
YY vs. OO	0.013469465	0.003760309	0.006654001
YY vs. OMM	0.04561755	0.012326182	0.023084325
OO vs. OMM	0.413560776	0.467994446	0.430431068

Y-Y	Left	Right	Total
avg	15.75	16.25	32
stdev	4.856267428	3.685557398	8.286535263
sem	2.428133714	1.842778699	4.143267632

O-O	Left	Right	Total
avg	7	7.5	14.5
stdev	1.414213562	1	2.380476143
sem	0.426401433	0.301511345	0.717740563

OMM	Left	Right	Total
avg	8.5	8.5	17
stdev	3.109126351	2.380476143	5.416025603
sem	0.937436867	0.717740563	1.632993162

Average			
	Left	Right	Total
YY	15.75	16.25	32
OO	7	7.5	14.5
ONBE	8.5	8.5	17

SEM			
	Left	Right	Total
Control	2.428133714	1.842778699	4.143267632
7d RS	0.426401433	0.301511345	0.717740563
7d RS + Mino	0.937436867	0.717740563	1.632993162

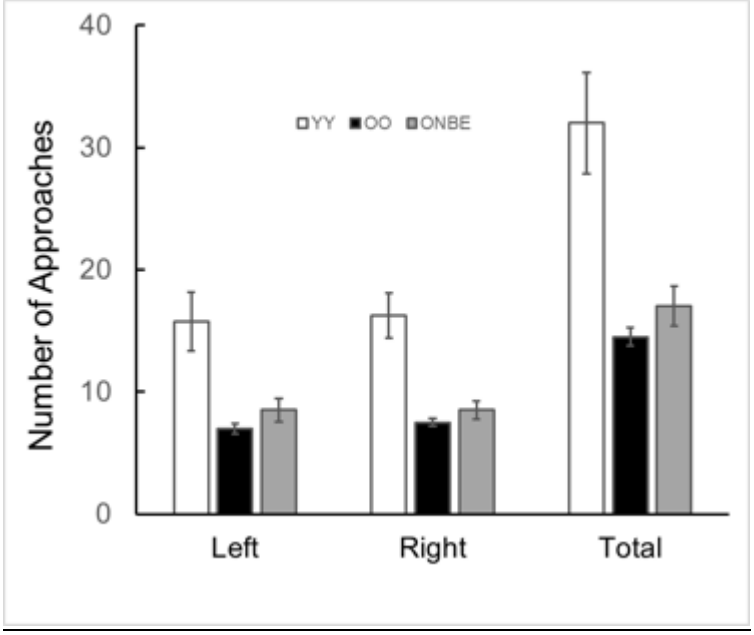
40
30
20
10
0
Number of Approaches
YY
OO
ONBE
Left
Right
Total

Neuroinflammation Excel Sheets (Excel 5)

	CD68+	H+	CD68/H
OA-1,2	63	457	
OA-5,6	33	341	
OA-8,9	15	298	
OA-10,11	39	290	
OA-3,4	Null signal		
Total	150	1386	0.108225
OB-1,2	52	297	
OB-4,5	46	310	
OB-6,3	46	327	
OB-7,8	8	311	
OB-9,10	13	298	
Total	165	1543	0.106935
OC-1,2	8	464	
OC-3,4	64	385	
OC-5,6	33	337	
OC-7,8	27	293	
OC-9,10	Null signal		
Total	132	1479	0.089249
OMM3-0,1	86	585	
OMM3-2,3	62	487	
OMM3-4,5	58	527	
OMM3-6,7	58	496	
Total	264	2095	0.126014
O5-1,2	2	394	
O5-3,4	10	345	
O5-5,6	12	512	
O5-7,8	11	475	
O5-9,10	25	555	
Total	60	2281	0.026304
O6-1,2	37	602	
O6-3,4	35	664	
O6-5,6	19	504	
O6-7,8	9	541	
Total	100	2311	0.043271
O7-1,2	33	585	
O7-3,4	29	573	
O7-5,6	32	492	
Total	94	1650	0.05697
D-14,15	16	598	
D-16,17	16	510	
D-18,19	11	601	
D-21,22	9	475	
Total	52	2184	0.02381
G-23,24	12	489	
G-26,27	45	599	
G-27,28	17	726	
G-29,30	21	484	
Total	95	2298	0.04134
B-31,32	22	619	
B-33,34	17	523	
B-35,36	23	534	
B-37,38	26	486	
Total	88	2162	0.040703
A-__0,__1	8	580	
A-__2,__3	22	520	
A-__4,__5	31	490	
A-__6,__7	31	498	
Total	92	2088	0.044061

IgG Ctl

B&C settings on Fiji (ImageJ): 709-1300

	CD68+	H+	CD68/H
YA-1,2	0	285	
YA-3,4	4	744	
YA-5,6	1	403	
Total	5	1432	0.00349162
YB-1,2	4	374	
YB-3,4	5	675	
YB-5,6	1	560	
YB-8,9	1	371	
Total	11	1980	0.00555556
YC-1,2	29	512	
YC-3,4	13	406	
YC-5,6	44	347	
Total	86	1265	0.06798419
YMM1-8,9	17	541	
YMM1-10,	8	520	
Total	25	1061	0.02356268
Y4-1,2	0	532	
Y4-3,4	1	821	
Y4-5,6	0	363	
Y4-7,8	2	879	
Total	3	2595	0.00115607
Y5-1,2	0	268	
Y5-3,4	8	418	
Y5-5,6	0	320	
Y5-7,8	0	379	
Total	8	1385	0.00577617
Y6-1,2	12	489	
Y6-3,4	2	431	
Y6-5,7	0	419	
Y6-8,9	10	479	
Total	24	1818	0.01320132
A-72,73	25	634	
A-74,75	21	591	
A-76,77	10	706	
Total	56	1931	0.02900052
B-78,79	31	664	
B-80,81	19	752	
B-82,83	26	668	
B-84,85	8	499	
Total	84	2583	0.03252033
D-86,87	12	645	
D-88,89	20	549	
D-90,91	23	527	
Total	55	1721	0.03195816

	Ave	Std Error	P-value	
YY	0.025149	0.014973		*
YNBE	0.018935	0.006		
OO	0.107606	0.007509	1.2542E-05	
ONBE	0.039494	0.004269	*	0.2728

Compiled Cohort Averages

0.108225	0.026304	0.00115607	0.003492
0.106935	0.043271	0.00577617	0.005556
0.089249	0.05697	0.01320132	0.067984
0.126014	0.02381	0.02900052	0.023563
	0.04134	0.03252033	
	0.040703	0.03195816	
	0.044061		

Neurogenesis Excel Sheets (Excel 6)

Old+Abt--Injured	Mean No. of Ki67+/H+	Standard Error			
	182	26.80795902			
	Image ID	Ki67+/H+	Section	Sum for all sections	Extrapolated total
O+Abt1					
Section 3	384,385	1	2	2	224
	386,387	1			
	388,389	0			
	390,391	0			
	393,394	0			
O+Abt2					
Section 1	395,396	1	1	3	168
	397,398	0			
	399,400	0			
	401,402	0			
Section 2	403,404	1	2		
	405,406	1			
	407,408	0			
	409,410	0			
O+Abt3					
Section 3	411,412	1	1	1	112
	413,414	0			
	415,416	0			
	417,418	0			
	419,420	0			
O+Abt4					
Section 1	421,422	0	1	6	224
	423,424	0			
	425,426	0			
	427,428	0			
	429,430	0			
	431,432	1			
	433,434	0			
	435,436	0			
	437,438	0			
Section 2	439,440	0	2		
	441,442	0			
	443,444	1			
	445,446	0			
	447,448	1			
	449,450	0			
Section 3	451,452	0	3		
	453,454	1			
	455,456	0			
	457,458	1			
	459,460	0			
	461,462	0			
	463,464	0			
	465,466	1			
	467,468	0			

Old+Abt--Uninjured	Mean No. of Ki67+/H+	Standard Error			
	194.133333	41.57264058			
	Image ID	**Ki67+/H+**	**Section Sum**	**Sum for all sections**	**Extrapolated total**
OJA1					
Section 1	116,117	0	1	5	186.6666667
	118,119	1			
	120,121	0			
	122,123	0			
	124,125	0			
	126,127	0			
	128,129	0			
Section 2	130,131	1	2		
	132,133	1			
	134,135	0			
	136,137	0			
	138,139	0			
	140,141	0			
Section 3	142,143	0	2		
	144,145	2			
	146,147	0			
	148,149	0			
	150,151	0			
OJA2					
Section 2	152,153	1	2	6	224
	154,155	1			
Section 3	156,157	1	1		
	158,159	0			
Section 4	160,161	0	3		
	162,163	3			
OJA3					
Section 2	164,165	2	3	3	336
	166,167	1			
	168,169	0			
OJA4					
Section 3	170,171	0	1	1	112
	172,173	1			
	174,175	0			
	176,177	0			
OJA5					
Section 3	182,183	1	1	2	112
	184,185	0			
	186,187	0			
	188,189	0			
Section 4	190,191	0	1		
	192,193	1			
	194,195	0			
	196,197	0			

Old+Vehicle--Injured	Mean No. of Ki67+/H+	Standard Error			
	197.1666667	26.00907961			
	Image ID	**Ki67+/H+**	**Section Sum**	**Sum for all**	**Extrapolated total**
O+Veh1					
Section 1	198,199	0	0	3	112
	200,201	0			
	202,203	0			
	204,205	0			
	206,207	0			
Section 2	208,209	1	1		
	210,211	0			
	212,213	0			
Section 3	214,215	2	2		
	216,217	0			
	218,219	0			
O+Veh2					
Section 1	222,223	1	1	3	168
	224,225	0			
	226,227	0			
Section 4	228,229	1	2		
	230,231	1			
O+Veh3					
Section 1	232,233	1	1	6	336
	234,235	0			
	236,237	0			
	238,239	0			
	240,241	0			
	242,243	0			
	244,245	0			
Section 3	246,247	1	5		
	248,249	2			
	250,251	1			
	252,253	0			
	254,255	0			
	256,257	1			
	258,259	0			
	260,261	0			
O+Veh4					
Section 2	262,263	3	3	6	224
	264,265	0			
	266,267	0			
	268,269	0			
Section 3	270,271	1	1		
	272,273	0			
	274,275	0			
	276,277	0			
Section 4	278,279	0	2		
	280,281	2			

O+Veh5					
Section 1	282,283	1	1	5	186.6666667
	284,285	0			
	286,287	0			
Section 2	288,289	1	1		
	290,291	0			
	292,293	0			
Section 3	294,295	2	3		
	296,297	0			
	298,299	1			
O+Veh6					
Section 1	300,301	2	2	5	140
	302,303	0			
	304,305	0			
	306,307	0			
	308,309	0			
Section 2	311,312	0	1		
	313,314	0			
	316,317	1			
	318,319	0			
Section 3	320,321	0	1		
	322,323	1			
	324,325	0			
	326,327	0			
	328,329	0			
Section 4	330,331	0	1		
	332,333	1			
	334,335	0			
	336,337	0			
	338,339	0			
	340,341	0			
O+Veh7					
Section 1	342,343	1	1	4	149.3333333
	344,345	0			
	346,347	0			
	348,349	0			
Section 3	350,351	0	1		
	352,353	1			
	354,355	0			
Section 4	356,357	1	2		
	358,359	0			
	360,361	1			
O+Veh8					
Section 2	362,363	0	2	7	261.3333333
	364,365	2			
	366,367	0			
	368,369	0			
Section 3	370,371	0	2		
	372,373	1			
	374,375	1			
Section 4	376,377	2	3		
	378,379	1			
	380,381	0			
	382,383	0			

Old+Vehicle--Uninjured	Mean No. of Ki67+/H+	Standard Error			
	186.6666667	39.59797975			
	Image ID	**Ki67+/H+**	**Section Sum**	**Sum for all sections**	**Extrapolated total**
OJV1					
Section 1	4,5	0	0	3	168
	6,7	0			
	8,9	0			
Section 3	10,11	1	3		
	12,13	2			
	14,15	0			
OJV2					
Section 2	16,17	1	1	4	149.3333333
	18,19	0			
	20,21	0			
	22,23	0			
	24,25	0			
	26,27	0			
Section 3	28,29	0	0		
	30,31	0			
	32,33	0			
	34,35	0			
	36,37	0			
	38,39	0			
Section 4	40,41	0	3		
	42,43	1			
	44,45	0			
	46,47	0			
	48,49	2			
	50,51	0			
OJV3					
Section 3	52,53	0	0	2	112
	54,55	0			
	56,57	0			
	58,59	0			
	60,61	0			
Section 4	62,63	0	2		
	64,65	2			
	66,67	0			
	68,69	0			
	70,71	0			
OJV4					
Section 3	72,73	0	0	4	224
	74,75	0			
	76,77	0			
	78,79	0			
	80,81	0			
Section 4	82,83	2	4		
	84,85	0			
	86,87	1			
	88,89	0			
	90,91	1			

OJV5					
Section 2	92,93	0	3	5	280
	94,95	2			
	96,97	0			
	98,99	1			
	100,101	0			
	102,103	0			
Section 4	104,105	1	2		
	106,107	1			
	108,109	0			
	110,111	0			
	112,113	0			
	114,115	0			

	Mean	**Std Error**	**P value**	
O+Veh Uninj	186.6666667	29.51459149	0.887189024	
O+Abt Uninj	194.1333333	41.57264058	N.S.	
O+Veh Inj	197.1666667	26.00907961		0.724032429
O+Abt Inj	182	26.80795902		N.S.
O+Veh Uninj	**O+Abt Uninj**	**O+Veh Inj**	**O+Abt Inj**	
168	186.6666667	112	224	
149.3333333	224	168	168	
112	336	336	112	
224	112	224	224	
280	112	186.6666667		
		140		
		149.3333333		
		261.3333333		

Neuroinflammation Excel Sheets (CD68+ Cell Frequency; Excel 7)

Old+Abt--Injured	**Mean Freq. of CD68+ cells per total cells**	**Standard error**		
	0.10516924	0.01008303		
	Images	**CD68+**	**H+**	**Freq.**
Old+Abt1				
Section 1	120,121	54	535	
Section 2	122,123	50	521	
Section 3	124,125	75	698	
Section 4	126,127	36	566	
	Sum	215	2320	0.092672
Old+Abt2				
Section 1	128,129	64	437	
Section 2	130,131	63	476	
Section 3	132,133	55	446	
	Sum	182	1359	0.133922
Old+Abt3				
Section 2	134,135	59	513	
Section 3	136,137	72	515	
Section 4	138,139	32	535	
	Sum	163	1563	0.104287
Old+Abt4				
Section 1	140,141	45	500	
Section 2	142,143	43	480	
	Sum	88	980	0.089796

Old+Abt--Uninjured	Mean Freq. of CD68+ cells per total cells	Standard error		
	0.119014987	0.020637536		
	Images	**CD68+**	**H+**	**Freq.**
OJA1				
Section 1	43,44	62	663	
Section 2	45,46	58	636	
Section 3	47,48	87	716	
Section 4	49,50	90	684	
	Sum	297	2699	0.110041
OJA2				
Section 1	51,52	25	441	
Section 2	53,54	44	465	
Section 3	55,56	46	466	
	Sum	115	1372	0.083819
OJA3				
Section 1	60,61	80	399	
Section 2	62,63	103	434	
Section 3	65,66	83	380	
Section 4	67,68	49	364	
	Sum	315	1577	0.199746
	Images	**CD68+**	**H+**	**Freq.**
OJA4				
Section 1	69,70	74	555	
Section 2	71,72	49	531	
Section 3	73,74	27	452	
Section 4	75,76	56	560	
	Sum	206	2098	0.098189
OJA5				
Section 1	77,78	56	474	
Section 2	79,80	62	505	
Section 3	81,82	30	454	
	Sum	148	1433	0.10328

Old+Vechicle--Injured	Mean Freq. of CD68+ cells per total cells	Standard error		
	0.124161198	0.0086475		
	Images	**CD68+**	**H+**	**Freq.**
Old+Veh1				
Section 1	83,84	62	556	
	Sum			0.111511
Old+Veh2				
Section 1	85,86	41	570	
Section 2	87,88	63	479	
	Sum	104	1049	0.099142
Old+Veh3				
Section 1	89,90	92	466	
Section 2	91,92	72	396	
Section 3	93,94	44	399	
Section 4	95,96	29	376	
	Sum	237	1637	0.144777
Old+Veh4				
Section 3	97,98	55	537	
Section 4	99,100	68	551	
	Sum	123	1088	0.113051
	Images	**CD68+**	**H+**	**Freq.**
Old+Veh5				
Section 3	101,102	91	520	
	Sum			0.175
Old+Veh6				
Section 2	103,104	60	529	
Section 3	105,106	60	403	
Section 4	107,108	59	526	
	Sum	179	1458	0.122771
Old+Veh7				
Section 2	109,110	41	523	
Section 4	111,112	70	495	
	Sum	111	1018	0.109037
Old+Veh8				
Section 2	113,114	74	509	
Section 3	115,116	62	485	
Section 4	117,118	56	515	
	Sum	118	1000	0.118

Old+Vehicle--Uninjured	Mean Freq. of CD68+ cells per total cells	Standard error		
	0.141158957	0.020724562		
	Images	**CD68+**	**H+**	**Freq.**
OJV1				
Section 1	4,5	35	516	
Section 2	6,7	85	557	
Section 3	9,10	88	508	
Section 4	11,12	130	465	
	Sum	338	2046	0.1652
OJV2				
Section 1	13,14	119	706	
Section 2	15,16	144	677	
Section 3	17,18	152	591	
	Sum	415	1974	0.210233
OJV3				
Section 1	21,22	66	472	
Section 2	23,24	66	535	
Section 3	25,26	23	342	
	Sum	155	1349	0.1149
OJV4				
Section 1	27,28	73	642	
Section 2	29,30	38	502	
Section 3	31,32	47	538	
Section 4	33,34	50	504	
	Sum	208	2186	0.095151
OJV5				
Section 1	35,36	45	515	
Section 2	37,38	70	583	
Section 3	39,40	72	602	
Section 4	41,42	92	619	
	Sum	279	2319	0.12031

	Mean	Std Error	P-value	
O+Veh Uninj	0.141158957	0.020724562	0.470684483	
O+Abt Uninj	0.119014987	0.020637536	N.S.	
O+Veh Inj	0.124161198	0.0086475		0.211890179
O+Abt Inj	0.10516924	0.01008303		N.S.
Old+Vehicle--Uninjured	**Old+Abt--Uninjured**	**Old+Vechicle--Injured**	**Old+Abt--Injured**	
0.165200391	0.110040756	0.111510791	0.092672414	
0.210233029	0.083819242	0.09914204	0.133922001	
0.114899926	0.199746354	0.144777031	0.104286628	
0.095150961	0.098188751	0.113051471	0.089795918	
0.120310479	0.103279833	0.175		
		0.122770919		
		0.109037328		
		0.118		

Neuroinflammation Excel Sheets (CD68+ Particle Size; Excel 8)

Old+Abt Injured TA

Old+Abt 1				
	Label	Area	Mean	**% Area**
1	C1-Old+Abt-Section 1_120,121.tif	1447680	1479.905	4.995
2	C1-Old+Abt-Section 2_122,123.tif	1447680	3253.355	8.194
1	C1-Old+Abt-Section 3_124,125.tif	1447680	2110.857	4.264
1	C1-Old+Abt-Section 4_126,127.tif	1447680	2343.36	2.659
			Ave % Area	**5.028**
Old+Abt 2				
1	C1-Old+Abt2-Section 1_128,129.tif	1447680	3.046	3.081
2	C1-Old+Abt2-Section 2_130,131.tif	1447680	13.414	6.852
3	C1-Old+Abt2-Section 3_132,133.tif	1447680	11.641	8.127
			Ave % Area	**6.02**
Old+Abt 3				
1	C1-Old+Abt3-Section 2_134,135.tif	1447680	10.369	1.755
2	C1-Old+Abt3-Section 3_136,137.tif	1447680	12.337	8.035
3	C1-Old+Abt3-Section 4_138,139.tif	1447680	14.631	6.404
			Ave % Area	**5.398**
Old+Abt 4				
1	C1-Old+Abt4-Section 1_140,141.tif	1447680	9.875	6.774
2	C1-Old+Abt4-Section 2_142,143.tif	1447680	9.361	3.701
			Ave % Area	**5.2375**

Old+Abt Uninjured TA

OJA1				
	Label	Area	Mean	**% Area**
1	C1-OJA1-Section1_43,44.tif	1447680	10.941	9.575
2	C1-OJA1-Section2_45,46.tif	1447680	13.258	8.005
3	C1-OJA1-Section3_47,48.tif	1447680	7.692	6.61
4	C1-OJA1-Section4_49,50.tif	1447680	10.234	6.47
			Ave % Area	**7.665**
OJA2				
1	C1-OJA2-Section 1_51,52.tif	1447680	6.438	4.044
2	C1-OJA2-Section 2_53,54.tif	1447680	4.458	3.644
3	C1-OJA2-Section 3_55,56.tif	1447680	6.2	1.567
			Ave % Area	**3.085**
OJA3				
1	C1-OJA3-Section 1_60,61.tif	1447680	7.54	6.074
2	C1-OJA3-Section 2_62,63.tif	1447680	7.781	6.104
3	C1-OJA3-Section 3_65,66.tif	1447680	10.434	8.398
4	C1-OJA3-Section 4_67,68.tif	1447680	7.595	7.361
			Ave % Area	**6.98425**
OJA4				
1	C1-OJA4-Section 1_69,70.tif	1447680	14.687	2.858
2	C1-OJA4-Section 2_71,72.tif	1447680	6.101	2.939
3	C1-OJA4-Section 3_73,74.tif	1447680	7.284	2.654
4	C1-OJA4-Section 4_75,76.tif	1447680	7.617	3.801
			Ave % Area	**3.063**
OJA5				
1	C1-OJA5-Section 1_77,78.tif	1447680	6.709	3.844
2	C1-OJA5-Section 2_79,80.tif	1447680	9.85	7.856
3	C1-OJA5-Section 3_81,82.tif	1447680	10.534	5.319
			Ave % Area	**5.673**

Old+Vehicle Injured TA

Old+Veh 1				
	Label	Area	Mean	% Area
1	C1-Old+Veh1-Section 1_83,84.tif	1447680	9.119	7.306
			Ave % Area	**7.306**
Old+Veh 2				
1	C1-Old+Veh2-Section 1_85,86.tif	1447680	8.484	8.505
2	C1-Old+Veh2-Section 2_87,88.tif	1447680	8.905	9.705
			Ave % Area	**9.105**
Old+Veh 3				
1	C1-Old+Veh3-Section 1_89,90.tif	1447680	6.56	7.846
2	C1-Old+Veh3-Section 2_91,92.tif	1447680	12.01	7.932
3	C1-Old+Veh3-Section 3_93,94.tif	1447680	11	10.38
4	C1-Old+Veh3-Section 4_95,96.tif	1447680	6.056	5.85
			Ave % Area	**8.002**
Old+Veh 4				
1	C1-Old+Veh4-Section 3_97,98.tif	1447680	7.032	4.647
2	C1-Old+Veh4-Section 4_99,100.tif	1447680	8.713	9.14
			Ave % Area	**6.8935**
Old+Veh 5				
1	C1-Old+Veh5-Section 3_101,102.tif	1447680	9.129	9.513
			Ave % Area	**9.513**
Old+Veh 6				
1	C1-Old+Veh6-Section 2_103,104.tif	1447680	6.658	6.038
2	C1-Old+Veh6-Section 3_105,106.tif	1447680	12.779	9.885
3	C1-Old+Veh6-Section 4_107,108.tif	1447680	9.531	9.354
			Ave % Area	**8.425667**
Old+Veh 7				
1	C1-Old+Veh7-Section 2_109,110.tif	1447680	9.204	6.584
2	C1-Old+Veh7-Section 4_111,112.tif	1447680	7.739	9.721
			Ave % Area	**8.1525**
Old+Veh 8				
1	C1-Old+Veh8-Section 2_113,114.tif	1447680	9.685	12.586
2	C1-Old+Veh8-Section 3_115,116.tif	1447680	9.863	9.027
3	C1-Old+Veh8-Section 4_117,118.tif	1447680	7.936	8.903
			Ave % Area	**10.172**

Old+Vehicle Uninjured TA

OJV1				
Label	Area	Mean	**% Area**	
1	C1-OJV1-Section 1_4,5.tif	1447680	7.954	8.118
2	C1-OJV1-Section 4_11,12.tif	1447680	9.049	11.056
3	C1-OJV1-Section 3_9,10.tif	1447680	8.652	9.38
4	C1-OJV1-Section 2_6,7.tif	1447680	7.674	8.872
			Ave % Area	**9.3565**
OJV2				
1	C1-OJV2-Section 1_13,14.tif	1447680	19.751	15.407
2	C1-OJV2-Section 3_17,18.tif	1447680	9.843	9.622
3	C1-OJV2-Section 2_15,16.tif	1447680	13.723	11.4
			Ave % Area	**12.143**
OJV3				
1	C1-OJV3-Section 2_23,24.tif	1447680	5.72	7.376
2	C1-OJV3-Section 1_21,22.tif	1447680	6.167	8.534
3	C1-OJV3-Section 3_25,26.tif	1447680	3.177	4.959
			Ave % Area	**6.956333**
OJV4				
1	C1-OJV4-Section 1_27,28.tif	1447680	7.344	6.219
2	C1-OJV4-Section 2_29,30.tif	1447680	6.324	6.641
3	C1-OJV4-Section 3_31,32.tif	1447680	6.187	6.17
4	C1-OJV4-Section 4_33,34.tif	1447680	7.598	5.291
			Ave % Area	**6.08025**
OJV5				
1	C1-OJV5-Section 1_35,36.tif	1447680	5.172	4.694
2	C1-OJV5-Section 2_37,38.tif	1447680	9.442	11.507
3	C1-OJV5-Section 3_39,40.tif	1447680	7.428	7.029
4	C1-OJV5-Section 4_41,42.tif	1447680	11.425	10.783
			Ave % Area	**8.50325**

Old+Abt Inj	Old+Veh Inj	Old+Abt Uninj	Old+Veh Uninj			Mean	Std Error	P-value	
5.028	7.306	7.665	9.3565		**Old+Veh Uninj**	8.607867	1.053209		0.048615
6.02	9.105	3.085	12.143		**Old+Abt Uninj**	5.29405	0.96123		*
5.398	8.002	6.98425	6.956333333		**Old+Veh Inj**	8.446208	0.390636	0.000413	
5.2375	6.8935	3.063	6.08025		**Old+Abt Inj**	5.420875	0.213591	*	
	9.513	5.673	8.50325						
	8.425666667								
	8.1525								
	10.172								

References

1. Mehdipour, M. *et al.* Rejuvenation of three germ layers tissues by exchanging old blood plasma with saline-albumin. *Aging* **12**, 8790–8819 (2020).
2. Mehdipour, M. *et al.* Plasma dilution improves cognition and attenuates neuroinflammation in old mice. *Geroscience* (2020) doi:10.1007/s11357-020-00297-8.
3. Patterson, S. L. Immune dysregulation and cognitive vulnerability in the aging brain: Interactions of microglia, IL-1β, BDNF and synaptic plasticity. *Neuropharmacology* **96**, 11–18 (2015).
4. Fan, X., Wheatley, E. G. & Villeda, S. A. Mechanisms of Hippocampal Aging and the Potential for Rejuvenation. *Annual Review of Neuroscience* (2017) doi:10.1146/annurev-neuro-072116-031357.
5. Conboy, I. M., Conboy, M. J. & Rebo, J. Systemic problems: A perspective on stem cell aging and rejuvenation. *Aging* vol. 7 754–765 (2015).
6. Villeda, S. A. *et al.* The ageing systemic milieu negatively regulates neurogenesis and cognitive function. *Nature* **477**, 90–96 (2011).
7. Villeda, S. A. *et al.* Young blood reverses age-related impairments in cognitive function and synaptic plasticity in mice. *Nature Medicine* **20**, 659–663 (2014).
8. Katsimpardi, L. *et al.* Vascular and neurogenic rejuvenation of the aging mouse brain by young systemic factors. *Science (1979)* **344**, 630–634 (2014).
9. Smith, L. K. *et al.* β2-microglobulin is a systemic pro-aging factor that impairs cognitive function and neurogenesis. *Nature Medicine* **21**, 932–937 (2015).
10. Castellano, J. M. *et al.* Human umbilical cord plasma proteins revitalize hippocampal function in aged mice. *Nature* **544**, 488–492 (2017).
11. Shytikov, D., Balva, O., Debonneuil, E., Glukhovskiy, P. & Pishel, I. Aged Mice Repeatedly Injected with Plasma from Young Mice: A Survival Study. *BioResearch Open Access* **3**, 226–232 (2014).
12. Sha, S. J. *et al.* Safety, Tolerability, and Feasibility of Young Plasma Infusion in the Plasma for Alzheimer Symptom Amelioration Study: A Randomized Clinical Trial. *JAMA Neurology* **76**, 35–40 (2019).
13. Rebo, J. *et al.* A single heterochronic blood exchange reveals rapid inhibition of multiple tissues by old blood. *Nature Communications* **7**, (2016).
14. Chen, C.-C., Lu, J., Yang, R., Ding, J. B. & Zuo, Y. Selective activation of parvalbumin interneurons prevents stress-induced synapse loss and perceptual defects. *Molecular Psychiatry* **23**, 1614–1625 (2018).
15. Antunes, M. & Biala, G. The novel object recognition memory: neurobiology, test procedure, and its modifications. *Cognitive Processing* **13**, 93–110 (2012).
16. Mehdipour, M. *et al.* Rejuvenation of brain, liver and muscle by simultaneous pharmacological modulation of two signaling determinants, that change in opposite directions with age. *Aging* **11**, 5628–5645 (2019).
17. Harada, C. N., Natelson Love, M. C. & Triebel, K. L. Normal cognitive aging. *Clin Geriatr Med* **29**, 737–752 (2013).

18. van Praag, H., Kempermann, G. & Gage, F. H. Running increases cell proliferation and neurogenesis in the adult mouse dentate gyrus. *Nat Neurosci* **2**, 266–270 (1999).
19. Wu, H. P., Ioffe, J. C., Iverson, M. M., Boon, J. M. & Dyck, R. H. Novel, whisker-dependent texture discrimination task for mice. *Behav Brain Res* **237**, 238–242 (2013).
20. Lueptow, L. M. Novel Object Recognition Test for the Investigation of Learning and Memory in Mice. *J Vis Exp* 55718 (2017) doi:10.3791/55718.
21. Yousef, H. *et al.* Aged blood impairs hippocampal neural precursor activity and activates microglia via brain endothelial cell VCAM1. *Nature Medicine* **25**, 988–1000 (2019).
22. Lian, B. S. X. *et al.* Synergistic anti-proliferative effects of combination of ABT-263 and MCL-1 selective inhibitor A-1210477 on cervical cancer cell lines. *BMC Res Notes* **11**, 197 (2018).
23. Wang, H. *et al.* JQ1 synergizes with the Bcl-2 inhibitor ABT-263 against MYCN-amplified small cell lung cancer. *Oncotarget* **8**, 86312–86324 (2017).
24. Lin, Q.-H. *et al.* ABT-263 induces G(1)/G(0)-phase arrest, apoptosis and autophagy in human esophageal cancer cells in vitro. *Acta Pharmacol Sin* **38**, 1632–1641 (2017).
25. Lee, Y.-C., Wang, L.-J., Huang, C.-H., Shi, Y.-J. & Chang, L.-S. ABT-263-induced MCL1 upregulation depends on autophagy-mediated 4EBP1 downregulation in human leukemia cells. *Cancer Letters* **432**, 191–204 (2018).
26. Pan, J. *et al.* Inhibition of Bcl-2/xl With ABT-263 Selectively Kills Senescent Type II Pneumocytes and Reverses Persistent Pulmonary Fibrosis Induced by Ionizing Radiation in Mice. *Int J Radiat Oncol Biol Phys* **99**, 353–361 (2017).
27. Sharma, A. K. *et al.* The Senolytic Drug Navitoclax (ABT-263) Causes Trabecular Bone Loss and Impaired Osteoprogenitor Function in Aged Mice. *Front Cell Dev Biol* **8**, 354 (2020).
28. Chang, J. *et al.* Clearance of senescent cells by ABT263 rejuvenates aged hematopoietic stem cells in mice. *Nature Medicine* **22**, 78–83 (2016).
29. Kirkland, J. L. & Tchkonia, T. Senolytic Drugs: From Discovery to Translation. *Journal of Internal Medicine* **n/a**, (2020).
30. Yamaguchi, R. & Perkins, G. Finding a Panacea among Combination Cancer Therapies. *Cancer Research* **72**, 18 LP – 23 (2012).
31. Senatorov, V. v *et al.* Blood-brain barrier dysfunction in aging induces hyperactivation of TGFβ signaling and chronic yet reversible neural dysfunction. *Science Translational Medicine* **11**, eaaw8283 (2019).
32. Heinemann, U., Kaufer, D. & Friedman, A. Blood-brain barrier dysfunction, TGFβ signaling, and astrocyte dysfunction in epilepsy. *Glia* **60**, 1251–1257 (2012).
33. Yang, A. C. *et al.* Physiological blood–brain transport is impaired with age by a shift in transcytosis. *Nature* **583**, 425–430 (2020).
34. Walton, C. C., Begelman, D., Nguyen, W. & Andersen, J. K. Senescence as an Amyloid Cascade: The Amyloid Senescence Hypothesis. *Front Cell Neurosci* **14**, 129 (2020).
35. Balusu, S. *et al.* Identification of a novel mechanism of blood-brain communication during peripheral inflammation via choroid plexus-derived extracellular vesicles. *EMBO Mol Med* **8**, 1162–1183 (2016).

36. Cattaneo, A. *et al.* Association of brain amyloidosis with pro-inflammatory gut bacterial taxa and peripheral inflammation markers in cognitively impaired elderly. *Neurobiology of Aging* **49**, 60–68 (2017).
37. Bettcher, B. M. *et al.* Increases in a Pro-inflammatory Chemokine, MCP-1, Are Related to Decreases in Memory Over Time. *Front Aging Neurosci* **11**, 25 (2019).
38. Wang, L.-J. *et al.* Albendazole-Induced SIRT3 Upregulation Protects Human Leukemia K562 Cells from the Cytotoxicity of MCL1 Suppression. *Int J Mol Sci* **21**, 3907 (2020).
39. Ohgino, K. *et al.* Intracellular levels of reactive oxygen species correlate with ABT-263 sensitivity in non-small cell lung cancer cells. *Cancer Science* **n/a**, (2020).
40. Mukherjee, N. *et al.* MCL1 inhibitors S63845/MIK665 plus Navitoclax synergistically kill difficult-to-treat melanoma cells. *Cell Death Dis* **11**, 443 (2020).
41. Vogler, M. *et al.* The B-cell lymphoma 2 (BCL2)-inhibitors, ABT-737 and ABT-263, are substrates for P-glycoprotein. *Biochemical and Biophysical Research Communications* **408**, 344–349 (2011).
42. Tagscherer, K. E. *et al.* Apoptosis-based treatment of glioblastomas with ABT-737, a novel small molecule inhibitor of Bcl-2 family proteins. *Oncogene* **27**, 6646–6656 (2008).
43. Marschallinger, J. *et al.* Structural and functional rejuvenation of the aged brain by an approved anti-asthmatic drug. *Nat Commun* **6**, 8466 (2015).
44. Loeffler, D. A. AMBAR, an Encouraging Alzheimer's Trial That Raises Questions. *Front Neurol* **11**, 459 (2020).
45. Boada, M. *et al.* Amyloid-targeted therapeutics in Alzheimer's disease: Use of human albumin in plasma exchange as a novel approach for Aβ mobilization. *Drug News and Perspectives* (2009) doi:10.1358/dnp.2009.22.6.1395256.
46. Boada, M. *et al.* Efficacy and Safety of Plasma Exchange with 5% Albumin to Modify Cerebrospinal Fluid and Plasma Amyloid-β Concentrations and Cognition Outcomes in Alzheimer's Disease Patients: A Multicenter, Randomized, Controlled Clinical Trial. *J Alzheimers Dis* **56**, 129–143 (2017).
47. Cuberas-Borrós, G. *et al.* Longitudinal Neuroimaging Analysis in Mild-Moderate Alzheimer's Disease Patients Treated with Plasma Exchange with 5% Human Albumin. *J Alzheimers Dis* **61**, 321–332 (2018).
48. Boada, M. *et al.* Plasma exchange for Alzheimer's disease Management by Albumin Replacement (AMBAR) trial: Study design and progress. *Alzheimers Dement (N Y)* **5**, 61–69 (2019).

05/02/2022

To whom it may concern,

I grant Melod Mehdipour permission to use my data and notebook entries from Figure 4 of the manuscript *Plasma dilution improves cognition and attenuates neuroinflammation in old mice* (doi: 10.1007/s11357-020-00297-8) for Chapter 3 of his thesis.

Sincerely,

Taha Mehdipour

Email Confirmation from Professor Ok Hee Jeon:

Ok Hee Jeon <ojeon@korea.ac.kr>

Fri, Sep 10, 2021, 6:12 PM

to me

Hi, Melod. Hope you are doing well. Sure, You can add our collaborative work to your thesis. Let me know if you need anything.

Best
Okhee
--
Ok Hee Jeon, PhD

Assistant Professor
Department of Biomedical Sciences
Korea University College of Medicine
73, Goryeodae-ro, Seongbuk-gu, Seoul, Republic of Korea
Tel: +82-2-2286-1467

Conclusion

We used young (2-4 months of age) and old (18-24 months of age) mice—the equivalent of humans in their 20's and 80's, respectively—as a model to understand mammalian aging. We were interested in understanding the conserved effects of young vs aged systemic milieu on tissue health and regeneration. Representative organs of each of the three developmental germ layers, namely muscle (mesoderm) and brain (ectoderm) were the predominant focus of the presented work. In this dissertation we demonstrated that the inhibitory effects of aged blood—which dominates over the pro-regenerative properties of young blood—can be substantially abrogated by the dilution of aged plasma through neutral blood exchange (NBE). We also show that the dilution of aged plasma is sufficient to rejuvenate the tissues of old animals rapidly and robustly. We also show that NBE significantly improves muscle health by boosting myogenesis, increasing nascent myofiber size, and attenuating fibrosis *in vivo*. NBE substantially boosts hippocampal neurogenesis, attenuates neuroinflammation, and improves cognition in aged mice. We also found that the overall effects of NBE on the brain were more profound than those of the senolytic ABT263 (Navitoclax) even though both interventions act peripherally. Collectively, this work suggests that young blood factors may not be essential for rejuvenation. A neutral-age physiological fluid is adequate for rejuvenating multiple tissues simultaneously. The FDA approved Therapeutic Plasma Exchange (TPE) modality may also confer rapid translation to treat numerous inflammatory, fibrotic, and metabolic diseases in older people. Summarily, we maintain that it is possible to recalibrate the levels of systemic proteins to health/youth by removing factors that exert dominant progeric effects on tissues. We propose that this can be accomplished by calibrating the concentrations of TGFβ superfamily proteins to young levels. This is summarized in the schematic below:

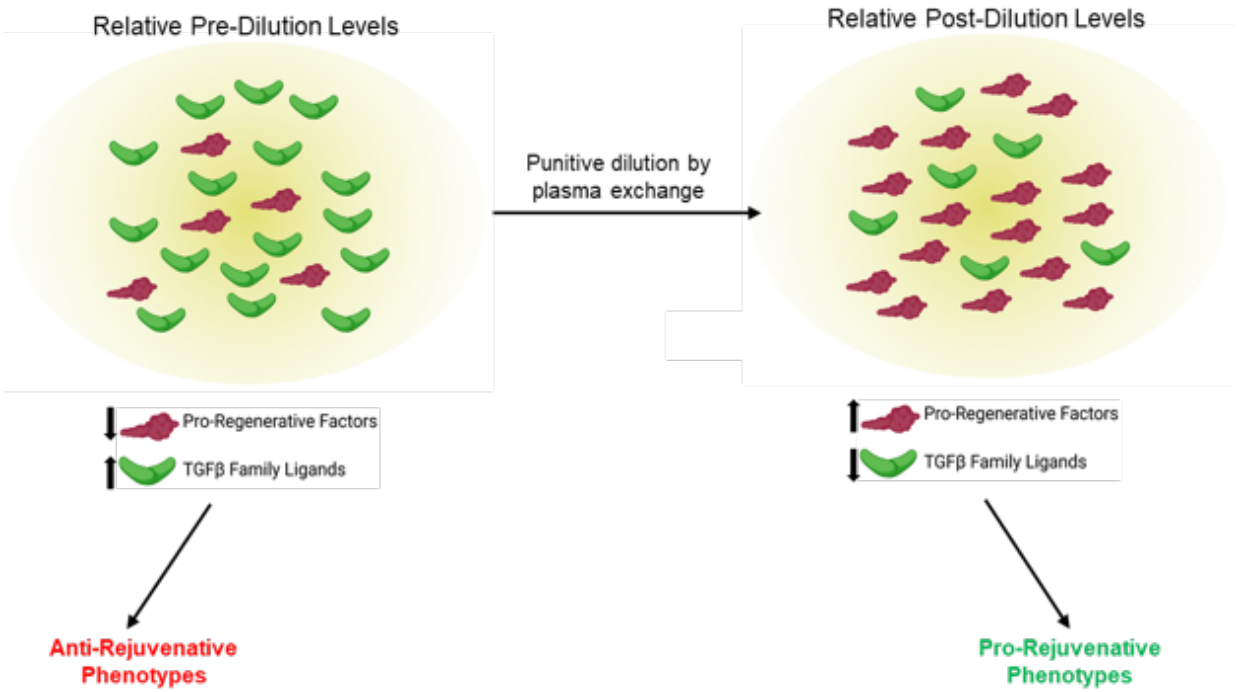

Image was created with biorender.com